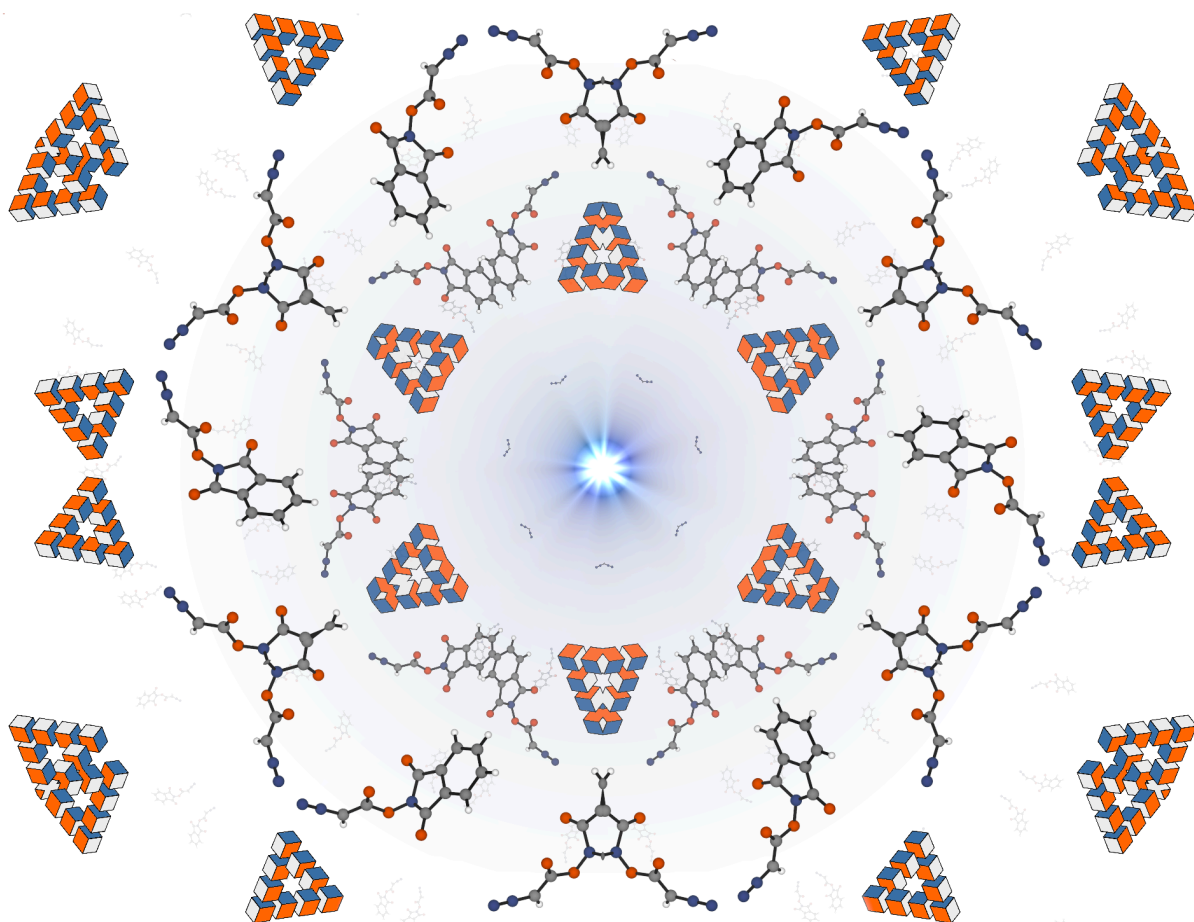


Asymmetric Synthesis using Redox-Active Diazocompounds as Chiral Carbon Atom Precursors

Matteo Costantini



Asymmetric Synthesis using Redox-Active Diazocompounds as Chiral Carbon Atom Precursors

Matteo Costantini

Academic dissertation for the Degree of Doctor of Philosophy in Organic Chemistry at Stockholm University to be publicly defended on Friday 19 November 2021 at 09.00 in Magnélisalen, Kemiska övningslaboratoriet, Svante Arrhenius väg 16 B.

Abstract

This thesis summarizes the development of general and efficient methods to synthesize enantiomerically enriched cyclopropane compounds. The works reported herein exploit the opportunity presented by redox-active esters to explore the orthogonality between asymmetric carbene-transfer and geminal radical generation. Together, these two processes enable the enantioselective manipulation of a carbon atom with multiple leaving groups, allowing sequential and systematic molecular assembly. This thesis discloses a unified approach to transform abundant alkene substrates into unrelated cyclopropane products, circumventing the need of specific methods, catalysts and carbene precursors for each individual case. The exploration of redox-active diazoacetate reagents in this strategy resulted in the discovery of the general enantioselective cyclopropanation method presented in Chapter 2. This method engages olefins, even aliphatic, to produce a variety of cyclopropane derivatives in high yields and selectivity. The late-stage diversification of the resulting products enables facile access to useful chiral building blocks and biologically important scaffolds in a more practical and sustainable way. The mechanism of this ruthenium-catalyzed cyclopropanation employing a novel redox-active carbene precursor is investigated in Chapter 3, disclosing the origin of the selectivity and performance of the system. Several techniques including gas evolution monitoring, benzhydrylium benchmarking, *in situ* high resolution mass spectroscopy and VTNA kinetic analysis are used to gain insight on this reaction. Chapter 4 describes the development of a key stereoselective photo-decarboxylation of cyclopropyl redox-active esters to obtain chiral *cis*-arylcyclopropanes. These are commonly used as conformationally restricted olefin isosteres in medicinal chemistry. The modular assembly of these challenging compounds is explored, along with the photophysical and photochemical features of the new efficient method. Finally, Chapter 5 describes the development of a robust protocol to transform cyclopropyl redox-active esters in versatile cyclopropylboronates by a new photo-organocatalyzed method, which is mediated by new non-symmetric diboronic acid monoesters. These findings originate from a detailed mechanistic investigation of a known borylation procedure by *in situ* NMR spectroscopy. The new method facilitates the synthesis of chiral cyclopropylboronates in a more sustainable and efficient way, and illustrates the opportunities bestowed by the new diboron species to enhance performance, robustness and stereoselectivity.

Keywords: *redox-active carbenes, mechanistic investigation, cyclopropanes, asymmetric catalysis, photochemistry.*

Stockholm 2021

<http://urn.kb.se/resolve?urn=urn:nbn:se:su:diva-197530>

ISBN 978-91-7911-640-8
ISBN 978-91-7911-641-5

Department of Organic Chemistry

Stockholm University, 106 91 Stockholm



Stockholm
University

ASYMMETRIC SYNTHESIS USING REDOX-ACTIVE
DIAZOCOMPOUNDS AS CHIRAL CARBON ATOM PRECURSORS

Matteo Costantini

Asymmetric Synthesis using Redox-Active Diazocompounds as Chiral Carbon Atom Precursors

Matteo Costantini

©Matteo Costantini, Stockholm University 2021

ISBN print 978-91-7911-640-8

ISBN PDF 978-91-7911-641-5

Front cover: "2021: A Chemical Odyssey" by Matteo Costantini, 2021

Printed in Sweden by Universitetsservice US-AB, Stockholm 2021

The time you enjoy
wasting is not wasted
time.

Abstract

This thesis summarizes the development of general and efficient methods to synthesize enantiomerically enriched cyclopropane compounds. The works reported herein exploit the opportunity presented by redox-active esters to explore the orthogonality between asymmetric carbene-transfer and geminal radical generation. Together, these two processes enable the enantioselective manipulation of a carbon atom with multiple leaving groups, allowing sequential and systematic molecular assembly. This thesis discloses a unified approach to transform abundant alkene substrates into unrelated cyclopropane products, circumventing the need of specific methods, catalysts and carbene precursors for each individual case. The exploration of redox-active diazoacetate reagents in this strategy resulted in the discovery of the general enantioselective cyclopropanation method presented in Chapter 2. This method engages olefins, even aliphatic, to produce a variety of cyclopropane derivatives in high yields and selectivity. The late-stage diversification of the resulting products enables facile access to useful chiral building blocks and biologically important scaffolds in a more practical and sustainable way. The mechanism of this ruthenium-catalyzed cyclopropanation employing a novel redox-active carbene precursor is investigated in Chapter 3, disclosing the origin of the selectivity and performance of the system. Several techniques including gas evolution monitoring, benzhydrylium benchmarking, *in situ* high resolution mass spectroscopy and VTNA kinetic analysis are used to gain insight on this reaction. Chapter 4 describes the development of a key stereoselective photo-decarboxylation of cyclopropyl redox-active esters to obtain chiral *cis*-arylcyclopropanes. These are commonly used as conformationally restricted olefin isosteres in medicinal chemistry. The modular assembly of these challenging compounds is explored, along with the photophysical and photochemical features of the new efficient method. Finally, Chapter 5 describes the development of a robust protocol to transform cyclopropyl redox-active esters in versatile cyclopropylboronates by a new photo-organocatalyzed method, which is mediated by new non-symmetric diboronic acid monoesters. These findings originate from a detailed mechanistic investigation of a known borylation procedure by *in situ* NMR spectroscopy. The new method facilitates the synthesis of chiral cyclopropylboronates in a more sustainable and efficient way, and illustrates the opportunities bestowed by the new diboron species to enhance performance, robustness and stereoselectivity.

Populärvetenskaplig sammanfattning

Inom kemin studeras atomers och molekylers egenskaper och denna kunskap nyttjas till att skapa föreningar och material som används i våra dagliga liv, till exempel läkemedel, färgämnen, bränsle, gödningsmedel och textilier. Organisk kemi fokuserar på molekyler som har kolskelett med andra atomer, och syftar till att utveckla strategier för syntes av dem från hållbara källor. En viktig egenskap hos organiska molekyler är att de kan finnas i två nästintill identiska former, på samma sätt som ena handen är spegelbilden av den andra. Denna egenskap kallas kiralitet. I denna avhandling beskrivs nya strategier för att erhålla kirala molekyler som är medicinskt intressanta och är baserade på treatomära skelett kallade cyklopropaner. Dessa föreningar innehåller särskilt intressanta farmaceutiska egenskaper och finns i många aktiva substanser. Syntesen av kirala cyklopropaner kräver dock specifika metoder för varje önskad molekyl, där svårtillgängliga reagens och material krävs. Denna avhandling undersöker och studerar nya metoder för att erhålla olika kategorier av kirala cyklopropaner och kretsar kring användandet av ett nytt och stabilt reagens kallat NHPI-DA, som kan generera en mängd olika kirala cyklopropaner från tillgängliga och billiga material. Cyklopropanprodukterna från reaktionerna kan sedan transformeras vidare i andra kemiska reaktioner. Denna avhandling utforskar några av dessa processer, särskilt de som kan aktiveras av blåa ljuskällor med samma energieffektivitet som LED-lampor i vanlig hushållsbelysning. Aktiveringen av energikrävande kemiska reaktioner med hjälp av synligt ljus kan både öka förståelsen av kemin och erbjuda stora möjligheter för en hållbarare kemisk produktion.

List of Publications

This report is based on the following articles:

- I. General Cyclopropane Assembly by Enantioselective Transfer of a Redox-Active Carbene to Aliphatic Olefins**
Montesinos-Magraner, M.[†]; Costantini, M.[†]; Ramirez-Contreras, R.; Muratore, M. E.; Johansson, M. J.; Mendoza, A.
Angew. Chem. Int. Ed. **2019**, 58, 5930–5935.
[†]: *The authors contributed equally.*
- II. Combined Experimental and Computational Study of Ruthenium N-Hydroxyphthalimidoyl Carbenes in Alkene Cyclopropanation Reactions**
Planas, F.[†]; Costantini, M.[†]; Montesinos-Magraner, M.; Himo, F.; Mendoza, A.
ACS Catal. **2021**, 11, 10950–10963
[†]: *The authors contributed equally.*
- III. Modular Enantioselective Synthesis of *cis*-Cyclopropanes through Self-Sensitized Stereoselective Photo-decarboxylation with Benzothiazolines**
Costantini, M.; Mendoza, A.
ACS Catal. *accepted*
Pre-print DOI: 10.33774/chemrxiv-2021-2f4mc
- IV. Photo-organocatalytic Decarboxylative Borylation Mediated by a Transient Non-Symmetrical Diboronic Acid Monoester**
Kohlhepp, S. V.; Montesinos-Magraner, M.; Costantini, M.; Mendoza, A. *Manuscript.*

Previous documents based on this work

This thesis is partly based on the author's half-time report titled "*Development of a redox-active carbene for the enantioselective assembly of cyclopropanes: applications in synthesis and mechanistic studies*" (presented on January 24th, 2020).

The introduction present in **Chapter 1** has been updated to include a more detailed background on the synthesis of cyclopropanes, as well as the development and applications of redox-active esters. References have been updated.

Chapter 2 (*Paper I*) has been revised in both the "introduction" and "results and discussion" sections. References have been updated.

Chapter 3 (*Paper II*) was not present in the half-time report and has been written entirely for this thesis.

Chapter 4 (*Paper III*), present in the half-time report, has been completely re-written considering the new developments of the project presented within the chapter.

Chapter 5 (*Paper IV*) was not present in the half-time report and has been written entirely for this thesis.

Table of contents

Abstract.....	i
Populärvetenskaplig sammanfattning	ii
List of Publications	iii
Previous documents based on this work.....	iv
Abbreviations	1
1. Introduction	1
1.1 Cyclopropanes and their importance.....	1
1.1.1 Synthesis of cyclopropanes	3
1.2 Carbenes and metal-carbene complexes.....	5
1.2.1 Rhodium-carbenes	6
1.2.2 Ruthenium carbenes.....	7
1.3 Redox-active esters	9
1.3.1 History and development of redox-active NHPI esters	9
1.3.2 Redox-active esters in decarboxylative reactions	10
1.4 Objectives and aims	11
2. General Asymmetric Synthesis of Cyclopropanes with a Single Redox-Active Diazocompound Reagent (NHPI-DA) (Paper I)	12
2.1 Introduction: Asymmetric syntheses of cyclopropanes	12
2.2 Aim of the project.....	14
2.3 Results and discussion.....	15
2.3.1 Reagent synthesis and reaction optimization	15
2.3.2 Substrate scope	17
2.3.3 Stereoselective diversification of the chiral redox-active cyclopropane intermediates.....	22
2.3.4 Application in synthesis	27
2.4 Conclusion and outlook.....	29
3. Combined Experimental and Computational Study of Ruthenium <i>N</i> -Hydroxyphthalimidoyl Carbenes in Alkene Cyclopropanation Reactions (Paper II)	30
3.1 Introduction	30
3.2 Aim of the project.....	31
3.3 Results and discussion.....	31

3.3.1 Kinetics of the dimerization reaction	31
3.3.2 Evaluation of migratory insertion complexes as active catalysts	35
3.3.3 Kinetics of the cyclopropanation reaction	37
3.4 Conclusions	39
4. Modular Enantioselective Synthesis of <i>cis</i> -Cyclopropanes through Self-Sensitized Stereoselective Photo-Decarboxylation with Benzothiazolines (Paper III)	41
4.1 Introduction	41
4.2 Aim of the project	43
4.3 Results and discussion	43
4.3.1 Optimization of the photo-decarboxylation reaction	43
4.3.2 Substrate scope	46
4.3.3 Photochemical characterization and mechanistic studies	49
4.3.4 Proposed mechanism	54
4.4 Conclusions and outlook	55
5. Photo-organocatalytic Decarboxylative Borylation Mediated by a Transient Non-Symmetrical Diboronate Acid Monoester	56
5.1 Introduction	56
5.2 Aim of the project	57
5.3 Results and discussion	58
5.3.1 NMR study of the decarboxylative borylation	58
5.3.2 Optimization of the decarboxylative borylation	60
5.3.3 Scope of the borocyclopropanation of olefins	62
5.3.4 Proposed mechanism	63
5.4 Conclusions and outlook	65
6. Concluding remarks	66
Appendix A – Contribution list	68
Appendix B – Reprint permissions	69
Appendix C – Experimental Data for Chapter 2-4	70
Acknowledgments	71
References	72

Abbreviations

Abbreviations are used in accordance with the standards of the subject.[§] Non-standard and unconventional abbreviations are listed below.

B ₂ cat ₂	Bis(catecholato)diboron
B ₂ pin ₂	Bis(pinacolato)diboron
BHT	2,6-Di- <i>tert</i> -butyl-4-methylphenol
BNAH	<i>N</i> -benzyl dihydronicotinamide
Box	bis(oxazoline)
bpy	1,1'-bipyridine
dba	Dibenzylideneacetone
DFT	Density functional theory
DOSP	<i>N</i> -(<i>p</i> -dodecylphenylsulfonyl)proline
DPPN	Diphenyl phosphoryl azide
DTBC	3,5-Di- <i>tert</i> -butyl-catechol
EDA	Electron donor-acceptor
Et-DA	Ethyl diazoacetate
EDG	Electron-donating group
EWG	Electron-withdrawing group
FG	Functional group
HAT	Hydrogen atom transfer
LED	Light-emitting diode
LG	Leaving group
MEOX	methyl-2-oxazolidinone-5-carboxylates
MEPY	methyl-2-oxopyrrolidine-5-carboxylates
NHPI	<i>N</i> -hydroxyphthalimide
NHPI-DA	<i>N</i> -hydroxyphthalimidoyl diazoacetate
NTTL	<i>N</i> -naphthaloyl-(<i>S</i>)- <i>tert</i> -leucinate
PET	Photoinduced electron transfer
Pheox	Phenyloxazoline
pin	pinacolato
PTTL	<i>N</i> -phthaloyl-(<i>S</i>)- <i>tert</i> -leucinate
PyBox	2,6-bis(oxazoline)pyridine
RPKA	Reaction progress kinetic analysis
rt	Room temperature
SET	Single-electron transfer
TCE	2,2,2-Trichloroethyl
TCSPC	Time-correlated single-photon counting
Teoc	2-(Trimethylsilyl)ethyloxycarbonyl
TFE	2,2,2-Trifluoroethyl
TPAP	Tetrapropylammonium perruthenate
TPCP	1,2,2-triphenylcyclopropanecarboxylate
VTNA	Variable-time normalization analysis

[§] The ACS Style Guide, American Chemical Society, Oxford University Press, New York 2006.

1. Introduction

1.1 Cyclopropanes and their importance

The cyclopropane structure is a moiety commonly found in the backbone of natural products and bioactive compounds, including pharmaceuticals and important agrochemical compounds (**Figure 1**). Due to their unique bonding and high strain energy, these molecules possess an alkene-like reactivity that allowed for the development of a variety of reactions, including ring-openings, cycloadditions and rearrangements among others.¹ Cyclopropanes are also very attractive for medicinal chemistry, and are commonly employed as (bio)isosteres in drug development, due to their rigidity, lower lipophilicity (compared to other aliphatics and aromatics), and slower metabolic oxidative degradation.^{1a, 2}

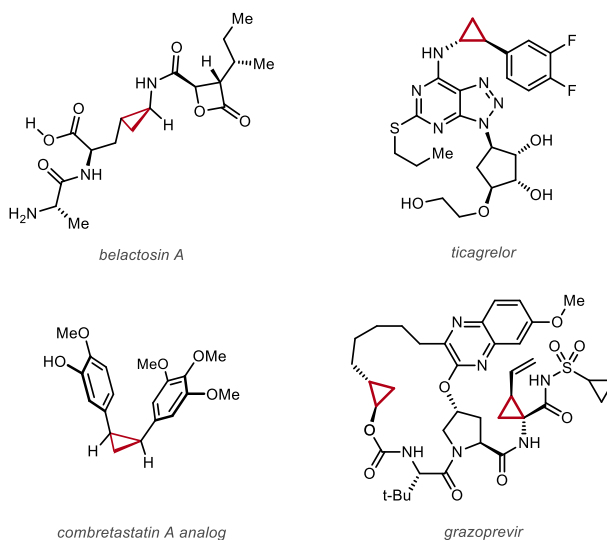


Figure 1: Examples of bioactive molecules containing the cyclopropane moiety.

These highly rigid molecules differ from other cycloalkanes for their decreased bond lengths and bond strength, due to the uncommon bonding that happens in cyclopropanes (**Figure 2**).^{1a, 2c, 3} Another feature of this moiety is the high strain energy of about 27.4 kcal/mol. This is only slightly higher than the one of cyclobutane (26.5 kcal/mol), suggesting the presence of some stabilization energy of electronic nature. Owing to their peculiar structure and reactivity, cyclopropanes have been object of numerous theoretical and experimental studies.^{1a, 1b, 2c, 3}

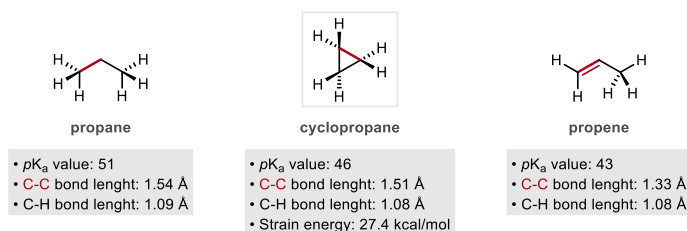


Figure 2: Properties of cyclopropane and its related compounds propane and propene.^{1a}

Several models were proposed to explain the peculiar reactivity and structure observed in these molecules.^{1b} The simplest one is based purely on the evaluation of its strain elements. The geometry of cyclopropanes requires an internal bond angle of 60° , far from the theoretical bond angle value of 109.5° in sp^3 -hybridized molecules. Moreover, the requirement of all the carbon atoms to be coplanar results in all the C-H bonds being eclipsed. The sum of the angular and torsional strain was initially proposed as the reason behind the reactivity of cyclopropanes. A more advanced explanation was given by the Förster-Coulson-Moffit model (**Figure 3**).⁴ This model suggests that C-C bonds have a higher p -character compared to regular alkanes. This results in the formation of *bent bonds*, with the electron density lying outside the cyclopropane ring. Conversely, the C-H bonds increase in s -character, explaining the higher acidity (see **Figure 2**).

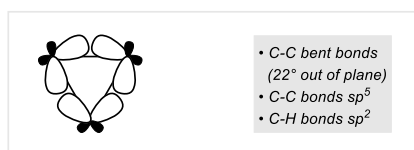


Figure 3: Representation of the Förster-Coulson-Moffit model.

Even though the Förster-Coulson-Moffit model was able to rationalize the presence of electron density outside the perimeter of the molecule, as evidenced by X-ray diffraction spectroscopy, it failed at explaining why some electron density was also observed in the center of the triangular structure. The Walsh theoretical model⁵ provides a more complete description of cyclopropanes. Walsh explained the change in the hybridization of the carbon atoms towards an increasing p -character in the C-C bonds while increasing the s -character of the C-H bonds using molecular orbitals (**Figure 4**). The lowest energy molecular orbital is formed by three sp^2 orbitals pointing towards the center, whereas the two HOMOs are originated from p -orbitals. This model can rationalize the experimental electron density and the alkene-like reactivity, as well as the different acidity and carbon-carbon bond length of cyclopropane compared to propane. Moreover, the electronic distribution provided by the Walsh model helps understanding the electronic factors contributing to the strain energy of this compound.

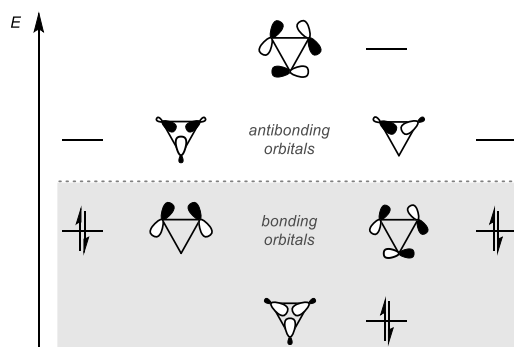
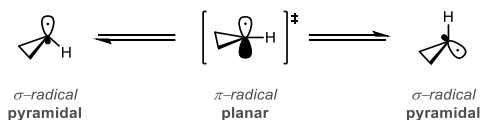


Figure 4: MO diagram of the Walsh model used to describe bonding in cyclopropanes.^{1a}

The particular bonding features of cyclopropanes also affect the stereoelectronic properties of cyclopropyl intermediates, among which cyclopropyl radicals are most relevant in the context of this thesis. These intermediates are configurationally unstable, pyramidal σ -radicals.⁶ The inversion of configuration for unconstrained cyclopropyl radicals (**Scheme 1**) is very rapid at room temperature, with a reaction rate constant of about 10^8 - 10^9 s⁻¹ and an associated energy barrier of ~ 1 kcal/mol.⁶ The inversion goes through a plane-symmetric π -radical transition state, which is the most stable form of conventional alkyl radicals. On these intermediates, the planar structure is favored to minimize steric hindrance among the substituents. This structure would instead enhance further the ring strain of the cyclopropane ring, leading to the aforementioned pyramidal configuration. It is evident how the prominent *s*-character of the cyclopropyl radical renders this intermediate similar to aryl radicals and differentiates them from the non-aromatic alkyl radicals, possessing *p*-character. Additionally, stereoselective radical substitution reactions are difficult on cyclopropane rings. Examples have been reported where the stereochemical stability of these species can be improved by having electronegative substituents,⁷ such as halogens or alkoxy groups, in the α -position of the radical in order to increase the energy barrier for the inversion.

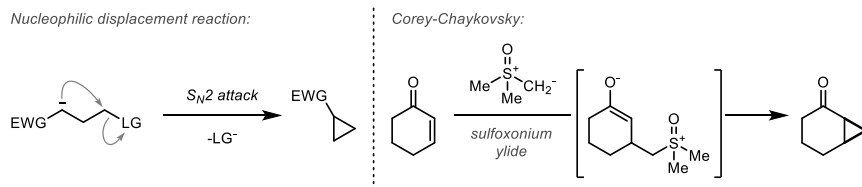


Scheme 1: Inversion of configuration of cyclopropyl radicals.

1.1.1 Synthesis of cyclopropanes

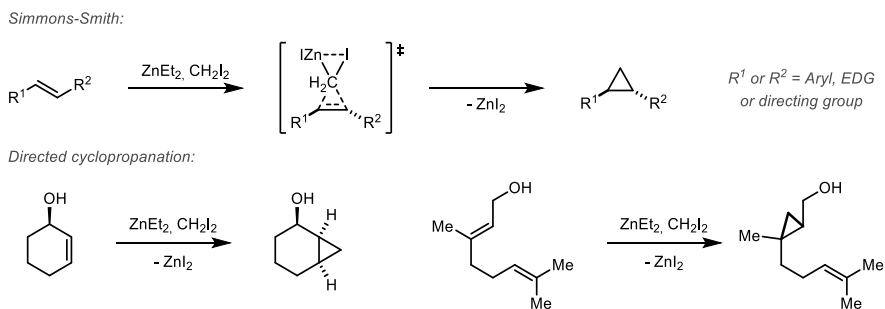
Due to their unique chemical properties, cyclopropanes have been employed in several fields of synthetic organic chemistry,^{2b, 8} ranging from asymmetric catalysis^{8a} to medicinal chemistry,^{2b} or the total synthesis of natural products.^{8b, 8c} Traditionally, these molecules have been synthesized by three main methods: nucleophilic displacement reactions, Simmons-Smith cyclopropanation, and carbene (free or

metal-bonded) cycloaddition. The first protocol involved an intramolecular S_N2 cyclization (**Scheme 2**) and was first reported by Perkin in 1884, where the cyclopropanation of diethyl malonate using 1,2-dibromoethane in the presence of base was described.⁹ Since then, analogous reactions of carbanions have been reported, most notably the addition of sulfoxonium ylides to enones, reported by Corey and Chaykovsky (**Scheme 2**).¹⁰



Scheme 2: Synthesis of cyclopropanes *via* intramolecular 3-*exo*-nucleophilic ring closure. Left: General concept. Right: The Corey-Chaykovsky reaction.¹⁰

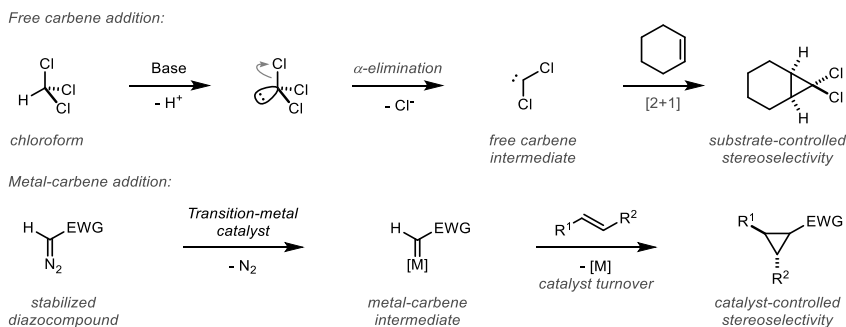
The Simmons-Smith reaction,¹¹ first published in 1958, is probably one of the most synthetically useful cyclopropanation methods due to the wide scope and stereospecificity of this process. This transformation operates through a zinc carbenoid intermediate, commonly generated *in situ* by treatment of diiodomethane with diethylzinc, and generally performs well with electron-rich substrates such as styrenes or enol ethers. (**Scheme 3**, top). Additionally, the intermediacy of zinc in this mechanism allows for Lewis basic substituents (alcohols, amines, etc.) to act as directing groups, displaying high levels of regio- and stereoselectivity (**Scheme 3**, bottom).^{8c, 12}



Scheme 3: Synthesis of cyclopropanes with zinc carbenoids. Top: General depiction of the Simmons-Smith cyclopropanation reaction.¹¹ Bottom: Examples of substrate-directed cyclopropanation.^{8c, 12}

By nature, carbenes are privileged intermediates in cyclopropane synthesis through [2+1] cycloadditions with olefins. It is known since 1954 that free dichlorocarbene (generated from chloroform in the presence of a strong base) react exothermally with olefins to yield cyclopropanes (**Scheme 4**, top).¹³ Despite the high reactivity of free

carbene intermediates, this powerful protocol has found applications in complex syntheses, such as that of (±)-ishwarane reported by Cory and McLaren.¹⁴



Scheme 4: Synthesis of cyclopropanes with free carbenes and metal-carbenes. Top: Addition of dichlorocarbene to cyclohexene reported in 1954.¹³ Bottom: General reaction scheme for the transition-metal catalyzed cyclopropanation of olefins using diazocompounds.^{1a}

More selective reactions can be achieved by the use of metal-carbene complexes (or metal carbenoids).¹⁵ These powerful species are most commonly obtained by the catalytic reaction of metal salts with diazocompounds, a reaction known since the beginning of the 20th century¹⁶ and further discussed in the next section. Once generated, these metal-bonded reagents can efficiently transfer in a stereospecific manner the carbene fragment onto an olefin substrate (**Scheme 4**, bottom). It is especially relevant in the context of this thesis to note that: 1) *diazocompounds lacking stabilization from an electron-withdrawing group or bearing a leaving group are highly unstable and therefore rarely employed in this transformation (see Chapter 2)*; 2) *slow addition or large excess of one of the reaction partners needs to be used to avoid dimerization of the diazoreagent (see Chapter 3)*; 3) *C–H insertion can outcompete cyclopropanation in specific cases*.^{8c, 17} Despite these limitations, this method is widely popular for the inter- and intramolecular synthesis of cyclopropanes.

1.2 Carbenes and metal-carbene complexes

Ever since their first observation more than 160 years ago, carbenes have attracted the attention of chemists for their unique structure and reactivity.^{15a} These compounds possess a neutral divalent carbon atom with two unshared valence electrons, and can be divided in two classes with distinct reactivities, *singlet* and *triplet carbenes*, depending on their electronic configuration (**Figure 5**).

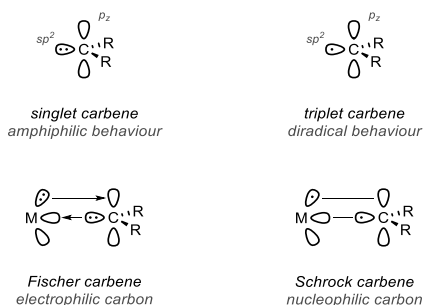


Figure 5: Two classes of carbenes and their related metal-carbene classes.

With a few important exceptions, carbenes are rarely stable in their free state and are often transient intermediates in chemical reactions. Notably, methyldene –the simplest carbene– is a highly reactive, short-lived intermediate that is often generated *in situ* from diazomethane or other precursors due to its instability. Despite the potential usefulness of functionalized methyldene derivatives, the presence of heteroatoms and other functional groups on this species greatly increases its instability and limits their synthetic utility.¹⁸ Particularly, boro-,^{18c} hydroxy-,^{18b} and aminomethyldenes^{18f} are too unstable to engage productively in carbene-transfer reactions, due to their known rapid oligomerization or decomposition *via* tunneling-enhanced hydrogen shift at extremely low temperatures.

One way to stabilize free carbenes and control their reactivity is by bonding with a metal center. The main types of coordinated carbenes are called *Fischer* and *Schrock carbenes*, named after their discoverers (**Figure 5**).^{15a, 19} Fischer-type carbenes are the result of a combination of late transition, low oxidation state metals (typically Cr⁰, W⁰, Mo⁰ or Fe⁰) with π -acceptor ligands and π -donor substituents on the carbene carbon, most commonly aromatic rings, alkoxy- or amino groups. Owing to the predominance of the C→M donation, the carbon center is electrophilic in nature. On the other hand, high oxidation state, early transition metals (Ti^{IV} or Ta^V among the most prominent examples) with strongly donating ligands are found in Schrock carbenes. These carbenes, which often have alkyl substituents on the carbon atom, behave as nucleophiles. Other types of metal-carbenes have properties that are in between these two extreme categories, and have demonstrated over the years to be most relevant for carbene-transfer catalysis.

1.2.1 Rhodium-carbenes

The metal-catalyzed extrusion of nitrogen from diazocompounds is one of the most efficient ways of generating carbenes. Dirhodium tetracarboxylates have been found to act as highly efficient catalysts for this reaction, opening the field to a variety of stereoselective transformations, including cyclopropanation, C–H insertion and ylide chemistry.^{15b} Rhodium-carbenes are highly electrophilic reactive intermediates that can be classified in three categories, based on their substitution pattern (**Figure 6**).

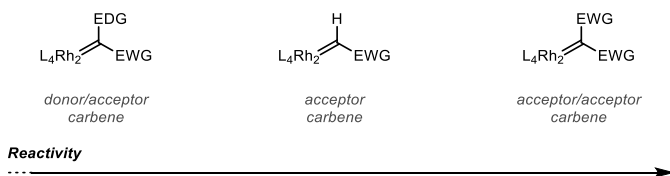


Figure 6: Categories of rhodium carbenes.

Most of the advances in the field of rhodium-carbene chemistry involves donor/acceptor ligands, due to the stability of their precursors and their easier to tame reactivity. The presence of both an electron-withdrawing group and an electron-donating group enables a number of highly selective intermolecular transformations that are not possible with other rhodium-carbenes. An intermediate reactivity is observed when using acceptor carbenes, whereas the presence of two electron-withdrawing groups imparts an extreme electrophilicity to acceptor/acceptor carbenes.^{15b} Because of the high stabilization of a negative charge on the carbene carbon offered by the presence of two electron-withdrawing groups, acceptor/acceptor carbenes are more prone to react via ylide intermediates compared to members of other categories.^{15b}

An important factor in the advance of this field was the development of highly selective chiral dirhodium catalysts. Most notably, chiral carboxylate (*ex.* DOSP, PTTL, TCP) and carboxamidate (*ex.* MEPY, MEOX) ligands (**Figure 7**) displayed high levels of enantioselectivity in cyclopropanation and C–H insertion reactions, due to the highly symmetrical three-dimensional arrangement of their rhodium complexes.²⁰

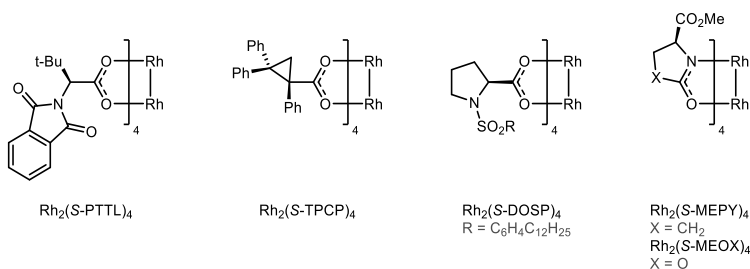


Figure 7: Some highly selective chiral rhodium complexes.

1.2.2 Ruthenium carbenes

Differently from other metal carbenes, ruthenium carbenes display a high selectivity towards C–C unsaturations and therefore a high tolerance to most organic functional groups. This affinity for carbon-carbon double bonds over other Lewis-basic functionalities is at the basis of the metathesis reaction, awarded with the Nobel prize in 2005.^{15b} Ruthenium complexes have also been employed in recent times for carbene-transfer reactions, in particular cyclopropanation reactions.²¹ Compared to

rhodium-carbenoids, ruthenium carbenes display significantly lower electrophilicity which enables selective mild carbene transfer to nucleophilic olefin substrates. On the other hand, choice of a proper ligand can affect the properties of these carbene intermediates to a considerable extent. Ruthenium complexes with porphyrins,²² pyridinebis(oxazoline)²³ and phenyloxazoline²⁴ ligands (**Figure 8**) possess remarkable activity in cyclopropanation reactions of activated olefins, and it is possible to tune the coordination environment to achieve high stereoselectivity.

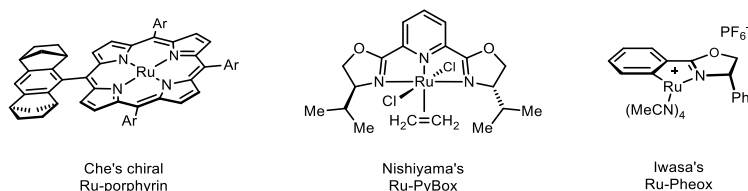
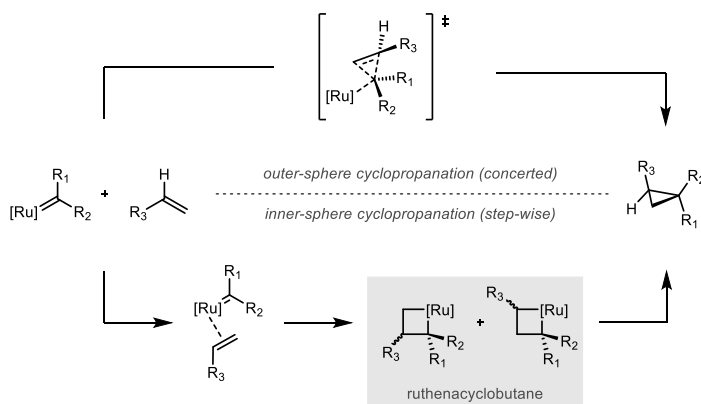


Figure 8: Examples of chiral ruthenium catalysts.²²⁻²⁵

Due to the electronic nature of ruthenium complexes, the mechanism for the carbene transfer reaction (shown in the context of cyclopropanation in **Scheme 5**) is not fully understood.²⁶ The reaction between the electrophilic ruthenium-carbene and the nucleophilic olefin could either take place through a concerted mechanism (**Scheme 5, top**) or through an associative mechanism, with the intermediacy of a ruthenacyclobutane reminiscent of the metathesis mechanism (**Scheme 5, bottom**). The latter intermediate can collapse to give the cyclopropane product, or alternatively give homologation or metathesis products.

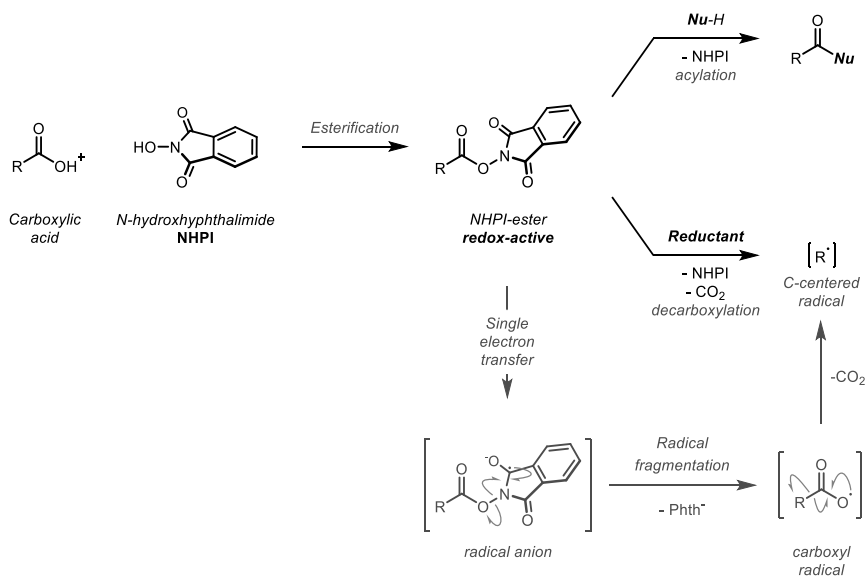


Scheme 5: Proposed mechanisms for the ruthenium-catalyzed cyclopropanation reaction.

1.3 Redox-active esters

1.3.1 History and development of redox-active NHPI esters

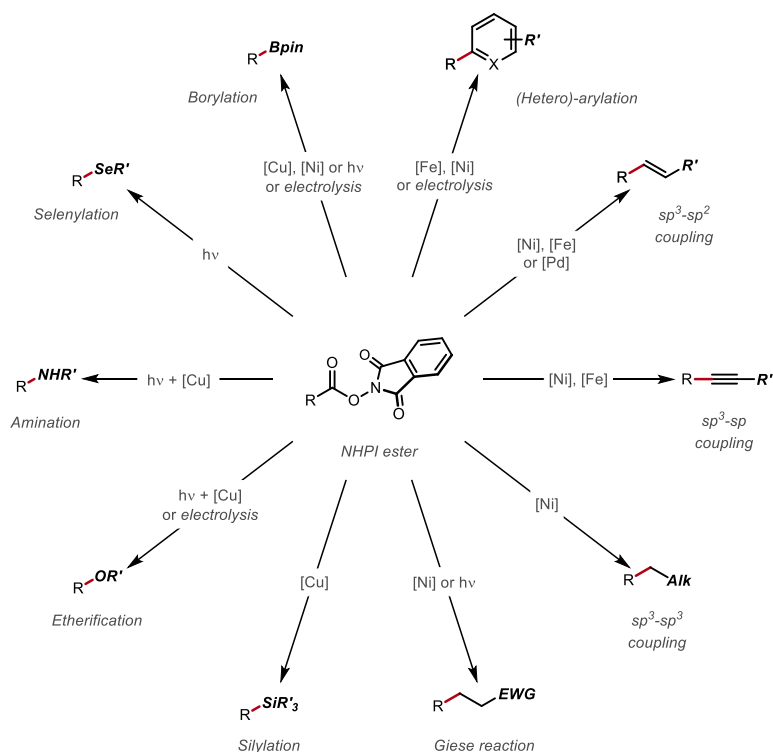
The use of activated esters has played a central role in chemical biology and medicinal chemistry, especially in peptide synthesis.²⁷ In this context, *N*-hydroxyphthalimidoyl (NHPI) esters were first reported by Nefken and Tesser in 1961 as efficient peptide coupling agents.²⁸ Among the advantages of this acyl donor, the authors cited the quick reaction times, high yields, ease of crystallization of the activated amino acids, and the convenient removal of NHPI by means of mildly basic extraction. The radical reductive decarboxylation of these esters under light irradiation was later demonstrated for the first time by Okada and co-workers in 1988.²⁹ This transformation was classically accomplished using Barton esters,³⁰ peracid derivatives,³¹ or conversion to haloalkanes followed by dehalogenation.³² In his work, Okada suggested that the radical decarboxylation of these redox-active esters occurs *via* single-electron transfer (SET) to the electron-poor phthalimide moiety (**Scheme 6**). The resulting radical anion would then fragment to generate phthalimide anion and a carboxyl radical, which in turn extrudes carbon dioxide to yield a carbon-centered radical.



Scheme 6: Synthesis and reactivity of NHPI esters as acyl donors and radical precursors.²⁸⁻²⁹

1.3.2 Redox-active esters in decarboxylative reactions

The abundance of carboxylic acids renders NHPI esters useful precursors of C(sp³) radicals, whose versatility and synthetic value is well established in organic synthesis. After Okada's seminal works,^{29, 33} redox-active esters found several applications in radical cross-coupling reactions capable of addressing the limitations of more traditional processes catalyzed by transition-metals. In particular, redox-active esters proved to be exceptional sources of alkyl (or less often, aryl) radicals that readily undergo reductive cross-coupling transformation, including challenging C–C or C–X bond-forming reactions (X = O, N, B, etc.).³⁴ A selection of these processes, some relevant for this thesis, are shown in **Scheme 7**. It is worth to mention that cyclopropane substrates have been successfully used in only a fraction of these reports, requiring almost always the stabilization of an *ipso*-aryl substituent on the cyclopropyl ring. The scarcity of use of cyclopropyl NHPI-esters in the literature clearly shows the challenge of taming cyclopropyl radicals (see **Section 1.1**) and efficiently employing these reactive intermediates in important radical coupling reactions.



Scheme 7: Selected applications of redox-active esters in radical cross-couplings.³⁴

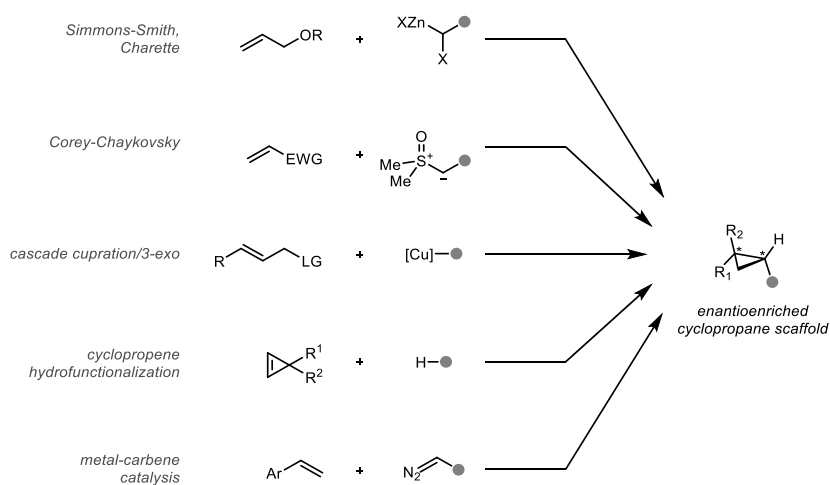
1.4 Objectives and aims

Despite the importance of functionalized cyclopropanes in various fields, state-of-the-art asymmetric syntheses of these compounds are limited by specific substrates, custom methods, and unstable precursors. The work presented in this thesis aims at addressing the current limitations by developing a unified asymmetric approach towards diverse cyclopropane products utilizing a stable carbene precursor with a geminal radical functionalization handle. In particular, Chapter 2 presents the enantioselective cyclopropanation of olefins using a novel redox-active diazocompound reagent. The focus of this work is set in the preparation of useful chiral building blocks and biologically important scaffolds from abundant materials over two steps. The work presented in Chapter 3 aims at unraveling the origin of the performance of the transition metal-catalyzed cyclopropanation of challenging aliphatic olefins described in Chapter 2, through a joint experimental and computational study. The goal of Chapter 4 is the highly stereoselective synthesis of medicinally relevant *cis*-aryl cyclopropanes. This is enabled by a novel photo-decarboxylation reaction, whose mechanism is studied in detail. Finally, Chapter 5 reports a robust photo-organocatalytic protocol to obtain versatile cyclopropylboronates with a superior degree of stereoselectivity from the chiral intermediates described in Chapter 2.

2. General Asymmetric Synthesis of Cyclopropanes with a Single Redox-Active Diazocompound Reagent (NHPI-DA) (Paper I)

2.1 Introduction: Asymmetric syntheses of cyclopropanes

Cyclopropanes are interesting molecules (see **Section 1.1**) that attracted the attention of organic chemistry since the identification of this motif within the structure of the natural product (+)-*trans*-chrysanthemic acid in 1924.³⁵ Because of this interest, different syntheses of enantiomerically enriched cyclopropanes have been developed.³⁶ Among these, the most versatile are shown in **Scheme 8**. First, the asymmetric Simmons-Smith-type (**Section 1.1.1**) cyclopropanation of allylic alcohols or ethers, developed by Charetté and co-workers, represents an efficient way to access highly substituted cyclopropanes using chiral dioxaborolane or phosphoric acid ligands to induce enantioselectivity.³⁷ Three major contributions by MacMillan and Feringa were reported exploiting 3-*exo*-cyclizations (**Section 1.1.1**). The first employs chiral organocatalysts to generate the desired products through Corey-Chaykovsky reaction on iminium ions,³⁸ while the second one generates the carbanion intermediate by asymmetric cupration of allylic electrophiles.³⁹ The last two methods shown in **Scheme 8** are the enantioselective hydrofunctionalization of cyclopropenes, mainly developed by the groups of Marek⁴⁰ and Gevorgyan,⁴¹ and metal-carbene catalysis employing chiral transition metal complexes (**Section 1.1.1** and **1.2**).⁴² Despite their efficiency, these state-of-the-art methodologies towards functionalized cyclopropanes rely on custom reagents and substrate-specific strategies.^{37-39, 40d, 41b, 43} A desirable alternative would be a unified strategy towards cyclopropanes with distinct functionalities.



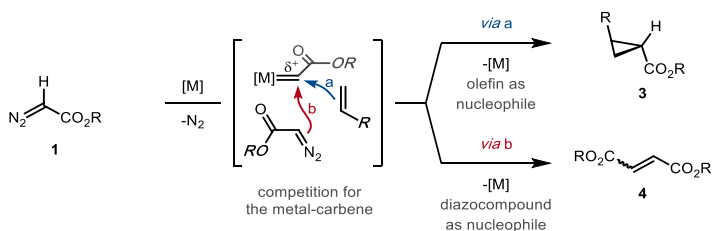
Scheme 8: State-of-the-art methods to access enantioenriched cyclopropanes.

The enantioselective cyclopropanation of olefins with diazocompounds is the route that offers the most general and attractive retrosynthetic disconnection, given the abundance of alkene materials and intermediates. However, this method suffers from severe limitations when it comes to aliphatic olefins, which are poorly reactive due to their lower nucleophilicity and are more challenging for diastereo- and enantioselectivity due to the flexibility and weak dispersive interactions of alkyl substituents.⁴⁴

The nucleophilicity of organic compounds can be described by Mayr's N parameter,⁴⁵ derived from the equation:

$$\log(k) = s_N(N + E) \quad (1)$$

In eq. 1, k is the reaction rate constant, s_N the nucleophile-specific sensitivity parameter, and N and E the nucleophilicity and electrophilicity parameters respectively (for details, see **Section 3.3.1**). The value of the parameter N can be used to rationalize the poor reactivity of non-nucleophilic alkenes, such as aliphatic ones, in cyclopropanation reactions (**Scheme 9**). Olefins **2** with a high N -value (*i.e.* styrenes, enol ethers, etc.), correlate to high nucleophilicity, can compete with diazocompounds **1** ($4 < N < 10$) for the electrophilic metal-carbene intermediate resulting in efficient cyclopropanation catalysis. Instead, olefins with low nucleophilicity ($N \leq 2$ for aliphatic olefins) lead to a decreased yield of the desired product **3** in favor of the dimer side-product **4**.



Scheme 9: Metal-catalyzed cyclopropanation: Cyclopropanation (pathway a) and the diazocompound dimerization side-reaction (pathway b).

To overcome the challenge posed by aliphatic substrates, some elegant strategies have recently been reported employing bulky cobalt-porphyrin or iridium-salen complexes,^{42e, 42f, 42k} or artificial enzymes (**Figure 9**).^{42i, 42j, 42l} These methods displayed high efficiency with unactivated substrates, generating the desired cyclopropane products in yields and enantioselectivities unachievable by other commonly used catalysts. However, such systems require expensive ligands and/or transition-metals,^{42e, 42f, 42k} or specific engineering of naturally occurring proteins^{42h-j, 42l} using technologies generally not available to the average synthetic chemist. Despite these advances in the field, a simple and general system for the asymmetric cyclopropanation of aliphatic olefins is still unachieved.

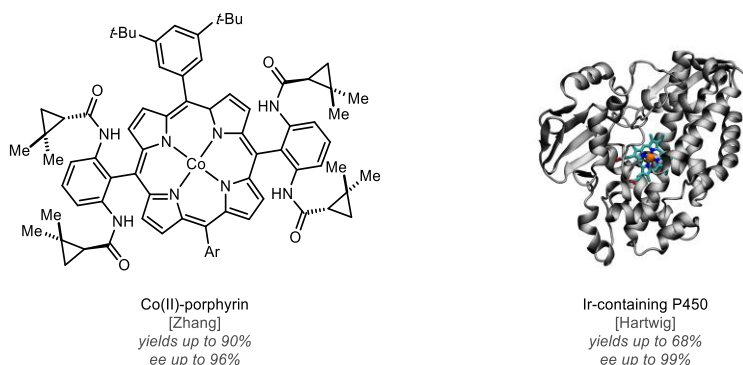


Figure 9: Selected efficient catalysts for the cyclopropanation of aliphatic olefins.^{42f, 42j, 42k}

Notably, functionalized carbenes that would lead to important cyclopropane scaffolds, such as alkyl-, hydroxy-, amino-, boryl-, selenyl-, heteroaryl- or alkenyl-methylidenes among others, are not stable enough to be used effectively in cyclopropanation reactions.¹⁸ Consequently, a simple and straightforward synthesis of functionalized cyclopropanes is yet to be achieved. Moreover, only a few leaving group-functionalized diazocompounds are present in the literature (**Figure 10**), and are reported to be poorly reactive in cyclopropanation reactions. Also, the studies on these carbene precursors have evidenced their tendency to undergo substitution prior to carbene transfer reaction.⁴⁶ Importantly, none of these compounds (or alternative leaving group-functionalized carbenes) have been used in asymmetric catalysis.

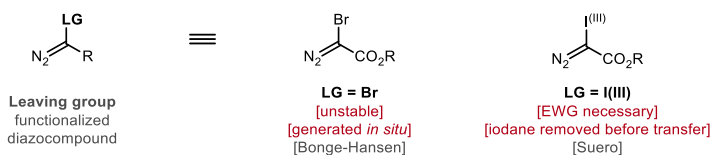
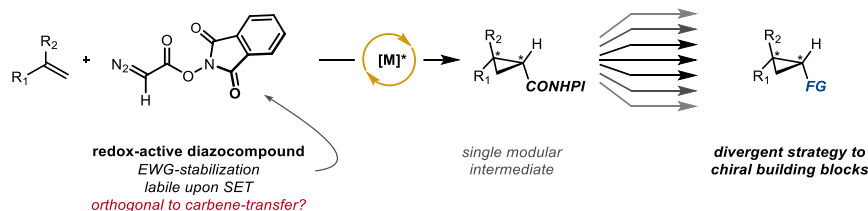


Figure 10: Reported leaving group-functionalized diazocompound.^{46a, 46b}

2.2 Aim of the project

We envisioned the asymmetric formal transfer of the aforementioned unstable methylidenes through the use of a novel diazocompound, decorated with a versatile leaving group that would allow for late-stage diversification of the resulting cyclopropane intermediates. The strategy presented herein would enable a unified synthesis of enantioenriched functionalized cyclopropanes from feedstock unfunctionalized olefins. To achieve this result, a diazocompound bearing an appropriate leaving-group was required. We hypothesized the use of *N*-hydroxyphthalimide ester (NHPI) as the leaving-group, owing to its versatility as acyl donor²⁸ and carbon-centered radical precursor^{33a, 34a-c, 34e-k, 34m-o, 34q} (**Scheme 10**). A reasonable concern in our approach was the orthogonality between the diazo moiety

and NHPI ester moieties, considering the lability of the latter in the presence of several transition metals, visible light or electron-rich organic molecules.

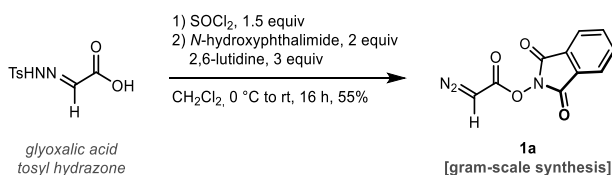


Scheme 10: Unified approach towards functionalized enantioenriched cyclopropanes.

2.3 Results and discussion

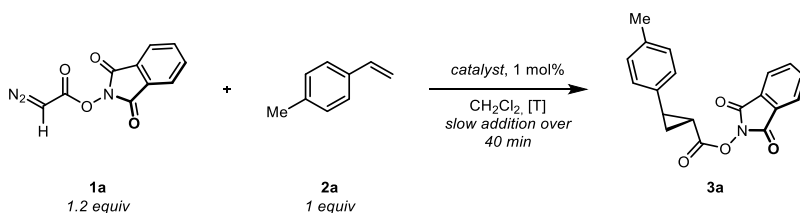
2.3.1 Reagent synthesis and reaction optimization

The first step towards the formal transfer of functionalized carbenes was the synthesis of the *N*-hydroxyphthalimidoyl diazoacetate (NHPI-DA) reagent **1a**. This compound had never been used in carbene transfer reactions.⁴⁷ Starting from cheap glyoxylic acid monohydrate, a gram-scale synthesis of **1a** was optimized to give the desired reagent in moderate yield as a crystalline, bench-stable solid that does not require solution storage unlike other diazoacetate reagents, allowing for easy handling (**Scheme 11**). Differential scanning calorimetry studies also showed that, compared to the benchmark ethyl diazoacetate, NHPI-DA is a more stable (safer) carbene precursor.⁴⁸

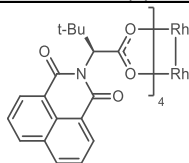


Scheme 11: Synthesis of NHPI-DA **1a**. Reaction conditions: SOCl₂ (1.5 equiv), glyoxylic acid tosyl hydrazone (1 equiv), dry CH₂Cl₂, rt, 16 h, then *N*-hydroxyphthalimide (2 equiv), 2,6-lutidine (3 equiv), dry CH₂Cl₂, rt, 4 h.

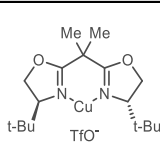
We tested the performance of **1a** in a model cyclopropanation reaction using styrene **2a** (**Table 1**). To minimize the dimerization side reaction, the carbene precursor was added over the course of 40 minutes to a solution of the olefin and catalyst. Extensive screening indicated that common rhodium, copper and palladium catalysts were ineffective and poorly selective in the cyclopropanation with NHPI-DA (**1a**) (**Table 1**, entries 1-3). A clear improvement in terms of diastereoselectivity was observed when using Nishiyama's ruthenium Pybox catalyst^{23b}, albeit in moderate yield and enantioselectivity (**Table 1**, entry 4). In contrast with these results, the electron-rich ruthenium catalyst (*S*)-RuPheox developed by the group of Iwasa²⁴⁻²⁵ was found to be highly efficient in this transformation (**Table 1**, entries 5,6).



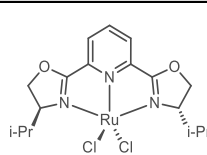
Entry	Catalyst	T (°C)	3a (%)	d.r. (<i>trans</i> : <i>cis</i>)	<i>ee</i> _{<i>trans</i>} (%)
1	Pd(OAc) ₂	rt	69	4.5:1	-
2	Rh ₂ (<i>S</i> -NTTL) ₄	rt	82	1:1	19
3	(<i>S</i>)-Cu-Box	rt	49	4:1	88
4	(<i>S</i>)-RuCl ₂ -PyBox	rt	63	20:1	80
5	(<i>S</i>)-RuPheox	rt	92	> 20:1	94
6	(<i>S</i>)-RuPheox	0	98	> 20:1	94



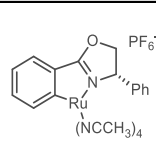
Rh₂(*S*-NTTL)₄



(*S*)-Cu-Box



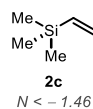
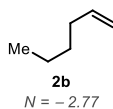
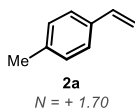
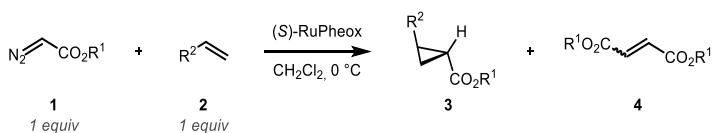
(*S*)-RuCl₂-PyBox



(*S*)-Ru-Pheox

Table 1: Summary of the optimization for the cyclopropanation of **2a** reaction employing **1a**. Reactions were performed at 0 °C under inert atmosphere, by adding a 0.2 M solution **1a** in dry CH₂Cl₂ to a solution of the indicated olefin and (*S*)-RuPheox in dry CH₂Cl₂ over 40 minutes (final concentration: 0.1 M). Yields and diastereomeric ratio determined by ¹H NMR using 1,1,2,2-tetrachlorethane as an internal standard. Enantiomeric ratio determined by chiral HPLC.

To further study the properties of NHPI-DA (**1a**) as a carbene-transfer reagent, we compared the performance of different diazo compounds with distinct properties. In these experiments, the diazo compound was treated with an equimolar amount of one of three model olefins (**2a-c**) in the presence of the catalyst (*S*)-RuPheox (**Table 2**). The diazoesters employed in this study were selected based on their ester residues, ranging from aliphatic (**1b-d**), to bulky aromatic (**1e**) and electron-poor esters (**1f,g**). To eliminate substrate-specific effects that would prevent a direct comparison, the diazo compounds were added to the reaction mixture in one portion. The olefin substrates were selected on the basis of their distinct nucleophilicity, tabulated by Mayr and co-workers using the *N* parameter.⁴⁵ The test showed that **1a** outperforms the other diazo reagents **1b-g** independently of the nature of the alkene substrate. These results could be due to the strong electron-withdrawing nature of the NHPI ester, which would decrease the nucleophilicity of compound **1a** and disfavor the formation of the dimer side-product (**4a-c**). This effect is studied in detail in **Chapter 3** of this thesis.

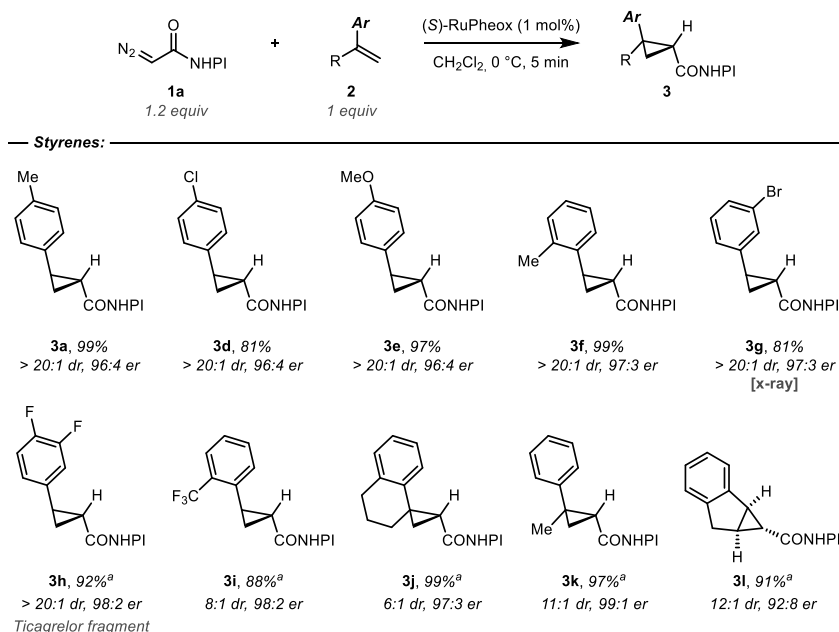


Entry	Diazoester	R ¹ =	3a (%)	4 (%)	3b (%)	4 (%)	3c (%)	4 (%)
1	1b	<i>t</i> -Bu	26	68	5	89	< 5	90
2	1c	Et	36	61	8	87	< 5	98
3	1d	Bn	48	53	7	84	< 5	92
4	1e	BHT	61	10	< 10	10	< 5	9
5	1f	TFE	66	30	23	72	7	86
6	1g	TCE	78	17	26	69	9	82
7	1a	NHPI	99	< 5	72	22	41	> 22

Table 2: Performance comparison of various diazo compounds **1a-g**. Reactions were performed at 0 °C under inert atmosphere, by adding in one portion a 0.2 M solution of the indicated diazoester in dry CH₂Cl₂ to a solution of the indicated olefin and (*S*)-RuPheox (1 mol%) in dry CH₂Cl₂ (final concentration: 0.1 M). Yields determined by ¹H NMR using 1,1,2,2-tetrachlorethane as an internal standard.

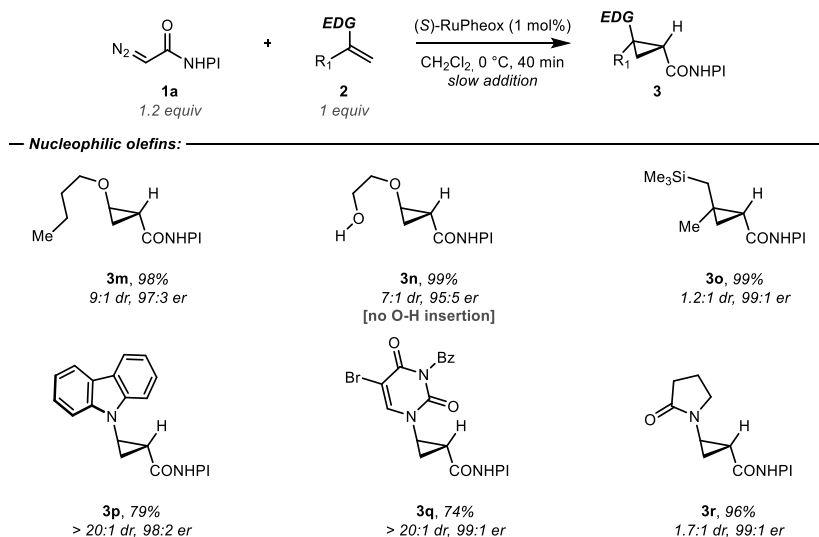
2.3.2 Substrate scope

With the optimized conditions in hand, we set out to explore the scope of the cyclopropanation reaction. Styrenes are known to be efficient partners for carbene transfer reactions, and indeed a variety of styrene substrates with various steric and electronic properties gave very good results in terms of yield and selectivity (**Scheme 12**). Unlike other reported cyclopropanations (see **Section 1.1.1**), optimal performance without slow addition was observed in several cases (**3a,d-g**). This way, we could derivatize electron-rich (**3e**) and electron-poor styrenes (**3d,g-i**) with excellent results. Also, 1,1-disubstituted substrates could be employed (**3j,k**), as well as the 1,2-disubstituted cyclic indene (**3l**).



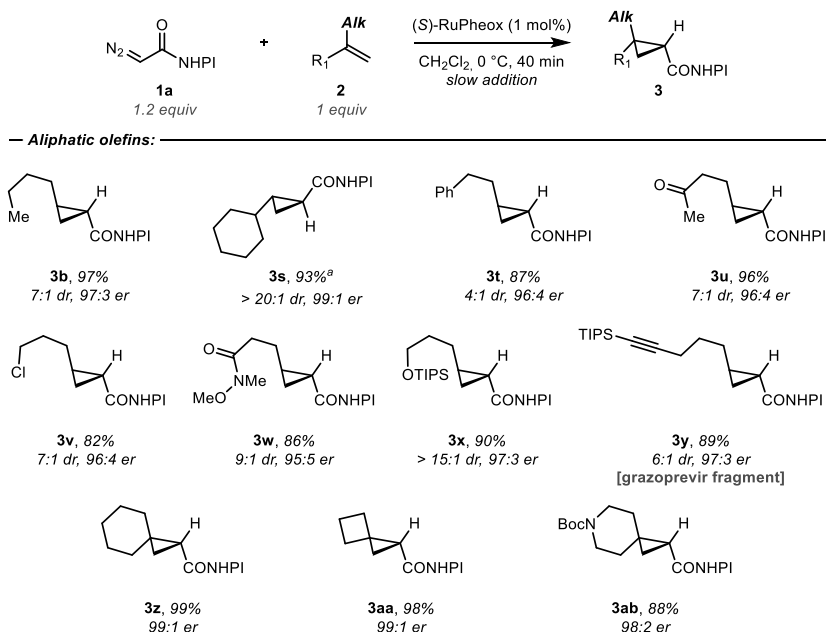
Scheme 12: Scope of the cyclopropanation of styrenes with **1a**. Reactions were performed at 0 °C under inert atmosphere, by adding in one portion a 0.2 M solution of **1a** (1.2 equiv) in dry CH₂Cl₂ to a solution of the indicated olefin **2** (1 equiv) and (*S*)-RuPheox (1 mol%) in dry CH₂Cl₂ (final concentration: 0.1 M). Reported yields are isolated. Diastereomeric ratio determined by ¹H NMR of the crude mixture. Enantiomeric ratio determined by chiral HPLC.
^a: **1a** was slowly added over 40 min to the reaction mixture.

Different nucleophilic olefins such as enol ethers (**3m,n**), allyl silanes (**3o**), enamines (**3p**) or enamides (**3q,r**) were also used for this transformation, yielding a variety of highly enriched donor-acceptor cyclopropane products, including the nucleoside analog **3q** (Scheme 13). It is worth to note that no O–H insertion was observed during the synthesis of **3n**. Different stereoelectronics features in the olefin substrates normally require tuning of both the diazocompound and the transition-metal complex (see Section 2.1). In this context, it is surprising the large structural diversity that can be accommodated next to the reactive olefin, without adjusting the carbene precursor nor the chiral catalyst.



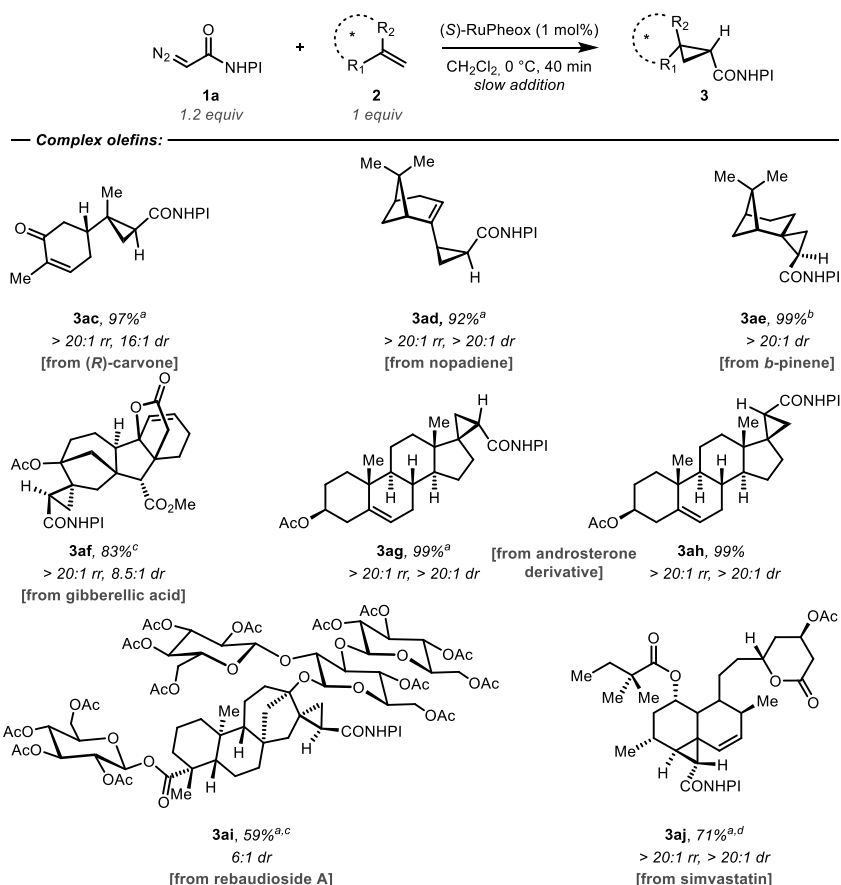
Scheme 13: Scope of the cyclopropanation of nucleophilic olefins with **1a**. Reactions were performed at 0 °C under inert atmosphere, by adding a 0.2 M solution of **1a** (1.2 equiv) in dry CH₂Cl₂ to a solution of the indicated olefin **2** (1 equiv) and (*S*)-RuPheox (1 mol%) in dry CH₂Cl₂ over the course of 40 min (final concentration: 0.1 M). Reported yields are isolated. Diastereomeric ratio determined by ¹H NMR of the crude mixture. Enantiomeric ratio determined by chiral HPLC.

As mentioned before, aliphatic olefins have been reported to be poor substrates for the asymmetric cyclopropanation reaction and highly desired given their abundance in raw materials and synthetic intermediates. In stark contrast with the literature, our system proved to be general and highly efficient for a wide range of unactivated aliphatic alkenes (**Scheme 14**). Several functional groups were tolerated, including Lewis basic ketone and Weinreb amides (**3u,w**), usually prone to carbonyl ylide side-reactions, as well as chloride (**3v**), protected alcohol (**3x**), and carbazole substituent (**3p**). No cyclopropene by-product was detected from alkyne (**3y**). When using methylene cycloalkanes, enantiopure spiro(hetero)cycles were obtained in excellent yields (**3z-ab**), showing that both linear and branched substrates can efficiently take part in this transformation.



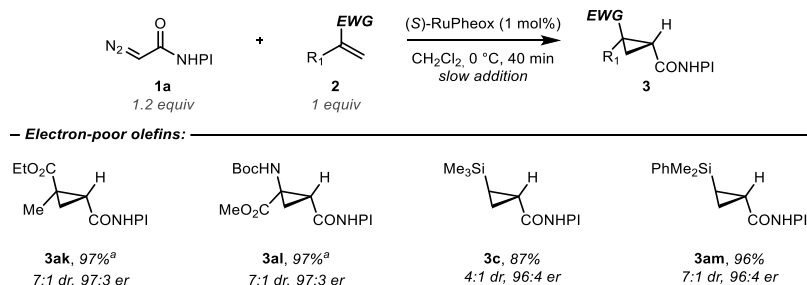
Scheme 14: Scope of the cyclopropanation of aliphatic olefins with **1a**. Reactions were performed at 0 °C under inert atmosphere, by adding a 0.2 M solution of **1a** (1.2 equiv) in dry CH₂Cl₂ to a solution of the indicated olefin **2** (1 equiv) and (S)-RuPheox (1 mol%) in dry CH₂Cl₂ over the course of 40 min (final concentration: 0.1 M). Reported yields are isolated. Diastereomeric ratio determined by ¹H NMR of the crude mixture. Enantiomeric ratio determined by chiral HPLC. ^a: (R)-catalyst was used.

The surprising performance of this system in aliphatic olefins opened new possibilities to explore their reactivity in more complex settings. We employed natural aliphatic olefins as models for functionally-, structurally- and stereochemically-complex substrates for the cyclopropanation reaction (**Scheme 15**). The combination of NHPI-DA with the metallacyclic RuPheox catalyst was able to discriminate olefins based on their nucleophilicity, leading to the selective modification of carvone (**3ac**), nopadiene (**3ad**), gibberellic acid (**3af**), as well as an acetylated androsterone derivative (**3ag,3ah**) and the cholesterol-regulating drug simvastatin (**3aj**). Additionally, highly congested olefins such as β -pinene (**3ae**) and rebaudioside A (**3ai**) could also be cyclopropanated effectively using our methodology. Again, complete tolerance of ketone (**3ac**) and ester moieties (**3af-aj**) was observed, as well as complete regioselectivity with 1,3-dienes (**3ad,aj**) or other cyclic internal olefins (**3ac,af-ah**). Notably, complete facial selectivity was achieved on the steroid substrate by simply switching to a different enantiomer of the catalyst (**3ag,ah**).



Scheme 15: Scope of the cyclopropanation of complex olefins with **1a**. Reactions were performed at 0 °C under inert atmosphere, by adding a 0.2 M solution of **1a** (1.2 equiv) in dry CH₂Cl₂ to a solution of the indicated olefin **2** (1 equiv) and (*S*)-RuPheox (1 mol%) in dry CH₂Cl₂ over the course of 40 min (final concentration: 0.1 M). Reported yields are isolated. Diastereomeric ratio determined by ¹H NMR of the crude mixture. Enantiomeric ratio determined by chiral HPLC. ^a: (*R*)-catalyst was used. ^b: **1a** added over 6 h, catalyst (2 mol%). ^c: **1a** (3 equiv) added over 16 h, catalyst (3 mol%), rt. ^d: **1a** (3 equiv) added over 24 h, catalyst (5 mol%), rt.

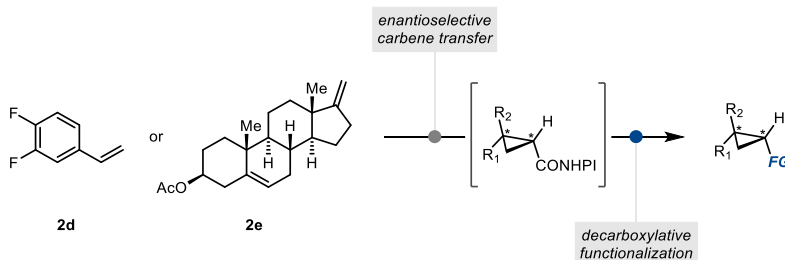
For completion, we explored electron-deficient olefins such as acrylates derivatives (**3ak,al**) and bulky vinylsilanes (**3ac,am**; $-0.26 < N < 1.03^{45}$). Although reported as poorly nucleophilic olefins, these substrates readily underwent carbene transfer, affording interesting substrates such as the cyclopropyl amino acid **3al** in good yields (**Scheme 16**), without detecting N–H insertion by-products.



Scheme 16: Scope of the cyclopropanation of electron-poor olefins with **1a**. Reactions were performed at 0 °C under inert atmosphere, by adding a 0.2 M solution of **1a** (1.2 equiv) in dry CH₂Cl₂ to a solution of the indicated olefin **2** (1 equiv) and (*S*)-RuPheox (1 mol%) in dry CH₂Cl₂ over the course of 40 min (final concentration: 0.1 M). Reported yields are isolated. Diastereomeric ratio determined by ¹H NMR of the crude mixture. Enantiomeric ratio determined by chiral HPLC. ^a: **1a** added over 6 h, catalyst (2 mol%).

2.3.3 Stereoselective diversification of the chiral redox-active cyclopropane intermediates

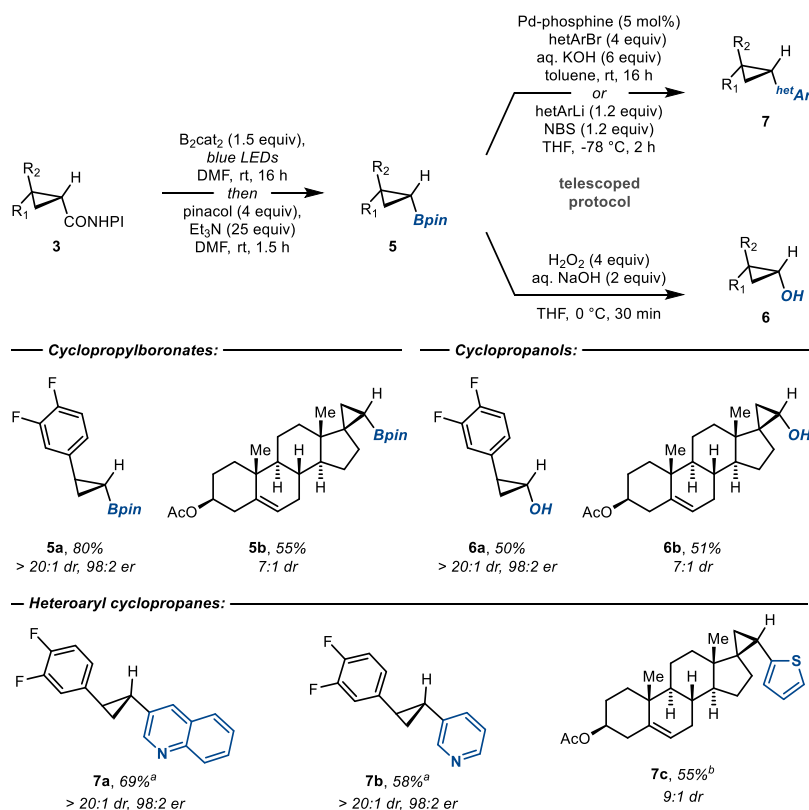
The late-stage diversification of the cyclopropyl NHPI esters is key to use these intermediates as general precursors in a unified synthesis of functionalized cyclopropanes. Having established the scope of our methodology, we selected two representative olefins from the aromatic and aliphatic series (**2d,e**) to explore this concept (**Scheme 17**).



Scheme 17: Divergent approach for the synthesis of enantioenriched functionalized cyclopropanes.

Following a variation of Aggarwal's decarboxylative borylation,^{34g} the two-step enantioselective synthesis of cyclopropylboronates was achieved, obtaining **5a,b** in good yield and selectivity (**Scheme 18**). This procedure employs readily available olefin starting materials, and is a valid alternative to the asymmetric hydroboration of cyclopropenes^{41b} or the borocyclopropanation of allylic ethers.^{18c} The resulting cyclopropylboronates were converted through a telescoped borylation/stereoretentive oxidation using hydrogen peroxide to cyclopropanols **6a,b** (**Scheme 18**). Overall, this strategy allows the synthesis of chiral cyclopropanols that are still challenging with alternative methods like the Kulinkovich reaction, which is a powerful method to

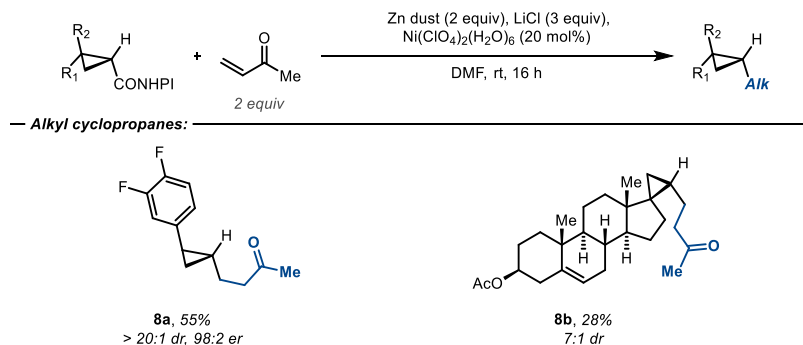
generate cyclopropanols from alkenes and esters.⁴⁹ Despite several advances in the field, an asymmetric version to obtain enantiopure products is yet to be achieved. Alternatively, heteroaryl substituents could be installed via palladium-catalyzed cross-coupling of the intermediate cyclopropylboronates, affording products **7a-c**. This route represents a surrogate to the use of problematic heteroaryl methylidenes (Scheme 18). On the other hand, direct decarboxylative arylation of the cyclopropyl redox-active esters **3** was unsuccessful, probably due to the challenging reactivity of cyclopropyl radical intermediates.



Scheme 18: Synthesis of enantioenriched cyclopropylboronates. Reactions were performed under inert atmosphere. Synthesis of borylcyclopropanes **5**: **3** (1 equiv), B₂cat₂ (1.5 equiv) dry DMF (0.1 M), blue LEDs (450 nm), rt, 16 h. Then, pinacol (4 equiv), Et₃N (25 equiv) dry DMF (0.1 M), rt, 1.5 h. Synthesis of cyclopropanols **6**: 30% wt. aq. H₂O₂ (4 equiv), 3 M aq. NaOH (2 equiv), THF, 0 °C, 30 minutes. ^a: Pd(dba)₂ (5 mol%), P(*o*-furyl)₃ (0.1 equiv), ArBr (4 equiv), 3 M aq. KOH (6 equiv), toluene (0.05 M), rt, 16 h. ^b: 2-thienyl-Li (1.2 equiv), *then* NBS (1.2 equiv), dry THF, -78 °C, 2 h. Reported yields are isolated. Diastereomeric ratio determined by ¹H NMR of the crude mixture. Enantiomeric ratio determined by chiral HPLC.

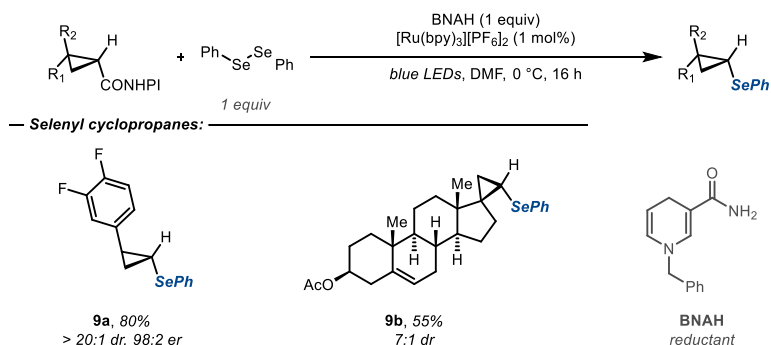
Radical alkylation with Michael acceptors^{34j} led to enantioenriched alkyl-substituted cyclopropanes **8a,b** in moderate yields, avoiding the use of aliphatic diazocompounds and problematic alkylidene intermediates (Scheme 19). This route gives access to

aliphatic cyclopropanes that would require longer routes or flow-technology using state-of-the-art cyclopropanations developed by Charette and co-workers.^{18g, 37}



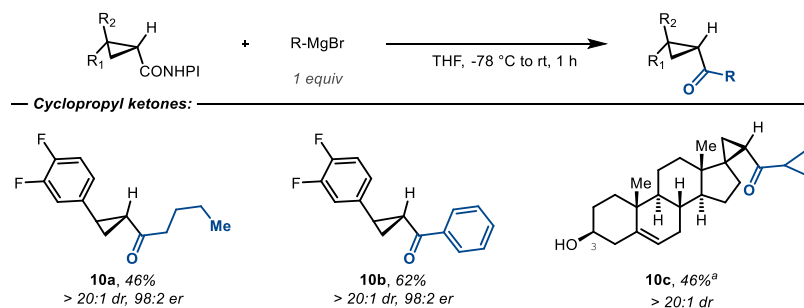
Scheme 19: Synthesis of enantioenriched alkyl cyclopropanes. Reactions were performed under inert atmosphere. **3** (1 equiv), methyl vinyl ketone (2 equiv), Zn dust (2 equiv), LiCl (3 equiv), Ni(ClO₄)₂(H₂O)₆ (20 mol%), dry DMF (0.4 M), rt, 16 h. Reported yields are isolated. Diastereomeric ratio determined by ¹H NMR of the crude mixture. Enantiomeric ratio determined by chiral HPLC.

The single-electron chemistry of NHPI esters could also be exploited to generate selenylcyclopropanes **9a,b**^{34b} circumventing the use of the unavailable selenylmethylidene, representing the first asymmetric synthesis of selenylcyclopropanes to the best of our knowledge (**Scheme 20**).



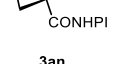
Scheme 20: Synthesis of enantioenriched selenylcyclopropanes. Reactions were performed under inert atmosphere. **3** (1 equiv), PhSeSePh (1 equiv), *N*-benzylidihydronicotinamide (1 equiv), [Ru(bpy)₃][PF₆]₂ (1 mol%), dry DMF (0.03 M), blue LEDs (450 nm), 0 °C, 16 h. Reported yields are isolated. Diastereomeric ratio determined by ¹H NMR of the crude mixture. Enantiomeric ratio determined by chiral HPLC.

As stated before, NHPI esters have the dual advantage of being both radical precursors and acyl donors.^{28, 33a, 34a-c, 34e-g, 34j, 34k, 34m-o} Taking advantage of this feature, we treated **3h** and **3ag** with different Grignard reagents to cleanly afford ketones **10a-c**. In all these reactions, no epimerization was observed despite the strongly basic environment, as shown in **Scheme 21**.



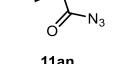
Scheme 21: Synthesis of enantioenriched cyclopropyl ketones. Reactions were performed under inert atmosphere. **3** (1 equiv), $RMgBr$ (1 equiv), dry THF (0.1 M), $-78\text{ }^{\circ}\text{C}$ to rt, 1 h. For **10c**: $[H_2N(OMe)Me]Cl$ (2.1 equiv), $n-BuLi$ (4.1 equiv), *then* $RMgBr$ (4 equiv). $-78\text{ }^{\circ}\text{C}$ to rt, 1 h. Reported yields are isolated. Diastereomeric ratio determined by 1H NMR of the crude mixture. Enantiomeric ratio determined by chiral HPLC. ^a: C-3 acetate cleaved.

Finally, a direct Curtius protocol to achieve cyclopropylamines was developed by our collaborators at AstraZeneca, and is included here for completeness. The optimization of the azide addition is summarized in **Table 3**. As it is shown, extensive experimentation revealed that either increasing the amount of azide source (entry 1) or increasing the temperature (entry 3) was ineffective for this transformation, yielding the desired product in small amounts. It was hypothesized that the reaction was hindered by an unfavorable thermodynamic equilibrium, between the azide/redox-active ester system and the acyl azide/*N*-hydroxyphthalimide anion, effectively regenerating the starting material. To test this hypothesis, TBSCl was used as an additive in the attempt of trapping the NHPI anion (entry 6). As it can be seen from **Table 3**, the approach was successful, yielding the product in 90% yield. A similar experiment employing aqueous HCl gave comparable results (entry 7). We reasoned that the silyl chloride was undergoing hydrolysis under the reaction conditions, generating HCl *in situ* and protonating the leaving group anion.

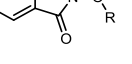


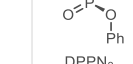
3an

$\xrightarrow[\text{solvent temperature}]{\text{Y-N}_3, \text{ additive}}$



11an



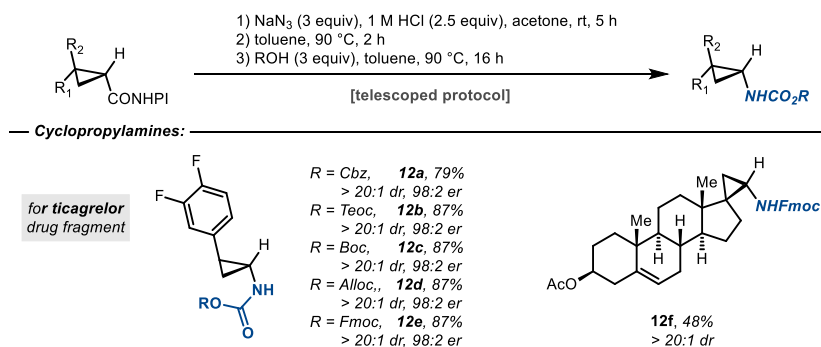


DPPN₃

Entry	Y-N ₃ (equiv)	Additive (equiv)	Solvent	T (°C)	11an (%)	3an (%)	
1	TMSN ₃ (6)	-	EtOAc	rt	36	60	Excess RN ₃ ineffective
2	DPPN ₃ (1.1)	Et ₃ N (2)	PhCH ₃	rt	29	70	
3	DPPN ₃ (1.1)	Et ₃ N (2)	PhCH ₃	60	18	82	Increase temperature ineffective
4	DPPN ₃ (3)	Imidazole (4)	PhCH ₃	rt	50	50	
5	NaN ₃ (3)	-	Acetone/H ₂ O	rt	29	66	Acidic buffer required
6	NaN ₃ (3)	TBSCl (2)	Acetone/H ₂ O	rt	90	8	
7	NaN ₃ (3)	aq. HCl (2.5)	Acetone	rt	91	5	

Table 3: Optimization of the azide addition to the NHPI ester. Yields determined by crude ¹H NMR using 1,3,5-trimethoxybenzene as an internal standard.

With the conditions optimized, the telescoped azide displacement/Curtius rearrangement protocol was performed on substrates **3h** and **3ag** employing different alcohol nucleophiles, yielding several protected cyclopropylamines including the ticagrelor (see **Figure 1**) fragments **12a-e**, as shown in **Scheme 22**.

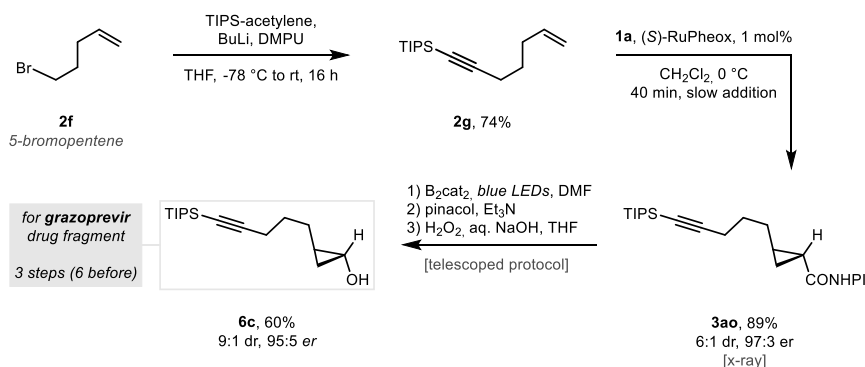


Scheme 22: Synthesis of enantioenriched cyclopropylamines. Step 1: **3** (1 equiv), NaN₃ (3 equiv), 1 M aq. HCl (2.5 equiv), acetone (0.1 M), rt, 5 h. Step 2: dry toluene (0.1 M), 90 °C, 2 hours. Step 3: ROH (3 equiv), dry toluene (0.1 M), 90 °C, 16 h. Reported yields are isolated. Diastereomeric ratio determined by ¹H NMR of the crude mixture. Enantiomeric ratio determined by chiral HPLC.

It is important to note that the synthesis of the cyclopropyl derivatives shown in this chapter did not require an individual synthesis of each carbene precursor, neither a tailored catalytic system for each compound. These results clearly show the potential of redox-active carbene precursor **1a** in the context of a unified synthesis of functionalized cyclopropanes.^{42e, 42l, 50}

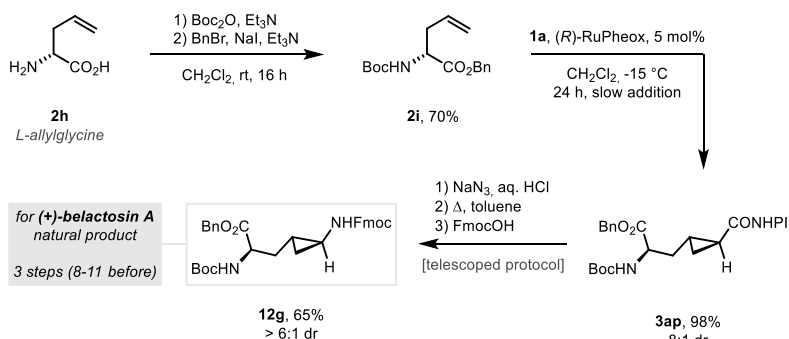
2.3.4 Application in synthesis

To further illustrate the strategic value of the enantioselective cyclopropanations with NHPI-DA, we applied our methodology to the synthesis of two drug fragments (**6c**, **12g**), a chiral building block (**5c**) and a natural product (**13**). As a first example, commercially available 5-bromopentene **2f** was transformed through a three-step process into cyclopropanol **6c**, a fragment of the drug grazoprevir (see **Figure 1**), through a telescoped borylation/oxidation reaction (**Scheme 23**). In contrast, six steps from chiral pool were required in the original synthesis, employing a nucleophilic displacement reaction to generate the cyclopropane ring, Baeyer-Villiger oxidation for the alcohol moiety, and double elimination of a dibromoalkane with a tailored amide base to generate the alkyne moiety.⁵¹



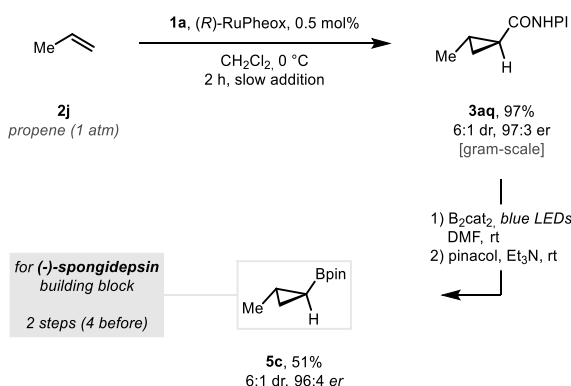
Scheme 23: Synthesis of fragment **6c**. Synthesis of **2g**: Ethynyltriisopropylsilane (1.2 equiv), *n*-BuLi (1.4 equiv), dry THF, -78 °C, 30 min, then DMPU (4 equiv), -78 °C, 15 min, then **2f** (1 equiv), -78 °C to rt, 16 h (74% isolated yield). Synthesis of **3ao**: **1a** (1.2 equiv), (*S*)-RuPheox (1 mol%), dry CH₂Cl₂, 0 °C, slow addition over 40 min (89% isolated yield). Synthesis of **6c**: B₂cat₂ (1.5 equiv), dry DMF, blue LEDs (450 nm), rt, 16 h, then pinacol (4 equiv), Et₃N (25 equiv), rt, 1.5 h. d) 30% aq. H₂O₂ (4 equiv), 3 M NaOH (2 equiv), THF, 0 °C, 30 min (60% isolated yield).

After protection, the amino acid L-allylglycine **2h** was converted to the cyclopropylamine **12g**, fragment of the bioactive natural product (+)-belactosin A (see **Figure 1**),⁵² via the intermediacy of cyclopropyl NHPI ester **3ap**. Again, the synthesis was performed in only three steps (**Scheme 24**) whereas the reported procedures required 8-11 steps from nitromethane and *tert*-butyl 2,3-dibromopropionate, including a non-diastereoselective asymmetric alkylation using a nickel complex as the chiral auxiliary.⁵²⁻⁵³



Scheme 24: Synthesis of fragment **12g**. Synthesis of **2i**: Boc_2O (1.2 equiv), Et_3N (1.2 equiv), dry CH_2Cl_2 , rt, 8 h, *then* NaI (1 equiv), BnBr (2 equiv), Et_3N (2.3 equiv), dry CH_2Cl_2 , rt, 16 h (70% isolated yield). Synthesis of **3ap**: **1a** (3 equiv), (*R*)- RuPheox (5 mol%), dry CH_2Cl_2 , -15°C , slow addition over 24 h (98% isolated yield). Synthesis of **12g**: NaN_3 (3 equiv), 1 M HCl (1.1 equiv), acetone, rt, 16 h, *then* FmocOH (3 equiv), toluene, 90°C , 16 h (65% isolated yield).

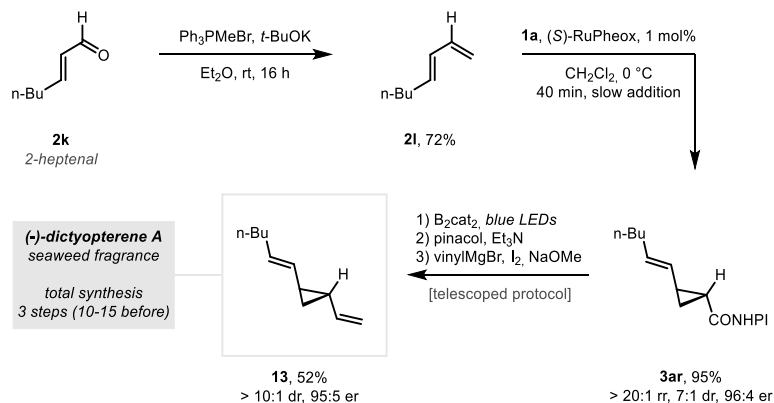
Cyclopropylboronate **5c** was employed for the total synthesis of (–)-spongidepsin.⁵⁴ Our synthetic procedure allowed for the synthesis of **5c** via a two-step protocol starting from propene gas (**2j**), the simplest prochiral olefin (**Scheme 25**). In contrast, the same building block was previously made by Simmons-Smith cyclopropanation of a chiral vinylboronate substrate.⁵⁴



Scheme 25: Synthesis of building block **5c**. Gram-scale synthesis of **3aq**: **1a** (1 equiv), (*R*)- RuPheox (0.5 mol%), dry CH_2Cl_2 , 0°C , slow addition over 2 h (97% isolated yield). Synthesis of **5c**: B_2cat_2 (1.5 equiv), dry DMF, blue LEDs (450 nm), rt, 16 h, *then* pinacol (4 equiv), Et_3N (25 equiv), rt, 1.5 h (51% isolated yield).

As a last example, **Scheme 26** shows the three-step enantioselective total synthesis of (–)-dictyopterene **A**⁵⁵ **12** starting from 2-heptenal (**2k**), followed by Wittig olefination and cyclopropanation of the resulting 1,3-diene **2l**. The key step of the synthesis was a telescoped decarboxylative borylation/vinylation following Zweifel's protocol⁵⁶ to install the second vinyl group of the desired cyclopropane. The previously reported synthesis of the same compound required several manipulations of a chiral

cyclopropylboronate, including TPAP or Dess-Martin oxidation, Julia-Kociensky olefination and Matteson homologation.⁵⁷



Scheme 26: Synthesis of natural product **13**. Synthesis of **2l**: Ph_3PMeBr (2 equiv), $t\text{-BuOK}$ (2 equiv), dry Et_2O , rt, 16 h (72% isolated yield). Synthesis of **3ar**: **1a** (1.2 equiv), (S)-RuPheox (1 mol%), dry CH_2Cl_2 , 0 °C, slow addition over 40 min (95% isolated yield). Synthesis of **13**: B_2cat_2 (1.5 equiv), dry DMF, blue LEDs (450 nm), rt, 16 h, then pinacol (4 equiv), Et_3N (25 equiv), rt, 1.5 h, then vinylmagnesium bromide (1.5 equiv), 1:1 dry THF:DMSO, rt, 30 min, then NaOMe (5 equiv), I_2 (1.2 equiv), 0 °C, 30 min (52% isolated yield).

2.4 Conclusion and outlook

In summary, a practical synthesis of the redox-active ester NHPI-DA **1a** was developed and its reactivity in cyclopropanation reactions has been explored. To this end, an asymmetric cyclopropanation reaction using the readily available catalyst RuPheox was optimized. This reaction was demonstrated to provide good yields, regio-, diastereo- and enantioselectivity on a broad range of substrates. Importantly, a large variety of olefins, including challenging aliphatic and electron-poor olefins, could be converted into enantiomerically enriched cyclopropanes equipped with a redox-active leaving group. The dual nature of the NHPI ester function as acyl donor and carbon-centered radical precursor enabled the diversification of these intermediates into a variety of synthetically useful compounds. The efficacy of this strategy was presented in the synthesis of biologically relevant molecules and natural products in a reduced number of steps. Diazocompound **1a** proved to be a versatile and useful functionalized methylenide precursor, enabling the generation of distinct cyclopropane families from a single intermediate without the need of custom reagents and circumventing the use of unstable carbenes. The methodology that has been reported herein simplifies the problem of functionalized methylenide transfer to olefins, rendering unnecessary the use of custom substrates and reagents, and represents an efficient unified synthesis of valuable enantioenriched cyclopropanes.

difficult. Computationally, the task of understanding the varied reactivity of ruthenium-carbene complexes is further complicated by the C_1 -symmetry of the Pheox ligand, originating four different carbene intermediates (**Figure 12**). The scarcity of data on the mechanistic aspects of this transformation, and the surprising performance of our previously disclosed system, led us to conduct a collaborative computational-experimental study with the Himo group, in order to gain better understanding of the main features of the ruthenium-catalyzed cyclopropanation of olefins using NHPI-DA (**1a**).

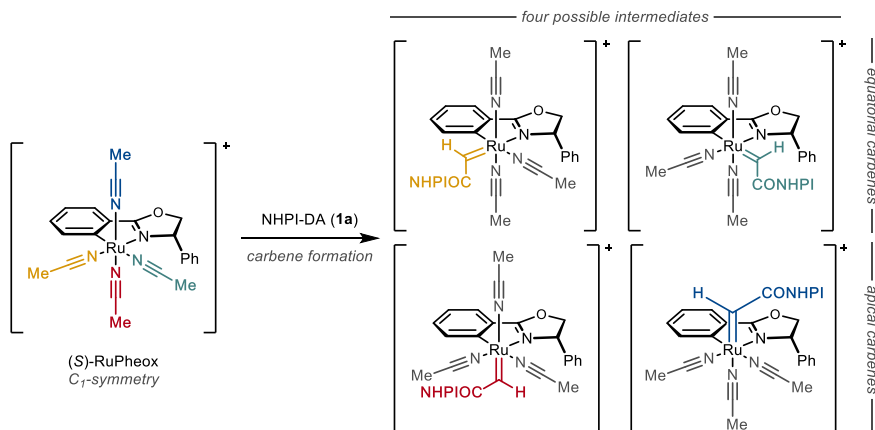


Figure 12: The four possible carbene intermediates from NHPI-DA (**1a**) and (*S*)-RuPheox.

3.2 Aim of the project

This work aims at expanding the knowledge on ruthenium-catalyzed carbene transfer reactions, including a detailed analysis of both the productive cyclopropanation pathway as well as the dimerization side-reaction to understand their interplay. The significant challenge of monitoring and analyzing these rapid transformations, with sufficient data density for advanced kinetic analyses, will require the use of advanced *in situ* techniques. The use of these methods could ultimately enable the identification of fleeting reaction intermediates. This collaborative work provides valuable insights on the complex mechanism of the reaction developed in **Chapter 2**, and may guide the future development of other carbene precursors.

3.3 Results and discussion

3.3.1 Kinetics of the dimerization reaction

The reactivity of the NHPI-DA/RuPheox combination was studied by means of N_2 evolution measurements. The latter technique^{62c} allowed us to continuously monitor the pressure inside a reaction vessel, which in turn enables to measure the conversion of NHPI-DA (**1a**) over time with high accuracy and data density.

Initially, we compared the kinetic profiles of the dimerization of NHPI-DA (**1a**) and the benchmark ethyl diazoacetate (**1c**; Et-DA) under identical catalytic conditions (**Figure 13**), and confirmed that full conversion was achieved in both experiments by ^1H NMR. It is evident from the kinetic traces that the dimerization of NHPI-DA (**1a**) is unconventionally slow (more than 15 minutes to complete) when compared to that of **1c**, that is fully consumed in less than 2 minutes.

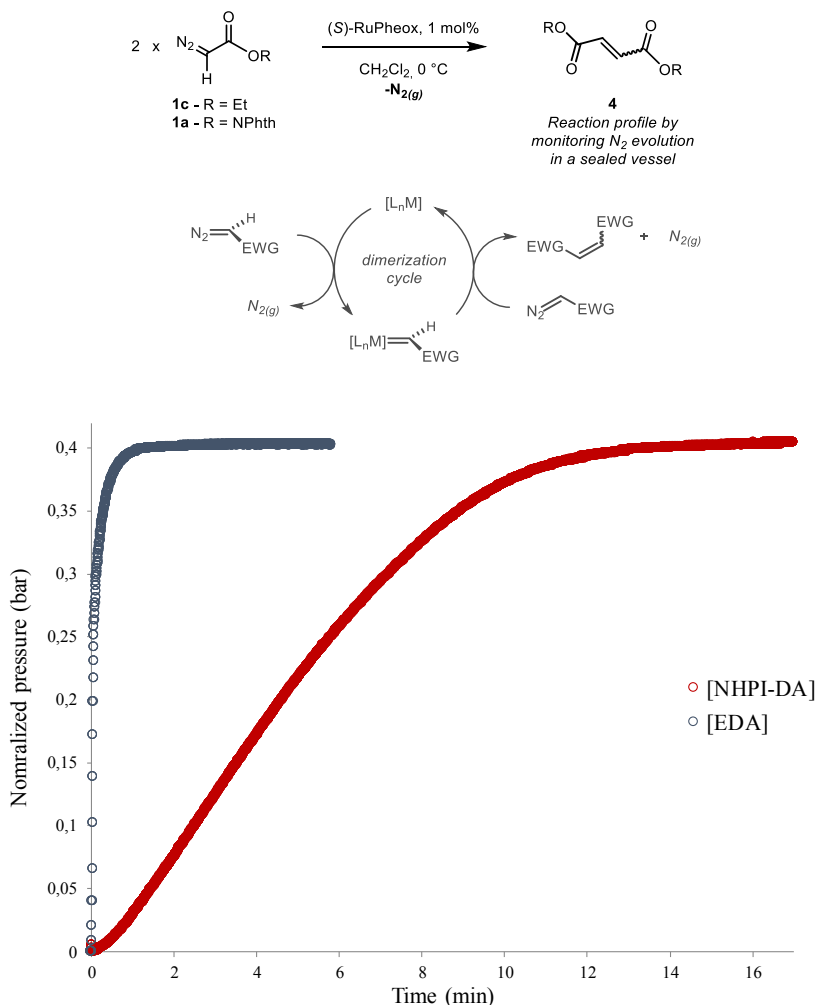


Figure 13: Normalized nitrogen evolution profiles of the dimerization of NHPI-DA (**1a**; red trace) and Et-DA (**1c**; blue trace) in the presence of (S)-RuPheox in CH_2Cl_2 at 0°C .

The reaction was also studied by high-resolution mass spectrometry (HRMS) to detect any intermediates formed during the reaction. Upon injection of a freshly mixed solution of **1a** and RuPheox in an electrospray ionization ESI-HRMS instrument, an interesting peak at m/z 527 was observed (**Figure 14**). This clear peak could not be

detected once the reaction was over, and showed an isotopic pattern consistent with that of the ruthenium-carbene species shown in **Figure 14**, despite its short-lived nature. However, any attempt of isolation and characterization of this species was not successful.

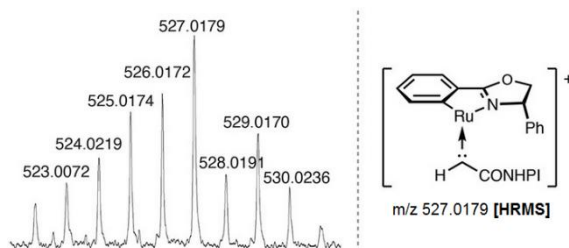


Figure 14: High resolution mass spectrum at $m/z = 527$, consistent with the formula $\text{C}_{25}\text{H}_{17}\text{N}_2\text{O}_5\text{Ru}$.

To assess the origin of the slower dimerization reaction in the case of NHPI-DA (**1a**), the nucleophilicity parameter ($N[\mathbf{1a}]$) was measured using the method reported by Mayr^{45c} that allows to determine the intrinsic nucleophilicity of diazocompounds towards a reference electrophile. This method has the advantage of being independent from any catalyst. This procedure is based on the measurement of the consumption of the colored benzhydrylium cation **14** ($\lambda_{\text{max}} = 569 \text{ nm}$) in the presence of the diazocompound by means of UV-visible spectroscopy. From the decay plot obtained with Et-DA (**1c**) and NHPI-DA (**1a**) under identical conditions, shown in **Figure 15**, the reaction constant (k_i) was estimated for each diazocompound **1**. This value was then used to determine the value of N according to the equation described in **Section 2.1** (eq. 1). It was calculated that NHPI-DA **1a** is significantly less nucleophilic than ethyl diazoacetate **1c** ($N[\mathbf{1a}] = 3.66$; $N[\mathbf{1c}] = 4.96^{45c}$), a quality that can be attributed to the electron-poor phthalimide moiety. The lower nucleophilicity of NHPI-DA (**Figure 13**) may explain the slower kinetics observed in the dimerization reaction (**Figure 11**), which is likely related to the enhanced performance of NHPI-DA in the cyclopropanation of olefins.

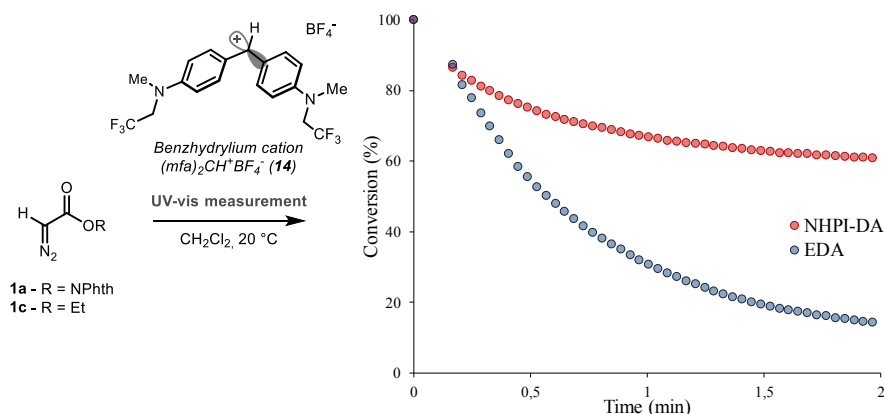
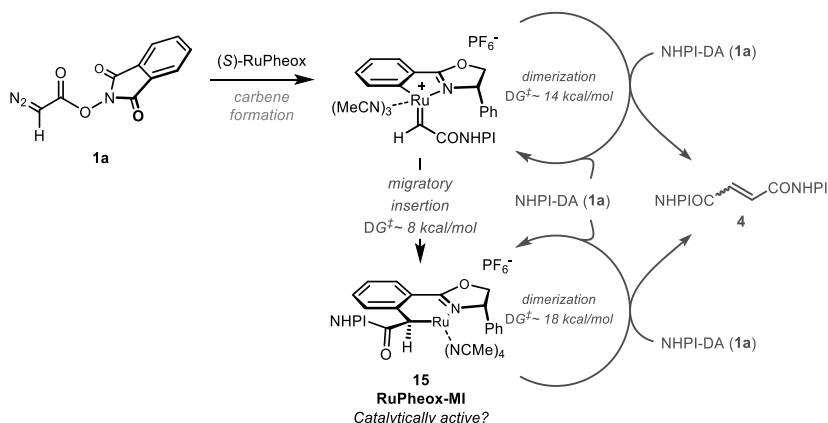


Figure 15: Measurement of the nucleophilicity parameter for NHPI-DA (**1a**) and Et-DA (**1c**) using benzhydrylium cation **14**.

In recent years, several C–H activation reactions of aromatic substrates with diazocompounds were reported, several of which employed ruthenium-based catalysts.⁶³ We realized that, when considering the intermediate metal-carbene species formed during the initial steps of both dimerization and cyclopropanation, it becomes evident that the migratory insertion of the carbene in the electron-rich Pheox ligand is possible (**Scheme 16**). This scenario, although not unprecedented in the literature, has not been shown to be involved in the catalytic activity of related complexes. Indeed it was calculated that the barrier for this migratory insertion step is low (8.2 kcal/mol relative to the carbene), even lower than that of the dimerization transition state (14.5 kcal/mol).⁶⁴



Scheme 16: Formation of the migratory insertion product **15** from the reaction of **1a** and RuPheox, and its catalytic activity in the dimerization reaction.

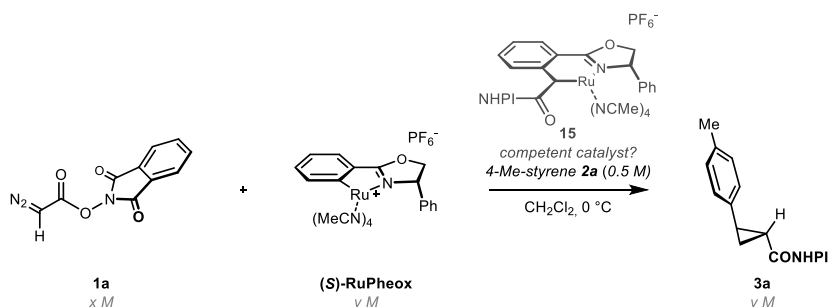
The low barrier for this process suggests that migratory insertion would take place preferentially over dimerization, possibly resulting in an alternative metallacyclic

complex (RuPheox-MI; **15**) catalyst (**Scheme 16**). In the eventuality that this migratory insertion would happen, the presence of **15** would also be consistent with the species detected by HRMS, as described above in **Figure 11**.

3.3.2 Evaluation of migratory insertion complexes as active catalysts

Calculations show that the barriers for the elementary steps of the catalysis with RuPheox-MI **15** are similar in energy to those of RuPheox, and this plausible pathway can have serious implications on the mechanism and selectivity of the NHPI-DA/RuPheox cyclopropanation. We therefore set out to assess the feasibility of the RuPheox-MI-mediated cyclopropanation reaction.

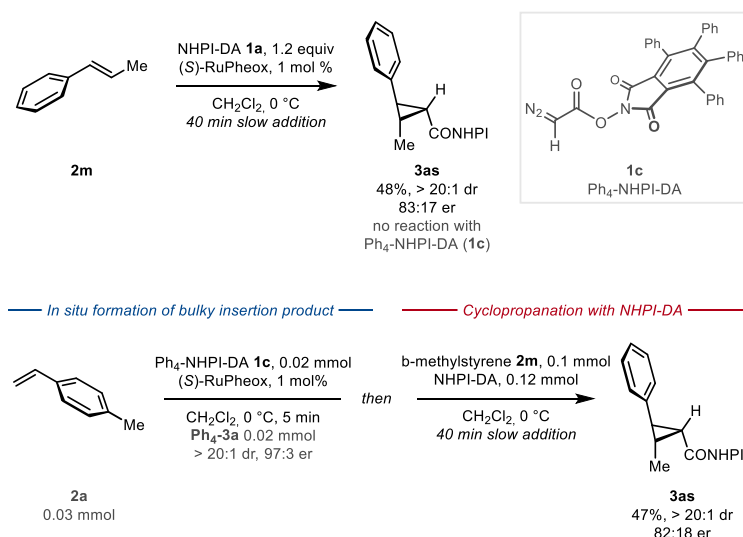
As stated previously, all attempts towards the isolation of the organometallic species formed during the reaction proved unsuccessful. We realized that the incorporation of the carbene structure into the ligand will have consequences on the stoichiometry and selectivity of the cyclopropanation. Intriguingly, calculations shown that a single diastereoisomer of the migratory insertion complex was preferentially formed from various stereoisomers of the carbene intermediate. Specifically, diazocompound **1a** would be consumed by RuPheox to activate the catalyst before being able to produce any product. This means that different ratios of NHPI-DA:RuPheox would result in different yields (and potentially enantioselectivities) of the cyclopropane product **3a**. To investigate this hypothesis, a set of experiments with different loadings of ruthenium catalyst from 1 mol% to 5 equivalents was performed (**Table 4**).



Entry	x (M)	y (M)	[cat] ₀ /[diazo] ₀	Yield (%)	er
1	0.1	0.001	0.01	97	96:4
2	0.2	0.1	0.05	95	93:7
3	0.1	0.1	1	96	94:6
4	0.05	0.1	2	97	96:4
5	0.02	0.1	5	95	96:4

Table 4: Stoichiometry experiments on the cyclopropanation of *p*-methylstyrene **2a** using NHPI-DA **1a** and (*S*)-RuPheox.

No variation was observed on the yield or the selectivity of the transformation, suggesting that the migratory insertion complex is not likely to be involved in the activation of the catalysis of the process. However, it is still possible that a small amount of RuPheox-MI could be more active in the cyclopropanation reaction than the initial RuPheox complex and be responsible for the majority of the conversion. To test this possibility, we synthesized a much bulkier diazocompound reagent (Ph₄-NHPI-DA; **1c**) and compared its selectivity and efficiency in carbene-transfer (Scheme 27). The rationale of this experiment is that, upon migratory insertion, a bulkier RuPheox-MI would be generated and this would be reflected on the stereoselectivity of the reaction. To maximize the possibility of detecting changes in the enantiomeric ratio of the product, we chose *trans*-β-methylstyrene **2m** as a substrate in this experiment for its modest performance in the NHPI-DA/RuPheox cyclopropanation. As shown in Scheme 27, NHPI-DA reacts with olefin **2m** to give **3as** in 48% and 83:17 e.r. as a single diastereomer under standard conditions.



Scheme 27: Control experiments aimed to observe the effect of potential catalysis by RuPheox-MI **15**. Reactions were performed under inert atmosphere. Top: Cyclopropanation of *trans*-β-methylstyrene (**2m**) with NHPI-DA (**1a**) under standard conditions. Bottom: Cyclopropanation experiment aimed at the observation of potential migratory insertion catalyst. Yields were measured by ¹H NMR using 1,1,2,2-tetrachloroethane as an internal standard.

In a different experiment, RuPheox was pre-activated with Ph₄-NHPI-DA (**1c**) and *p*-methylstyrene (**2a**; a good substrate for the cyclopropanation reaction) in substoichiometric amounts (Scheme 27, bottom). If migratory insertion would be operational, this step would incorporate Ph₄-NHPI-DA (**1c**) in the catalyst. This step would generate the migratory insertion product. Then, *trans*-β-methylstyrene (**2m**) followed by NHPI-DA (**1a**) were added to the mixture according to standard procedure. Analysis of the product **3as** revealed that the same yield and

stereoselectivity was obtained as under standard conditions. Although these experiments cannot rule out completely that the RuPheox-MI **15** is involved in the cyclopropanation catalysis, it does not appear to play a major role in the catalysis of the cyclopropanation reaction. Yet, this mechanistic possibility should be considered in the future when using carbenes derived from metallacyclic catalysts.

3.3.3 Kinetics of the cyclopropanation reaction

Next, we investigated the kinetics of the cyclopropanation reaction. We decided to employ two model olefins for our study, *p*-methylstyrene (**2a**) and 1-hexene (**2b**) representative of both aromatic and aliphatic substrates. N₂-evolution profiling revealed that both cyclopropanation reactions were significantly faster than the dimerization process (Figure 17), showing once more the slower kinetics of NHPI-DA (**1a**) towards the electrophilic metal-carbene.

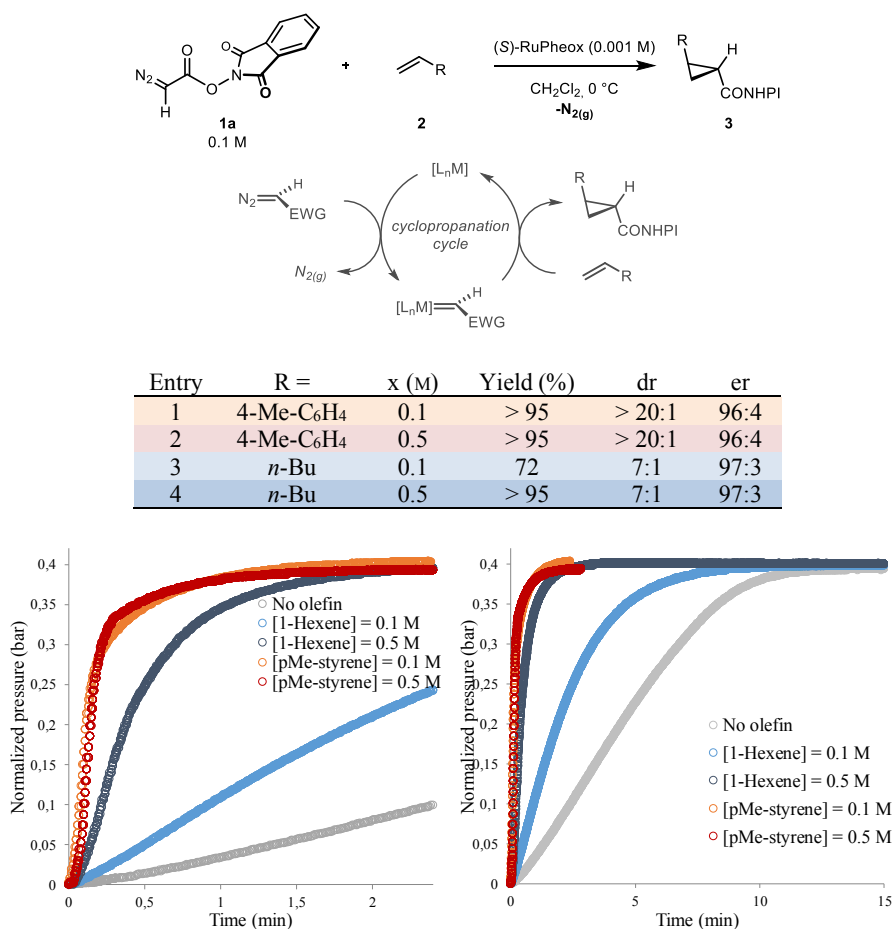


Figure 17: N₂ evolution profile of the cyclopropanation of *p*-methylstyrene (**2a**; red traces) and 1-hexene (**2b**; blue traces) using NHPI-DA (**1a**) and (S)-RuPheox (expansion on the right). For comparison, the dimerization profile is plotted in gray.

It is also evident that the rate of the reaction does not depend on the concentration of the olefin (zero-order kinetics) when the substrate is a good nucleophile, as in the case of styrene **2a** ($N = +1.70$). In contrast, in the case of the less nucleophilic 1-hexene (**2b**; $N = -2.77$) the rate was found to depend on the concentration of the olefin substrate. In this case, the slower rate of cyclopropanation allowed us to sample the reaction mixture at different conversions to evaluate the distribution of cyclopropanation and dimerization products. It was observed that the same value for the combined cyclopropane-dimer yield and conversion by nitrogen evolution was obtained until at least 56% conversion, as well as a constant cyclopropane:dimer ratio of 85:15 (**Figure 18**). In this regime, we could then calculate the nitrogen evolved from the cyclopropanation cycle from that of the total nitrogen pressure. This estimated data was used to determine the reaction order in 1-hexene using variable time normalization analysis (VTNA),⁶⁵ a technique that exploits the normalization of the time scale for the average concentration of each reaction component, effectively removing the kinetic effect of those reagents. This normalization results in the overlay of two or more reaction profiles, from which reaction orders and rate constants can be extrapolated. This results in first order kinetics up until at least 56% conversion and indicating that the substrate is probably involved in the rate-determining step (**Figure 18**). Moreover, the linearity of the resulting plot after the initial curvature revealed that the reaction has zero-order kinetics for NHPI-DA (**1a**).

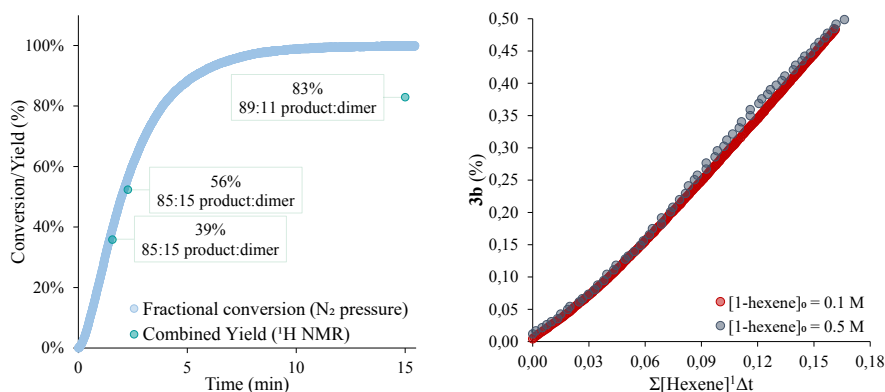


Figure 18: Left: N₂ evolution profile of the cyclopropanation of 1-hexene (**2b**) using NHPI-DA (**1a**) and 1 mol% (*S*)-RuPheox in CH₂Cl₂ at 0 °C, displaying a constant ratio of cyclopropane and dimer products up to 56% conversion. Right: VTNA analysis of extrapolated nitrogen pressure until 56% conversion, showing first order kinetics in 1-hexene (**2b**) and zero-order kinetics in NHPI-DA (**1a**).

The kinetic data shown until now is in line with a fast reaction of the diazocompound with the metal catalyst followed by a rate-determining cyclopropanation step. In the case of styrene **2a**, the cyclopropanation is no longer the RDS, consistent with a faster reaction of the metal-carbene with the olefin. A thorough computational study of all the possible stereoisomers of the metal-carbene and the evaluation of their relative

competence in cyclopropanation, favored the outer-sphere mechanism with decreased kinetic barriers (see **Paper II** for details).^{64,66} These kinetic results are well in agreement with the nucleophilicity of the olefins employed in the experiments ($N[2a] = 0.78$; $N[2b] = -2.77$), where a higher N value results in zero-order kinetics with respect to the olefin substrate. In this case, the RDS seems to be the formation of the metal-carbene intermediate. In contrast, a less nucleophilic alkene correlates to first-order kinetics, which suggest that it is involved in the rate-determining step or an association equilibrium before it. This is consistent with the nucleophilicity of the alkene determining the relative rate of cyclopropanation with respect to the dimerization cycle. Additionally, in the slower reactions with 1-hexene (**2b**), it was possible to detect by HRMS the same signal with $m/z = 527$ upon injection of the alkene. This intermediate could not be detected when the reaction was completed, or when *p*-methylstyrene (**2a**) was employed instead. The observation that this species could only be observed during dimerization or rate-limiting cyclopropanation is consistent with its accumulation in the catalytic cycle. Yet, we cannot completely rule out the possibility that the signal belongs to the migratory insertion complex (**Section 3.3.2**).

3.4 Conclusions

Overall, the mechanism of the RuPheox-catalyzed cyclopropanation of olefins with NHPI-DA (**1a**) appears to be a delicate equilibrium of multiple reaction pathways (**Figure 19**). We have calculated that RuPheox can react with NHPI-DA (**1a**) through a dissociative mechanism to give four possible metal-carbene intermediates.⁶⁴ The carbene formation step is rate-determining when nucleophilic styrene substrates are used, as evidenced by the kinetic analysis of the cyclopropanation reaction in **Figure 17**. These intermediates can then react with an additional molecule of diazocompound. The calculations support an inner-sphere mechanism for this process, where the nucleophile coordinates to the ruthenium complex before the formation of the dimer side-product. With kinetic profiling and nucleophilicity measurement, we have shown that NHPI-DA (**1a**) increases the performance of this transformation due to its intrinsically lower nucleophilicity, which results in slower dimerization kinetics relative to cyclopropanation. Although the optimization of the diazoester structure has been reported in various studies (**Section 3.1**),⁶⁰ herein it is demonstrated the importance of its overall nucleophilicity, giving a direction for further developments. The metal-carbene intermediates can also originate a new migratory insertion complex (RuPheox-MI, **15**), potentially active in the catalysis of the reaction. With a set of experiments, we can confidently rule out this possibility when using styrene substrates, although they should be considered in future studies employing different substrates or diazocompounds. Among various possibilities, DFT calculations deemed the cyclopropanation in this system to operate through an outer-sphere mechanism⁶⁴, although the calculations could not definitively point to which of the four possible carbenes is operational. VTNA analysis of the cyclopropanation of

1-hexene (**Figure 18**) revealed that this step is rate-determining when using poorly nucleophilic substrates, like aliphatic olefins.

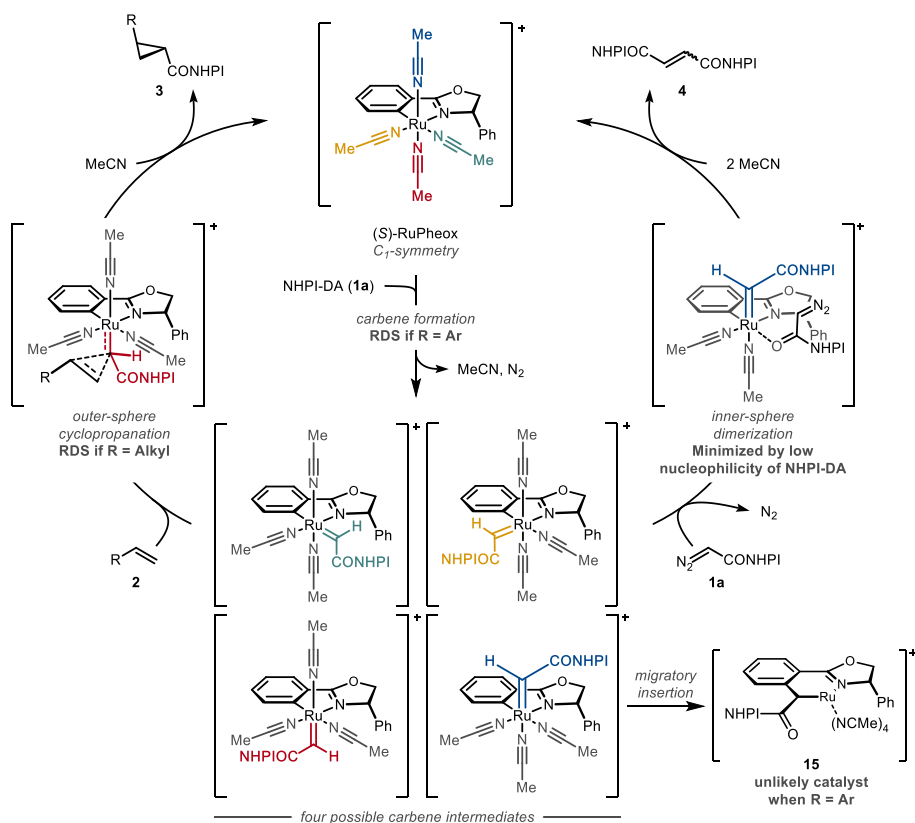


Figure 19: Mechanistic model of the cyclopropanation (right) and dimerization (left) reaction of NHPI-DA (**1a**) catalyzed by RuPheox.

This experimental and computational study proves that weakly nucleophilic diazocompounds are a viable option to increase the selectivity of cyclopropanation *vs* dimerization in problematic systems. In a broader sense, this study demonstrates the combination of experimental (nucleophilicity measurement, N₂ evolution monitoring, *in situ* HRMS analysis, VTNA) and computational (DFT) techniques to gain understanding in fast carbene-transfer reactions.

4. Modular Enantioselective Synthesis of *cis*-Cyclopropanes through Self-Sensitized Stereoselective Photo-Decarboxylation with Benzothiazolines (Paper III)

4.1 Introduction

A common strategy in the development of medicinal candidates is to restrict the flexibility of the ligand in its binding conformation.⁶⁷ In this process, it is essential that properties like size, shape and molecular weight of the analog are similar to those of the parent compound. Alkyl linkages, ubiquitous in medicinal candidates, require rigid analogs to improve the biological properties of lead compounds. One way to lock the conformation of a fragment is to replace the flexible aliphatic residues with alkene linkers. These moieties, however, are prone to metabolic oxidation, resulting in sub-optimal potency *in vivo*. To overcome these intrinsic issues of olefins, cyclopropanes have been widely used in the pharmaceutical industry to optimize the properties of drug candidates as rigid and metabolically stable alkyl chain analogs (**Figure 20**).^{2a, 2b, 68}

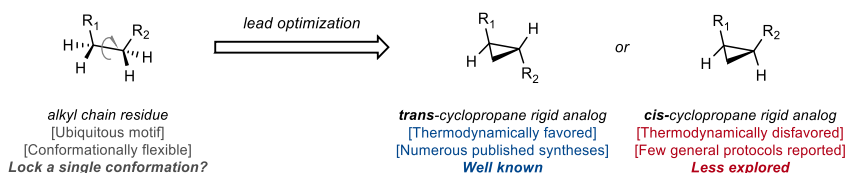


Figure 20: Cyclopropanes act as rigid conformationally restricted of alkyl chains.

Although several procedures towards *trans*-cyclopropanes have been developed throughout the years,³⁶ protocols to obtain their *cis*-diastereoisomer remained largely unexplored and the existing methods lead mostly to racemic products, resulting in additional steps of resolution.⁶⁹ In recent times, a number of enantioselective syntheses of *cis*-cyclopropyl esters by means of carbene transfer have emerged, requiring tailored transition-metal catalysts^{42e, 42f, 42k, 42l, 50} or engineered proteins^{42h, 42i, 42l} to access the disfavored *cis*-diastereomer. Nevertheless, these methods have had limited impact due to the unavailability of the advanced catalysts used. In particular, the direct asymmetric synthesis of *cis*-(di)arylcyclopropanes from olefins leads to interesting products but requires the enantioselective transfer of benzyldienes (**Figure 21**). The few existing methods still remain problematic, requiring allylic alcohols or enantiopure *Z*-vinylboronates starting materials, or stoichiometric iron-benzylidene complexes.⁷⁰ All these methodologies, however, suffer from the requirement of preformed substrates and often lack sufficient generality.

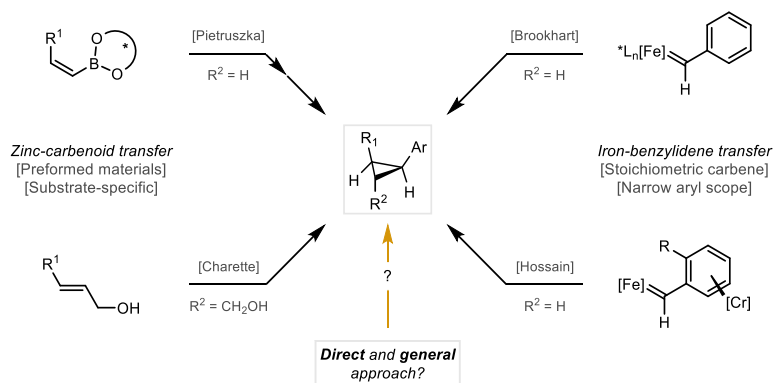
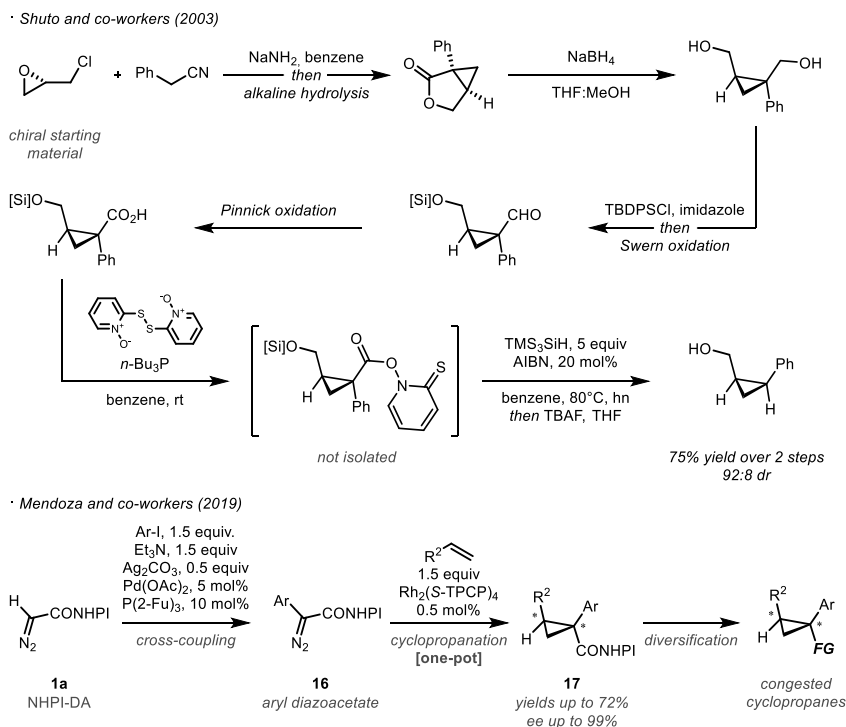


Figure 21: State-of-the-art in the enantioselective synthesis of *cis*-diarylcyclopropanes.^{70c-k}

A diastereoselective approach from the chiral pool was reported by Shuto and co-workers in a single example, where the authors performed a stereoselective decarboxylative reduction of a cyclopropyl Barton ester as the key step (**Scheme 28**, top).^{70a}

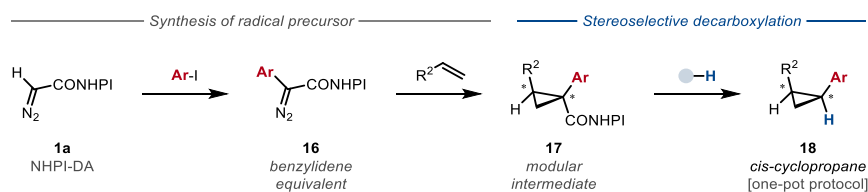


Scheme 28: Relevant background for the work in this thesis. Top: Shuto's decarboxylation of a cyclopropyl Barton ester.^{70a} Bottom: Synthesis of congested cyclopropanes using redox-active aryldiazoacetates **16** by Mendoza and co-workers.⁷¹

However, to yield the desired product in high yields and selectivity Shuto's protocol required a large excess of expensive tris(trimethylsilyl)silane as hydrogen atom donor, required to efficiently trap the *cis*-radical intermediate.^{70a} For this reason, and for the long synthetic sequence necessary to obtain chiral cyclopropyl Barton esters, this approach has not yet found further applications. Nevertheless, this result demonstrated that hydrogen atom transfer (HAT) in cyclopropyl radical intermediates could be used to obtain contra-thermodynamic stereoisomers of cyclopropanes. Such radical intermediates could be also generated from more accessible cyclopropyl redox-active esters **17**, readily synthesized through a protocol recently published by our group (Scheme 28, bottom).⁷¹ This procedure utilizes aryldiazocompound reagents **16**, in turn obtained from the palladium-catalyzed reaction of commercially available aryl iodides and NHPI-DA (**1a**).

4.2 Aim of the project

We aimed to convert olefins into *cis*-arylcyclopropanes by means of sequential asymmetric cyclopropanation with redox-active aryldiazoacetates and stereoselective decarboxylative reduction. In our previous project, we have shown how feedstock olefins can be transformed in valuable *trans*-cyclopropane building blocks using the single-carbon reagent NHPI-DA (**1a**).⁴⁸ Exploiting the single-electron chemistry of redox-active esters, this project aims at developing a highly selective, one-pot protocol towards the asymmetric synthesis of *cis*-arylcyclopropanes **18** from unfunctionalized olefins (Scheme 29). Conscious of the selectivity problem that arise from the decarboxylative reduction, this methodology would require the design of a reductant with the right steric and electronic properties that would allow for efficient hydrogen atom transfer (HAT) to the cyclopropyl radical. This method would simplify the synthesis of relevant cyclopropane material, avoiding the necessity of preformed chiral reagents.



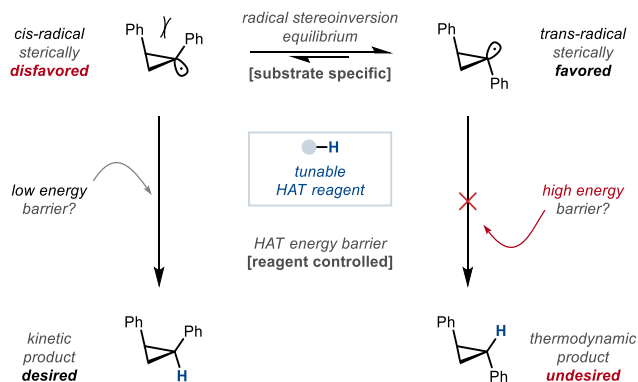
Scheme 29: One-pot synthesis of enantioenriched *cis*-arylcyclopropanes from olefins and aryl iodides.

4.3 Results and discussion

4.3.1 Optimization of the photo-decarboxylation reaction

The cyclopropyl radical is known to exist as a pyramidal σ -hybridized radical, with a very fast stereoinversion equilibrium ($k_{\text{inv}} \sim 10^8\text{-}10^9 \text{ s}^{-1}$) between the two *cis*- and *trans*-isomers,⁶ resulting in a mixture of products.^{6, 72} Consequently, our initial idea was contingent on the design of a hydrogen atom transfer (HAT) reagent capable of

kinetically steering the selectivity of the decarboxylation reaction towards the thermodynamically disfavored *cis*-product (**Scheme 30**). The challenge posed by this transformation in terms of efficiency and stereoselectivity is further complicated by the high reactivity of cyclopropyl radicals that makes them particularly prone to alternative side-reactions.



Scheme 30: Proposed model for the *cis*-selectivity of the decarboxylation reaction.

Redox-active ester **17a** was chosen as a model substrate for the screening of hydrogen atom donors, summarized in **Table 5**. We started by exploring known decarboxylation conditions. The nickel-catalyzed protocol using PhSiH_3 reported by Baran^{34j} afforded the desired cyclopropane *cis*-**18a** in low yields, although with good stereoselectivity (entry 1). Chloroform has been used as a safer alternative to tin reagents in decarboxylation of redox-active esters.⁷³ However, its use failed to achieve high yields and diastereomeric ratio (entry 2). We then moved onto the recent photochemical reductions employing dihydropyridines. Diethyl-substituted Hantzsch ester **19a**⁷⁴ in dichloromethane displayed low reactivity albeit good selectivity (entry 3), however no further improvement could be obtained by tuning the structure and electronics of the reductant (**19b-f**; entries 4-8). A clear improvement in terms of yield was observed when the solvent was replaced with DMSO (entry 9). The use of a related *N*-substituted nicotinamide **19g**⁷⁵ recently developed by our group was encouraging (entries 10), although only moderate yields of product **18a** were obtained. These results prompted us to search for a different reductant possessing a transferable hydrogen atom in a more sterically hindered position. Benzothiazolines **20**, in particular when substituted in the 2-position, have been employed as reductants in transfer hydrogenation reactions as a substitute to Hantzsch esters, often displaying better results compared to its bio-inspired counterpart.⁷⁶ More recently, these compounds have been reported to serve as acyl radical sources or hydrogen atom donors in photocatalytic reactions under visible light irradiation.⁷⁷ Although their ability to function as self-sensitized photoreductants or their reactivity in decarboxylative reductions was still unexplored, the fact that benzothiazolines like

dihydropyridines result in pro-aromatic radicals after HAT encouraged further study.^{77c}

Entry	HAT reagent	X (equiv)	Solvent	Yield (%)	dr (cis:trans)
1 ^{a,b}	PhSiH ₃	1.5	THF:DMF: <i>i</i> PrOH	30	90:10
2 ^{a,c}	CHCl ₃	solvent	CHCl ₃	43	77:23
3	19a	1.2	CH ₂ Cl ₂	41	88:12
4	19b	1.2	CH ₂ Cl ₂	n.d.	-
5	19c	1.2	CH ₂ Cl ₂	n.d.	-
6	19d	1.2	CH ₂ Cl ₂	n.d.	-
7	19e	1.2	CH ₂ Cl ₂	22	88:12
8	19f	1.2	CH ₂ Cl ₂	40	86:14
9	19a	1.2	DMSO	76	90:10
10	19g	1.2	DMSO	60	94:6
11	20a	1.2	DMSO	88	95:5
12	20b	1.2	DMSO	81	95:5
13	20c	1.2	DMSO	n.d.	-
14	20d	1.2	DMSO	92	89:11
15	20e	1.2	DMSO	54	88:12
16	20f	1.2	DMSO	44	90:10
17 ^a	20g	1.2	DMSO	< 10	97:3
18 ^a	20a	1.2	DMSO	n.d.	-

19a R¹ = Et, R² = H
19b R¹ = Et, R² = Ph
19c R¹ = Et, R² = Et
19d R¹ = Cy, R² = H
19e R¹ = Bn, R² = H
19f R¹ = Ph, R² = H

19g

20a R = Ph
20b R = *t*-Bu
20c R = 4-NO₂-Ph
20d R = 4-CF₃-Ph
20e R = 2,4,6-Me₃-Ph
20f R = Cy

Table 5: Optimization of the decarboxylative reduction of **17a**. Reactions were performed under inert atmosphere by stirring **17a** and the indicated reductant in the specified solvent under blue LEDs irradiation (450 nm) with fan cooling. Yields are measured by ¹H NMR using 1,1,2,2-tetrachloroethane as an internal standard. The diastereomeric ratio between *cis*-**18a** and *trans*-**18a** is measured by GC-MS after filtration of the crude through a plug of silica. ^a: No light irradiation. ^b: Reaction conditions: PhSiH₃ (1.5 equiv), Zn (0.5 equiv), NiCl₂(H₂O)₆ (10 mol%), 4,4'-di-*t*-Bu-2,2'-bipyridyl (20 mol%), THF:DMF:*i*PrOH 10:2:1, 40 °C. ^c: Reaction conditions: Et₃N (2 equiv), 4CzIPN (2 mol%), CHCl₃.

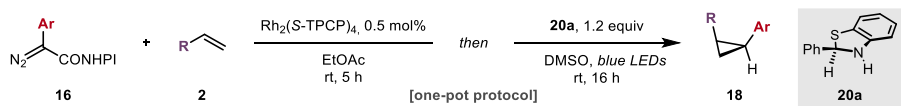
Several 2-substituted benzothiazolines were screened without additional photocatalysts (entries 11-16), giving promising results. Phenyl- and *tert*-butyl-benzothiazoline (**20a,b**), conveniently prepared and stored in multi-gram amounts, displayed remarkable results in terms of both yield and diastereoselectivity (entries 11,12), while other electron deficient (**20c,d**), bulky (**20e**) or aliphatic (**20f**) substituents lead to lower efficiency and/or selectivity (entries 13-16). Two control reactions in the absence of light resulted in low conversion, preliminarily indicating that light was required for this transformation to take place (entries 17,18). Importantly, the simplicity of these conditions only requiring the irradiation of the

substrate **17** and benzothiazoline **20** in DMSO enabled integration with the enantioselective cyclopropanation previously developed in the group, as shown below (Section 4.3.2).

4.3.2 Substrate scope

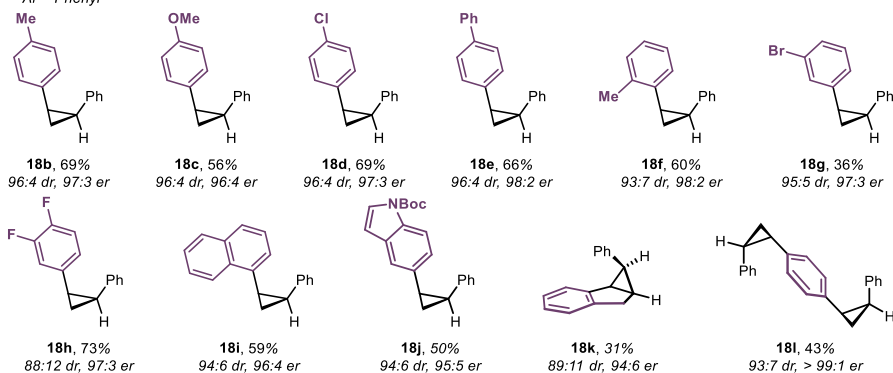
The scope of the one-pot cyclopropanation/reduction was explored using benzothiazoline **20a** and stoichiometric amounts of olefin **2** and diazocompound **16**. As shown in Scheme 31, both electron-poor (**18d,g,h**) and electron-rich styrenes (**18c,e**) could be converted in enantioenriched *cis*-diarylcyclopropanes **18b-l**, showing good overall yields and stereoselectivities. Naphthyl- and indole-substituted olefins were tolerated in this transformation yielding products **18i,j**, as well as the cyclic indene substrate (**18k**), albeit with slightly less stereoselectivity. This could be due to either a slower stereoinversion process, or the instability of the *cis*-radical intermediate. Pleasingly, we observed that divinyl benzene can take part in this transformation to generate the C_2 -symmetric product **18l** as a single enantiomer through a one-pot double cyclopropanation/double decarboxylation. Importantly, negligible loss of stereochemical information from the intermediate cyclopropyl esters⁷¹ was observed in all cases, demonstrating that the epimerization of the neighbouring stereogenic center does not occur during the photochemical reduction step.

Our modular approach enabled the enantioselective transfer of several aromatic fragments from aryl redox-active esters **16**. This way, *p*-methylstyrene (**2a**) can be transformed in several *cis*-cyclopropane products with different embedded functionalities (**18m-u**). Alkyne (**18p**), nitrile (**18r**), and ketone (**18t**) moieties were all tolerated in this transformation. Remarkably, this method allowed to turn commercially available 4-iodophenylalanine in a *cis*-cyclopropane-modified amino acid (**18u**) in two steps.



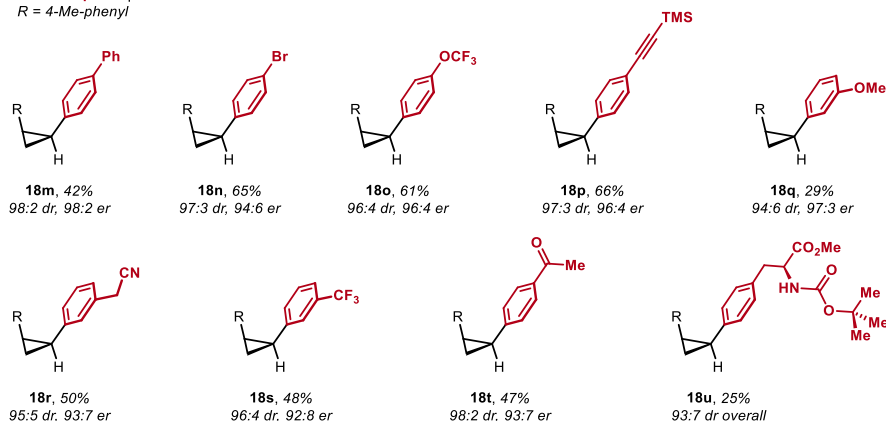
— Alkene scope

Ar = Phenyl



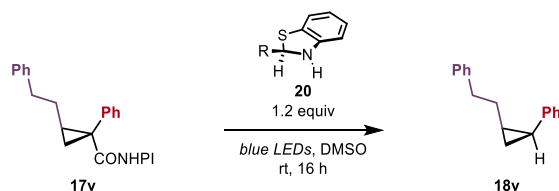
— Diazoscope scope

R = 4-Me-phenyl



Scheme 31: Substrate scope for the enantioselective synthesis of *cis*-cyclopropanes **18**. Reactions were performed under inert atmosphere. Reactions conditions: **16** (1 equiv), **2** (1 equiv), Rh₂(S-TPCP)₄ (0.5 mol%), dry EtOAc (0.05 M), rt, 5 h, then **20a** (1.2 equiv), dry DMSO (0.1 M), blue LEDs (450 nm), rt (fan cooling), 16 h. Reported yields are isolated. Diastereomeric ratio determined by chiral HPLC.

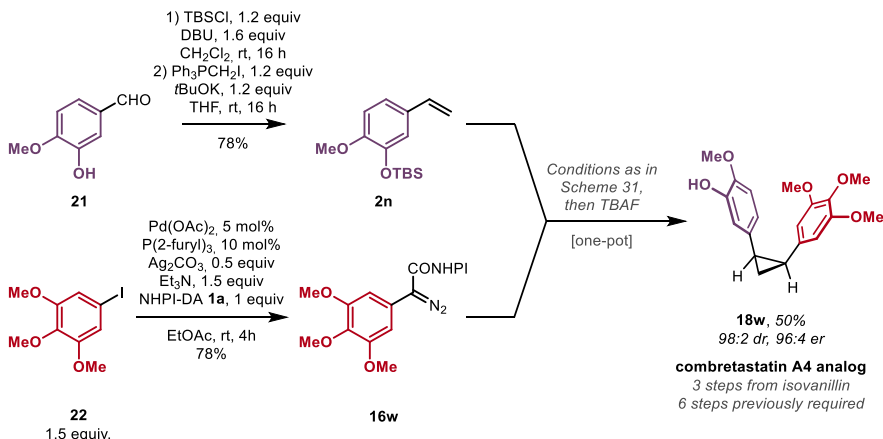
For aliphatic substrates, the reaction proved to be more challenging in terms of selectivity. When the reduction was carried out on NHPI cyclopropyl ester **17v**, poor diastereoselectivity was observed (**Table 6**). Fortunately, the use of bulkier benzothiazoline **20b** gave almost a two-fold increase in selectivity for the *cis*-product. Lowering the temperature had no effect on the selectivity, although the rate of the reaction decreased considerably.



Reductant	T (°C)	Conversion (%)	18v (%)	d.r. (<i>cis:trans</i>)
20a – R = Ph	rt	> 95	75	67:33
20b – R = <i>t</i> -Bu	rt	90	82	82:18
20a – R = Ph	– 40	50	28	70:30
20b – R = <i>t</i> -Bu	– 40	20	10	75:25

Table 6: Optimization for the reduction of aliphatic substrate **17v**. Reactions were performed under inert atmosphere. Reaction conditions: **17v** (1 equiv), **20** (1.2 equiv), dry DMSO (0.1 M), blue LEDs (450 nm), 16 h. Reported yields are isolated. Yields and diastereomeric ratio are measured by ^1H NMR using 1,1,2,2-tetrachloroethane as an internal standard.

To further prove the synthetic value of this methodology, we explored the enantioselective synthesis of the bioactive combretastatin A4 analog **18w** (Scheme 32). This molecule features extremely electron-rich aryl substituents, whose compatibility with highly electrophilic and reducible NHPI esters was unknown. To our delight, isovanillin (**21**) was converted in the TBS-protected olefin **2n** in 78% yield. The desired product was then obtained using a telescoped sequence of cyclopropanation/photo-decarboxylation/deprotection using diazo compound **16w**, in 39% overall yield from commercially available material. To put these results in perspective, twice as many steps and a resolution were previously required to obtain the same product in < 10% overall yield from comparable materials.^{70b}



Scheme 32: Enantioselective synthesis of combretastatin A4 analog **18w**. Reactions were performed under inert atmosphere. Reaction conditions as in Scheme 31, then TBAF·3H₂O (1.5 equiv), 2 h. Reported yields are isolated. Diastereomeric ratio determined by chiral HPLC.

4.3.3 Photochemical characterization and mechanistic studies

The decarboxylation of redox-active esters by benzothiazolines required light irradiation (**Table 5**), without any additional photocatalyst. Therefore, we set out to investigate the mechanism of the photo-decarboxylation reaction and in particular the role of visible light in the process. Initial studies on the photochemical properties of this system were done by means of UV-visible spectrometry, shown in **Figure 22**. The analysis revealed an increased absorbance in the visible range when the redox-active ester and benzothiazoline **20a** were mixed in DMSO, suggesting the formation of an electron donor-acceptor (EDA) complex⁷⁸ between the two reagents. The variation of this absorption feature with the relative concentration of the two species was studied with the continuous variation method.⁷⁹ Representation of the variation of absorbance with the molar fraction of the redox-active ester **17a** (Job plot) revealed a shallow maximum at $\chi_{17a} = 0.5$ (**Figure 22**). These data suggest that a 1:1 complex is formed between the electron-deficient NHPI ester **17a** and the electron-rich benzothiazoline **20a**. The light curvature around the maximum can be likely the result of a low binding constant for the complex, or alternatively indicate the formation of other complexes.

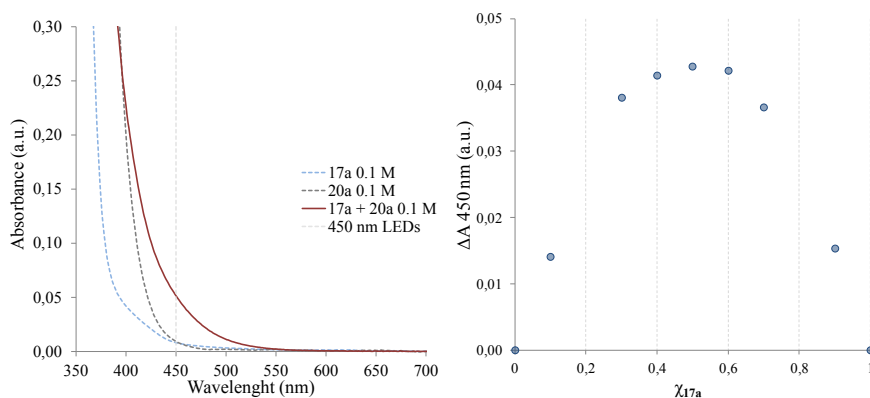


Figure 22: Initial spectroscopic investigation of the photo-decarboxylation reaction. Left: UV-visible spectra of benzothiazoline **20a** (gray dotted line), NHPI ester **17a** (blue dotted line) and the mixture of the two (red line). It is visible the increased absorbance in the 400-550 nm range. Right: Job plot of the mixture of **17a** and **20a** in DMSO, measured at 450 nm ($c_{\text{tot}} = 0.1$ M).

The EDA complex was further studied by fluorescence spectroscopy, showing clear new excitation and emission features when redox-active ester **17a** was mixed with benzothiazoline **20a** ($\lambda_{\text{max}} = 435$ nm; $\lambda_{\text{em}} = 490$ nm) as shown in **Figure 23**. Fluorescence lifetime measurements by time-correlated single photon counting (TCSPC) demonstrated the presence of a new species with a distinct fluorescence lifetime ($\tau = 1.4$ ns) compared to that of the initial benzothiazoline ($\tau_0 = 1.7$ ns). Stern-Volmer quenching experiments are commonly used to measure the kinetic features of photochemical transformations.⁸⁰ Two possible scenarios can be formulated between an excited-state species and a ground-state quencher (**Q**).

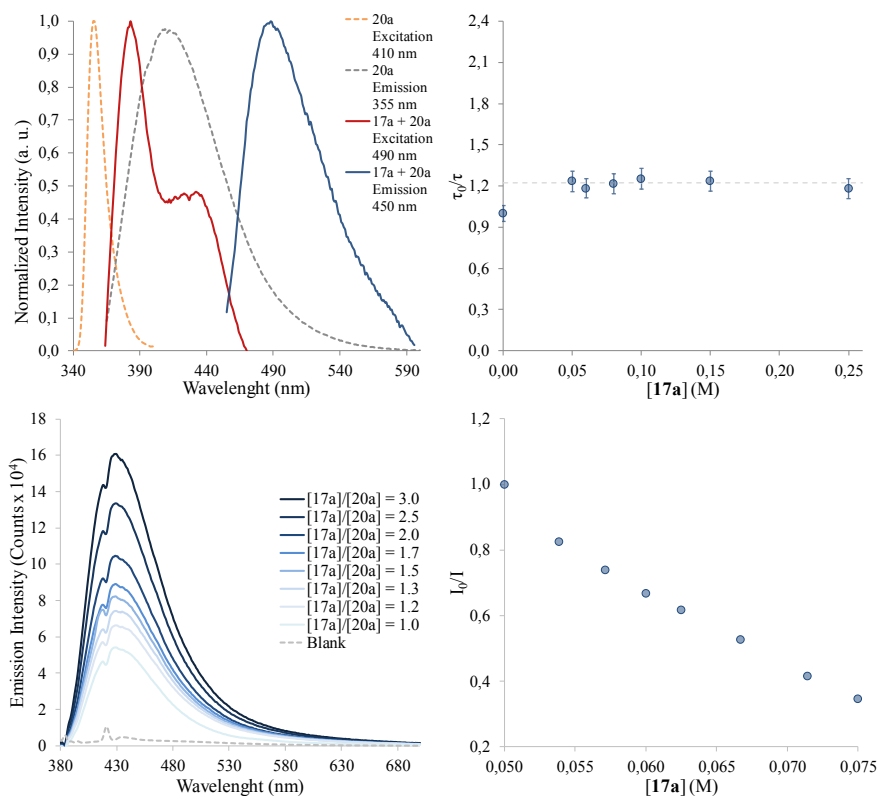


Figure 23: Fluorescence spectroscopy and Stern-Volmer experiments on the photodecarboxylation reaction. Top left: Normalized excitation and emission spectra of benzothiazoline **20a** ($c = 0.02$ M) and its EDA complex ($c = 0.1$ M) with redox-active ester **17a** in DMSO. Top right: Stern-Volmer lifetime plot of benzothiazoline **20a** ($c = 0.01$ M, $\tau_0 = 1.7$ ns) with redox-active ester **17a** ($\tau_{\text{EDA}} = 1.4$ ns) in DMSO. Bottom left: Emission profile of **17a** and **20a** in DMSO at increasing amounts of **17a**. The feature at $\lambda = 422$ nm is an artifact originated by subtraction of the blank (dotted gray) from the emission spectra. Bottom right: Steady-state Stern-Volmer quenching of **20a** with **17a** in DMSO.

The first one, the *dynamic quenching*, represents a situation in which an excited-state species is quenched by a collisional interaction with the quencher molecule **Q**. The second case, called *static quenching*, involves the formation of a complex between the fluorophore and the quencher **Q** with different luminescence properties. These scenarios are described by the Stern-Volmer relationships,^{80b} shown in equation 2 and 3:

$$\frac{I_0}{I} = 1 + k_q \tau_0 [Q] \quad (2)$$

$$\frac{I_0}{I} = (1 + K_a [Q])(1 + k_q \tau_0 [Q]) \quad (3)$$

In this equation, I_0 and I are the fluorescence intensity in the absence and in the presence of a quencher, respectively, k_q is the collisional quenching rate, K_a is the

association equilibrium constant, τ_0 is the lifetime of the excited species without the quencher, and $[Q]$ is the concentration of the quencher. In the case of dynamic quenching, plotting I_0/I (or τ_0/τ) vs $[Q]$ will result in a linear plot with a positive slope equal to the product $k_q\tau_0$. In the case of static quenching, I_0/I could instead show as a quadratic curve, differently from τ_0/τ . Typically, the latter ratio will keep constant with $[Q]$ if association is strong and/or the complex is either the dominant emissive species or not emissive at all. With increasing concentrations of the redox-active ester **17a** (which does not absorb in the visible region), the excited-state lifetime was found to be constant, further supporting the formation of a new species in the ground state (**Figure 23**). Although unusual, this observation indicates that the EDA complex is more emissive than the starting benzothiazoline, and discards any dynamic process from the excited state of the free benzothiazoline (**20a***).

The nuclear Overhauser effect is a powerful tool that allows for the detection of supramolecular aggregates by NMR spectroscopy, including EDA complexes.⁸¹ Indeed, the association between **17a** and **20a** was further corroborated by a series ^1H NMR 1D-NOE experiments that clearly evidenced the spatial proximity of the two species when mixed in equimolar amounts in DMSO (**Figure 24,25**).

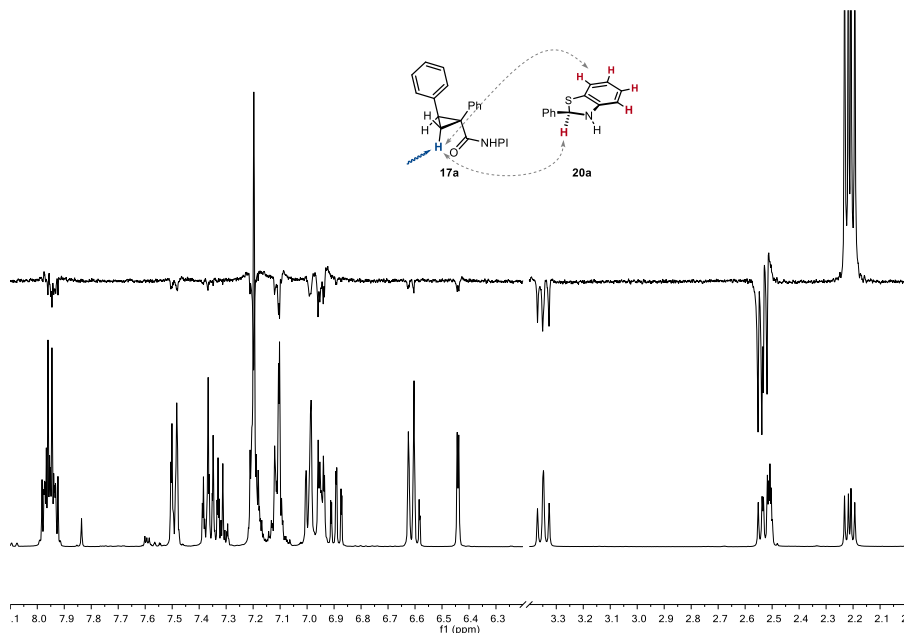


Figure 24: ^1H NMR 1D-NOE experiment of a 1:1 mixture of **17a** and **20a** in DMSO-d_6 . Irradiation at 2.21 ppm, mixing time 750 ms.

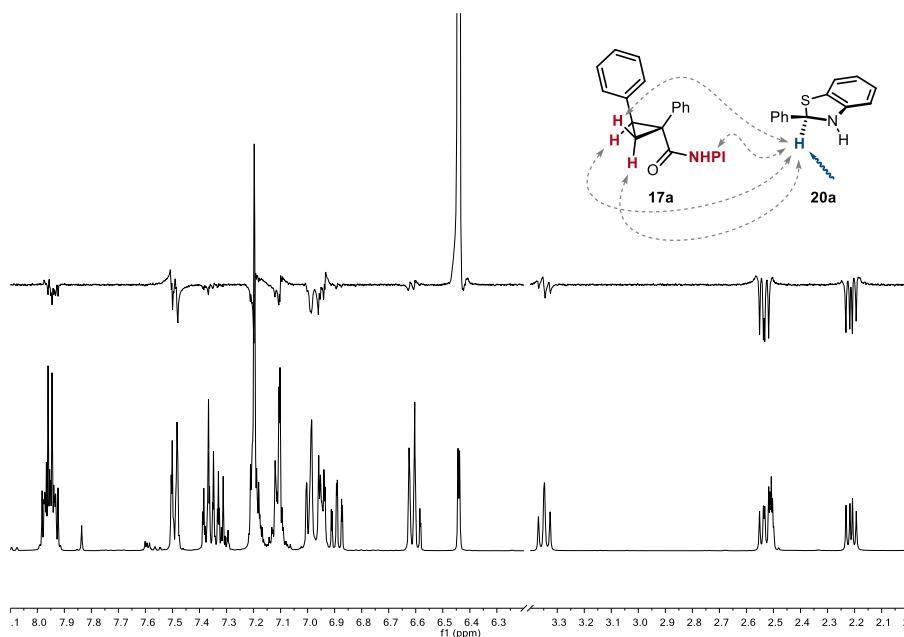


Figure 25: ^1H NMR 1D-NOE experiment of a 1:1 mixture of **17a** and **20a** in DMSO-d_6 . Irradiation at 6.44 ppm, mixing time 750 ms.

Lastly, the quantum yield of the reaction was measured. The quantum yield (Φ) is defined as the ratio of moles of product to the number of photons absorbed, measured in einstein. We calculated the quantum yield using eq. 4 (t = irradiation time; f = fraction of light absorbed by the mixture at 450 nm):

$$\Phi = \frac{\text{moles of } \mathbf{4a}}{\text{photon flux} \times t \times f} \quad (4)$$

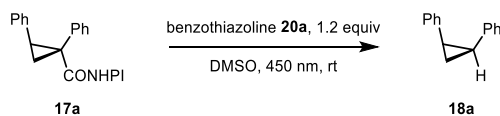
The parameter f can be estimated from the absorbance value as follows (eq. 5):

$$f = 1 - 10^{-A} \quad (5)$$

In our case, this parameter was calculated to be $f = 0.3920$. The photon flux of the spectrofluorometer light source, instead, was measured by standard ferrioxalate actinometry⁸² (eq. 6). In this system, Φ refers to the quantum yield for the potassium ferrioxalate actinometer ($\Phi = 1.01$), and f is the light fraction absorbed at 450 nm by the actinometer (0.99833).⁸²

$$\text{photon flux} = \frac{\text{moles of } \text{Fe}^{2+}}{\Phi \times t \times f} \quad (6)$$

The photon flux was determined after triplicate experiments to equal 3.68 ± 0.22 . Using these values, the quantum yield of the photo-decarboxylation reaction was measured in three separate experiments, summarized in **Table 7** below.

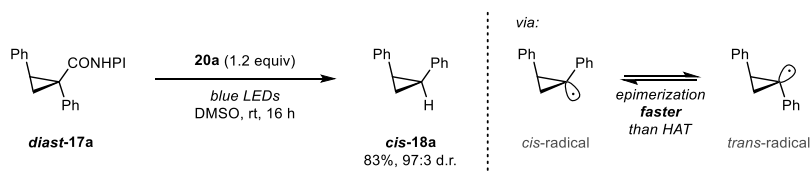


Entry	t (s)	18a (mol·10 ⁻⁵)	Φ	$\Delta \Phi$
1	57600	5.95	0.072	0.06
2	72000	7.65	0.074	0.05
3	86400	13.51	0.108	0.04

Table 7: Determination of the quantum yield of the photodecarboxylative reduction reaction of **17a** (1 mol·10⁻⁵). Moles of product **18a** measured by no-*D* ¹H NMR using 1,2,4,5-tetrachloro-3-nitrobenzene as an internal standard.

The quantum yield of the photochemical process was measured to be $\Phi = 0.09 \pm 0.03$, suggesting that a radical-chain mechanism is unlikely operational, opposite to related dihydropyridine systems.⁷⁵

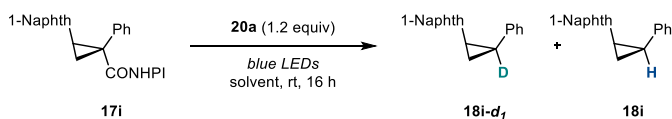
After characterizing the chromophore of this transformation, we additionally performed a set of experiments to obtain a complete mechanistic picture. The high levels of diastereoselectivity can be explained by two possibilities: a kinetically controlled HAT process (our initial hypothesis), or rapid a stereoretentive HAT before epimerization of the cyclopropyl radical. To discern which alternative is operational, the diastereomer **diast-17a** of our model substrate was synthesized by *Z*-selective desilylation of a silyl cyclopropane carboxylate precursor,⁸³ and subjected to the photodecarboxylative reduction conditions. We observed similar yield and stereoselectivity for **cis-18a**, indicating that the epimerization of the cyclopropyl radical happens at a faster rate than hydrogen atom transfer (**Scheme 33**).



Scheme 33: Stereoinversion experiment of **diast-17a**. The reaction was performed under inert atmosphere. Reaction conditions: **diast-17a** (1 equiv), **20a** (1.2 equiv), dry DMSO (0.1 M), blue LEDs (450 nm), 16 h. Yield is measured by ¹H NMR using 1,1,2,2-tetrachloroethane as an internal standard. Diastereomeric ratio determined by GC-MS.

Finally, we questioned which hydrogen atom in the benzothiazoline **20a** is transferred to the product. Benzothiazoline radical cations possess two hydrogen atoms that can be transferred during the HAT process, one at the benzylic position and the one bonded to nitrogen. To evaluate their relative contribution, we carried out a number of deuterium labeling experiments (**Table 8**). Firstly, the reaction of benzothiazoline **20a-d₁** bearing one deuterium atom at the benzylic position afforded the product in 56% yield and 70% deuterium incorporation (entry 1). On the other hand, the use of

the analog deuterated at nitrogen **20a-d₁'** resulted in negligible labeling and higher yield (77%, entry 2). Consistent with the previous observations, performing the reduction with doubly deuterated benzothiazoline **20a-d₂** yielded an almost fully deuterated cyclopropane product **20a-d₁** (entry 3). Finally, we ruled out any major involvement of the solvent in this transformation by employing DMSO-*d*₆ (entry 4). These results altogether suggest that the main hydrogen atom donor is the benzylic C–H bond, while the N–H moiety plays a minor role, possibly through the imine tautomer.⁸⁴



Entry	Reductant	Solvent	Yield (%)	d.r.	18i-d₁:18i
1	20a-d₁	DMSO	56	88:12	70:30
2	20a-d₁'	DMSO	77	92:8	< 5:95
3	20a-d₂	DMSO	52	88:12	> 90:10
4	20a	DMSO- <i>d</i> ₆	84	92:8	< 5:95

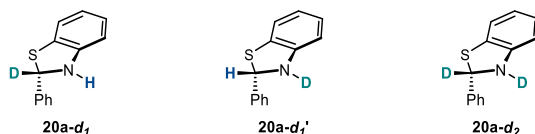
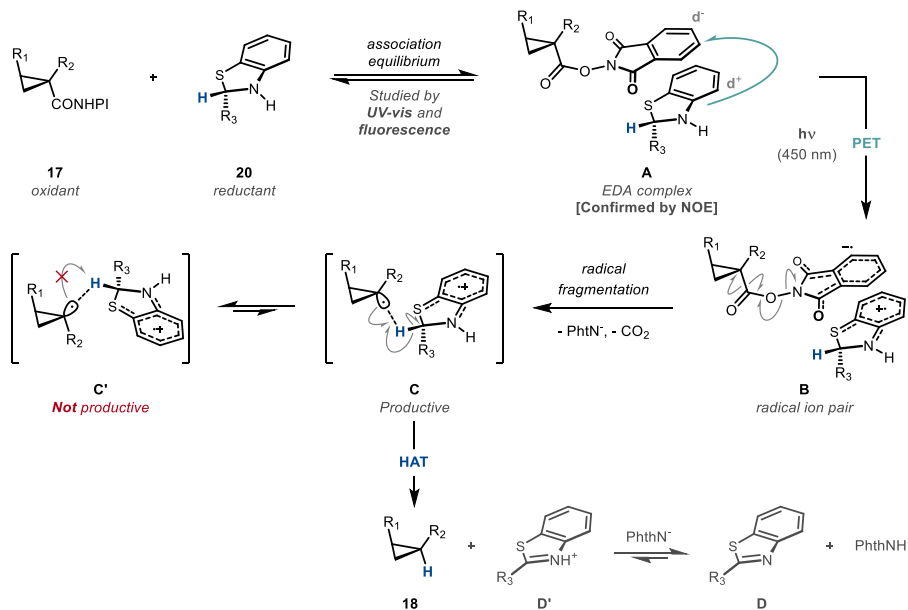


Table 8: Deuteration experiments. Reactions were performed under inert atmosphere. Reaction conditions: **17i** (1 equiv), **20a** (1.2 equiv), dry DMSO (0.1 M), blue LEDs (450 nm), 16 hours. Yields and diastereomeric ratios are measured by ¹H NMR using 1,1,2,2-tetrachloroethane as an internal standard.

4.3.4 Proposed mechanism

With this data in hand, the following mechanism can be proposed (**Scheme 34**). Redox-active esters **17** and benzothiazolines **20** associate in solution to form the EDA complex **A**, where electron-rich **20** acts as the donor and **17** acts as the acceptor. The formation of the EDA complex is validated by the photochemical studies described before (**Section 4.3.3**), as well as by the direct observation by ¹H NMR 1D-NOE experiments in DMSO (**Section 4.3.3**). Under visible light irradiation, photo-induced electron transfer (PET) occurs between the two species, generating ion pair **B**. After fragmentation of the NHPI moiety, with loss of CO₂ and phthalimide anion, the resulting cyclopropyl radical can abstract a hydrogen atom from the benzothiazoline radical cation (**C**), mainly from the benzylic C–H bond. This kinetically controlled HAT process selectively yields the *cis*-cyclopropane product **18**, together with a stoichiometric amount of benzothiazole by-product after loss of a proton. The alternative possibility of the cyclopropyl radical abstracting a hydrogen atom directly from benzothiazoline **20** would lead to a radical-chain mechanism that seems unlikely in this case based on the quantum yield measurements. It is worth noting that the benzothiazoline **20** plays a triple role as self-sensitized photoreductant (**A** → **B**),

highly stereoselective HAT reagent (**C** \rightarrow **18**), and Brønsted acid to neutralize the basic phthalimide by-product (**D'** \rightarrow **D**).



Scheme 34: Mechanistic model for the photodecarboxylative reduction.

4.4 Conclusions and outlook

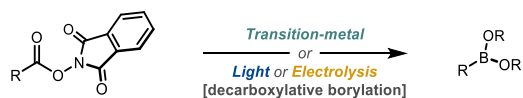
A general and highly selective methodology towards enantioenriched *cis*-diarylcyclopropanes was developed. This modular protocol allows for quick access to highly strained compounds starting from unfunctionalized olefins, ultimately facilitating the synthesis of rigid ligands and conformationally restricted medicinal candidates. These advances were enabled by the discovery of an EDA complex between benzothiazolines and NHPI esters, leading to a highly efficient and stereoselective photo-decarboxylation of cyclopropyl NHPI-esters. The mechanism underlying this transformation was thoroughly studied, revealing that, unlike dihydropyridines, benzothiazolines can act as self-sensitized photoreductants, highly stereoselective HAT reagent, and Brønsted acid. Aside from enantiomerically enriched *cis*-cyclopropanes, this work introduced benzothiazolines as a new platform to develop engineered HAT reagents for self-sensitized reactions.

5. Photo-organocatalytic Decarboxylative Borylation Mediated by a Transient Non-Symmetrical Diboronic Acid Monoester

5.1 Introduction

The direct conversion of simple available starting materials into valuable building blocks is central to the development of organic chemistry. Among such transformations, the conversion of carboxylic acids to boronic acid derivatives through redox-active esters (**Table 9**) has attracted significant attention in recent years.^{34e, 34g-i, 34q, 34w} This reaction involves the generation of a radical intermediate upon reduction of a redox-active ester and its subsequent borylation using a variety of diboron reagents, leading to boronic ester derivatives. For these transformations it is often required the use of transition-metal catalysts,^{34h, 34i, 34q} and/or the use B_2cat_2 or B_2pin_2 as the boron source.^{34e, 34g, 34i, 34q} In particular, B_2cat_2 has demonstrated to be an efficient borylating agent,⁸⁵ and has been adopted in the reductive borylation of several substrates including halides,⁸⁶ alcohols⁸⁷ and Katritzky's salts.⁸⁸ Despite the evident advantages of cheap and stable diboronic acid $B_2(OH)_4$ as the borylating agent, its use is generally uncommon and has been utilized only once in the context of decarboxylative borylation requiring an expensive iridium catalyst.^{34h}

We have recently demonstrated the enantioselective synthesis of cyclopropyl-boronates in a two-step protocol based on the transfer of a redox-active carbene and decarboxylative borylation (see **Chapter 2**).⁴⁸ This approach enabled the synthesis of pharmaceutically and synthetically relevant borylated cyclopropanes with high stereoselectivity. We observed that among the various methods reported, the photochemical protocol reported by Aggarwal and co-workers^{34g} was the one that performed best with the highly reactive cyclopropyl radical intermediates. However, we found that yield and reaction time were dependent on the different batches of solvent and B_2cat_2 used in the reaction.



Author (year)	R =	Boron source (equiv)	Conditions (equiv)	Solvent	Yield (%)
Glorius (2017) ^{34c}	Aryl	B ₂ pin ₂ (3.5)	Cs ₂ CO ₃ (0.5) Pyridine (1.5) <i>Blue LEDs</i>	EtOAc	28-89
Aggarwal (2017) ^{34g}	1 ^{ary} , 2 ^{ary} , activated 3 ^{ary}	B ₂ cat ₂ (1.25)	<i>Blue LEDs</i>	DMA	25-90
Li (2017) ^{34h}	1 ^{ary} , 2 ^{ary}	B ₂ (OH) ₄ (4)	[Ir] (0.01) 45 W CFL	DMF	40-84
	1 ^{ary} , 2 ^{ary}	B ₂ pin ₂ (4)	[Ir] (0.01) 45 W CFL	DMF: MeCN:H ₂ O	54-84
Baran (2017) ³⁴ⁱ	1 ^{ary} , 2 ^{ary} , 3 ^{ary}	B ₂ pin ₂ ·MeLi (3)	NiCl ₂ ·6H ₂ O (0.1) dMeO-bpy (0.13) MgBr ₂ ·Et ₂ O (1.5)	THF:DMF	23-87
Baran, Blackmond (2018) ^{34q}	1 ^{ary} , 2 ^{ary} , 3 ^{ary}	B ₂ pin ₂ (3)	Cu(acac) ₂ (0.3) LiOH·H ₂ O (15) MgCl ₂ (1.5)	Dioxane:DMF	35-85
Baran (2021) ^{34w}	1 ^{ary} , 2 ^{ary} , activated 3 ^{ary}	B ₂ cat ₂ (1.5)	LiBr (0.3) <i>graphite electrodes</i>	CH ₂ Cl ₂ :DMF	38-84

Table 9: State-of-the-art in the decarboxylative borylation of redox-active esters. CFL: compact fluorescent lightbulb. dMeO-bpy: 4,4'-dimethoxy-2,2'-bipyridine.

5.2 Aim of the project

The fluctuations in the performance of the decarboxylative borylation of redox-active cyclopropyl esters indicate that an unknown parameter, critical for this reaction, has remained unnoticed. Although kinetic studies are particularly primed to find new directions for reaction development,^{65, 89} the acquisition of high-density time profiles in photochemical reactions are particularly difficult. We recognized that the recent implementation of NMR monitoring in visible-light photochemical reactions using optic fibers by Gschwind and co-workers,⁹⁰ while not commonly employed, would allow us to gather relevant information on this system. Thus, we set out to unravel the mechanistic details that were responsible for the variable performance of our decarboxylative borylations. We were aware that these findings could have a broader impact beyond our case-study, given the increasing number of radical borylation methods using B₂cat₂.⁸⁶⁻⁸⁸ Additionally, given the importance of chiral cyclopropyl-boronate products **5** in medicinal chemistry and asymmetric synthesis, we aimed at developing an improved borylation system. Ideally, it would be able to efficiently turn redox-active esters, including the highly reactive cyclopropyl esters **3**, in boronate derivatives in the absence of any transition-metal catalyst or external photocatalyst.

5.3 Results and discussion

5.3.1 NMR study of the decarboxylative borylation

We began our investigation monitoring the reaction profile by *in situ* ^1H NMR spectroscopy, which has the advantage of being a non-destructive and high-resolution technique. The decarboxylative borylation reactions, unlike other reactions with highly absorbing photo-catalysts, are essentially transparent reactions that require powerful light input to perform. This posed the challenge of accurately reproducing the photochemical conditions required for this reaction within an NMR spectrometer. As a solution, we utilized three optic fibers⁹⁰ to guide blue light from the same LED emitters that we used in preparative experiments to the sample under analysis. Given the known ability of amide solvents to be involved in radical chain mechanisms,⁹¹ we opted for the use non-deuterated solvents in the NMR experiments to allow the detection of any solvent-derived species, as well as to avoid affecting the reaction rate due to possible kinetic isotope effects. Preliminary experiments showed similar results when using DMF instead of DMA as the reaction solvents, in agreement with Aggarwal's findings,^{34g} and we therefore decided to employ DMF to study the system to facilitate NMR monitoring. It was observed that under rigorously dried and anhydrous conditions, the reaction of NHPI ester **23** displays two different regimes: after an initial fast conversion, the reaction adopts a slower, steady zero-order regime (**Figure 26**). Based on this observation, and the different performances from different solvent sources, we hypothesized that water content in the solvent and starting materials could be a source of irreproducibility and we therefore decided to test its effect in the reaction. As shown in **Figure 26**, as little as 12.5 mol% of water in the mixture resulted in increased initial rate, followed by a zero-order regime with the same slope as the reaction run under anhydrous conditions. This rate-enhancing effect is amplified by the presence of additional water (25-75 mol%), where the zero-order regime is no longer observed, and the reaction is complete within 90 minutes. Thanks to the *in situ* reaction monitoring, we could also witness the decomposition of the catechol boronate product **24** at high conversion. Moreover, the onset of this process was dominant earlier with higher water concentration, even though it occurred with identical rate. From these experiments, it is clear that the water content of the solvent plays a critical role in defining the overall performance of the decarboxylative borylation.

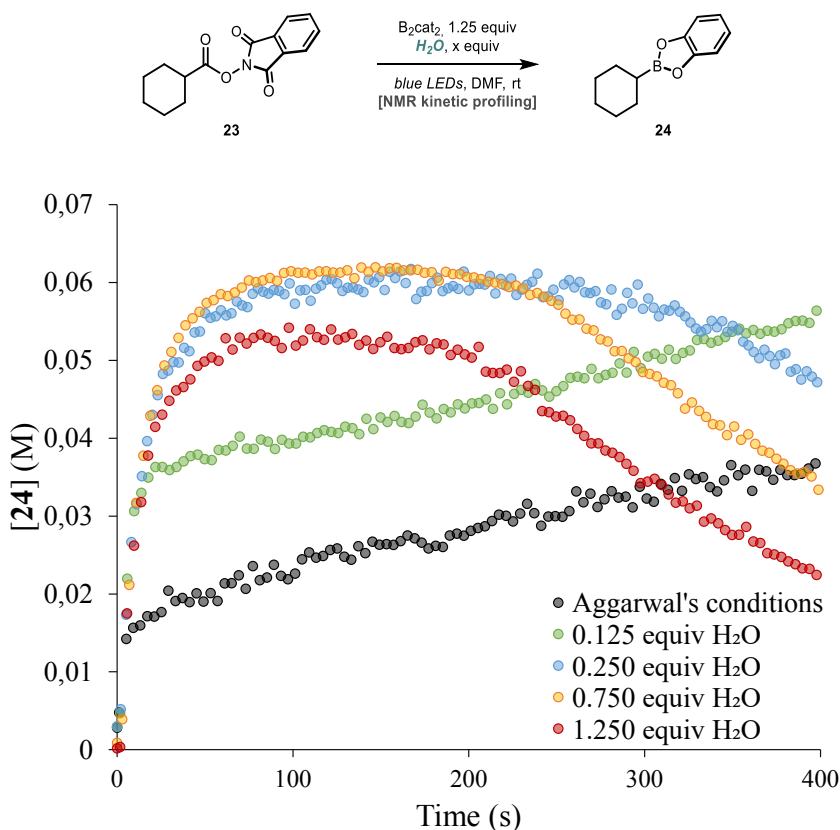


Figure 26: Kinetic profiles of the decarboxylative borylation reaction mediated by B_2cat_2 in the presence of water.

A careful speciation of these reactions revealed that B_2cat_2 was present in the reaction media only in the absence of moisture, whereas a new species became dominant in the presence of water. The abundance of this species correlates with the longer fast initial regimes, suggesting that it is a more competent reagent than B_2cat_2 for this transformation. This species was identified as the non-symmetrical diboron reagent (cat)BB(OH) $_2$ and confirmed by independent synthesis. NMR titration of B_2cat_2 with H_2O (Figure 27, left) or $B_2(OH)_4$ with catechol **25a** (Figure 27, right) demonstrated that the mixed boron species (cat)BB(OH) $_2$ is the thermodynamically favored species under the reaction conditions. Importantly, the formation of B_2cat_2 from $B_2(OH)_4$ and catechol **25a**, even with superstoichiometric amounts was never observed (Figure 27, right). This is probably due to the water formed in the condensation towards (cat)BB(OH) $_2$.

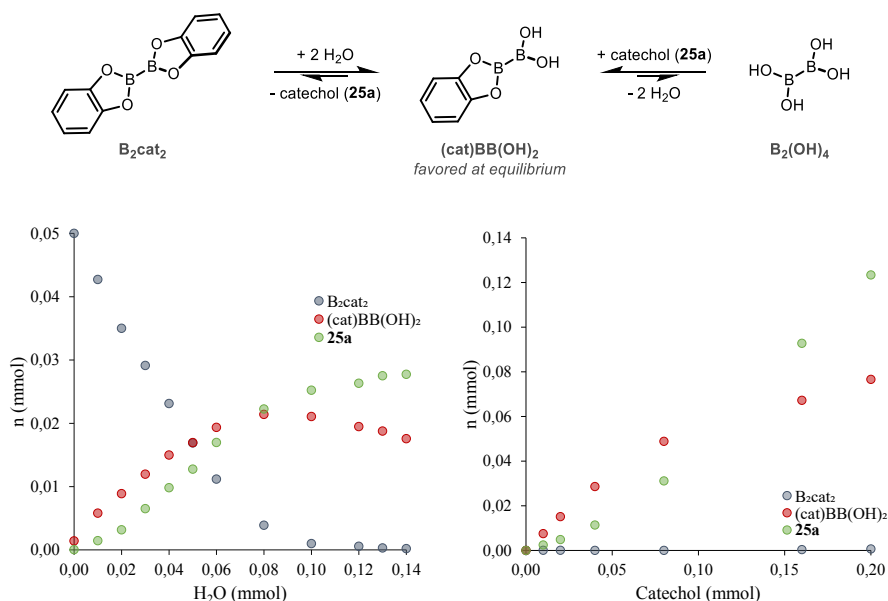
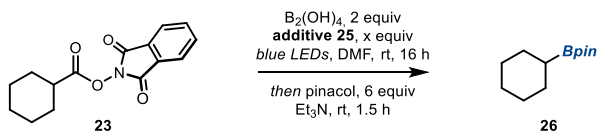


Figure 27: NMR titrations of diboron species involved in the decarboxylative borylation reaction. Left: NMR titration of B_2cat_2 with water in DMF. $[B_2cat_2]_0 = 0.1$ M. Right: NMR titration of $B_2(OH)_4$ with catechol **25a** in DMF. $[B_2(OH)_4]_0 = 0.1$ M.

5.3.2 Optimization of the decarboxylative borylation

Our initial observations suggested that the yield of this transformation can suffer from product decomposition. In contrast to catecholboronates, free boronic acids display a much higher stability towards degradation. We hypothesized that a stoichiometric amount of $B_2(OH)_4$ in combination with a catalytic catechol **25** would allow to generate the highly efficient $(cat)BB(OH)_2$ reagent, while keeping the concentration of water high enough to hydrolyze any catechol boronate product to the boronic acid. It was already reported by Aggarwal that the stoichiometric combination of catechol **25a** and tetrahydroxydiboron $B_2(OH)_4$ (believed to generate B_2cat_2 *in situ*) was effective although less efficient than B_2cat_2 in the decarboxylative borylation.^{34g} We were aware that in order to obtain catalysis with substoichiometric amounts of catechol, the latter would necessarily have a higher affinity towards $B_2(OH)_4$ than the boronic acid product.



Entry	Additive	x (equiv)	Yield (%)
1	-	-	25
2	25a	0.2	78
3	25b	0.2	41
4	25c	0.2	97
5	25c	0.1	80
6	25d	0.2	64
7	25e	0.2	14
8	25f	0.2	15
9	25g	0.2	46

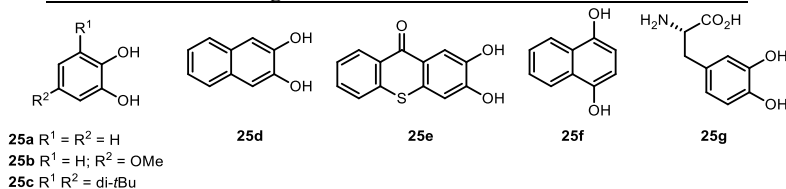


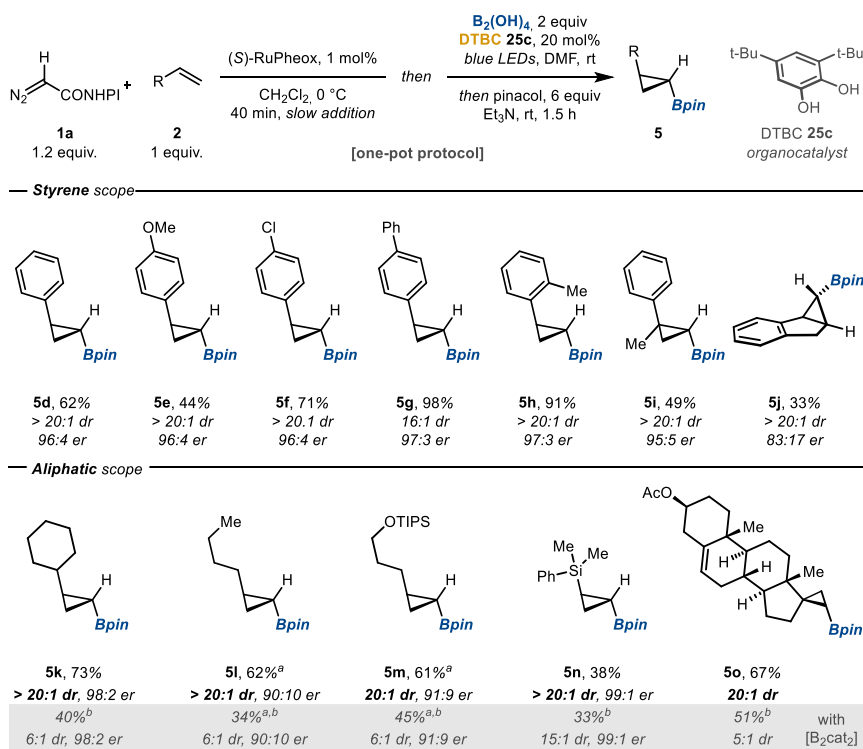
Table 10: Additive screening for the decarboxylative borylation reaction. Reactions were performed under inert atmosphere. Reaction conditions: Redox-active ester **23** (1 equiv), B₂(OH)₄ (2 equiv), additive **25** (x equiv), dry DMF, blue LEDs (450 nm), rt, 16 h, then pinacol (6 equiv), Et₃N (60 equiv), rt, 1.5 h. Yields are measured by ¹H NMR using 1,1,2,2-tetrachloroethane as an internal standard.

Indeed, the use of 20 mol% catechol **25a** could generate the desired boronic acid product at a faster rate compared to the reaction with B₂cat₂ (Table 10, entry 2). Using these conditions, we were able to screen different dihydroxybenzene catalysts without preparing the corresponding diboronic esters (Table 8). While poor reactivity was observed with *m*-methoxycatechol **25b** (entry 3), the electron-rich and sterically hindered 3,5-di-*tert*-butylcatechol (DTBC, **25c**) appeared to be the fastest and higher yielding catalyst for this transformation, displaying good performance in the borylation reaction using loadings as low as 10 mol% (entries 4,5). Only moderate yields were obtained using 2,3-dihydroxynaphthalene (**25d**; entry 6). In contrast, thioxanthone **25e**, 1,4-dihydroxynaphthalene (**25f**) and L-DOPA derivative **25g** displayed poor efficiency (entries 7-9). During the progress of the reaction, it was possible to detect a steady concentration of a DTBC containing species, while no free DTBC was observed. We confirmed by independent synthesis that the reaction does not proceed through the intermediacy of B₂(DTBC)₂, analogous to Aggarwal's system. Instead, we were able to determine by HRMS and NMR titration experiments that the non-symmetrical (DTBC)BB(OH)₂ species was dominant in the equilibrium and B₂(DTBC)₂ was poorly soluble in DMF at the reaction concentration. The fact that there were no precipitate in preparative experiments and B₂(DTBC)₂ was not detected by ¹H NMR of the reaction mixture, strengthens the notion that

(DTBC)BB(OH)₂ is the active diboron species in the system. Currently, our group is gathering additional kinetic data to further corroborate this hypothesis.

5.3.3 Scope of the borocyclopropanation of olefins

The simplicity of this photo-organocatalytic system enabled a telescoped cyclopropanation/decarboxylative borylation protocol using NHPI-DA **1a**, resulting in a formal enantioselective borocyclopropanation of unactivated olefins (**Scheme 35**).



Scheme 35: Scope of telescoped cyclopropanation/borylation reaction. Reactions were performed under inert atmosphere. Reaction conditions: **1a** (1 equiv), (S)-RuPheox (1 mol%), dry CH₂Cl₂, 0 °C, slow addition over 40 minutes. Then, B₂(OH)₄ (2 equiv), 3,5-di-*tert*-butylcatechol **25c** (0.2 equiv), dry DMF, blue LEDs (450 nm), rt, 5 h, then pinacol (6 equiv), Et₃N (60 equiv), rt, 1.5 h. Reported yields are isolated. Diastereomeric ratios determined by ¹H NMR. Enantiomeric ratios determined by chiral HPLC or chiral GC-MS. ^a: Enantiomeric ratio determined after oxidation-benzoylation of the pinacolboronate. ^b: Reaction performed with B₂cat₂ (1.25 equiv) instead of B₂(OH)₄ and 3,5-di-*tert*-butylcatechol, and dry DMA instead of dry DMF as the solvent.

Initially, we evaluated the performance of nucleophilic styrenes (**5d-j**), including ortho-substituted (**5h**), 1,1'-disubstituted (**5i**) and cyclic 1,2-disubstituted olefins (**5j**), with good results and enantioselectivities. The presence of electron-donating (**5e,g**) and electron-withdrawing (**5f**) groups was tolerated in this transformation. Aliphatic

olefins are known to be challenging not only for their poor reactivity, but for their intrinsic low stereoselectivities due to their flexible side chains. To our delight, we observed good results in terms of diastereoselectivity and yields with unactivated substrates (**5k-o**), including branched (**5k**) and linear (**5l,m**) aliphatic olefins, as well as the complex steroid derivative **5o**. Additionally, these reaction conditions were compatible with the presence of silylated moieties, both linked to oxygen (**5m**) or directly to the cyclopropane ring (**5n**). For comparison, we have also run the same borylations with B_2cat_2 , observing consistently lower diastereoselectivities and yields. While the difference in yield may be a consequence of the higher water content and substoichiometric catechol catalyst, the difference in diastereoselectivity suggests that the cyclopropyl radical is captured by a more selective diboron species. Given the enhanced steric bulk around the boronic ester unit in $(DTBC)BB(OH)_2$, we logically expect this to be the source of the differential stereoselectivity observed.

5.3.4 Proposed mechanism

Based on the mechanism generally accepted in decarboxylative borylations with B_2cat_2 ,^{34g, 86a} we propose the mechanism shown in **Figure 28**. $B_2(OH)_4$ reacts with one molecule of DTBC **25c** to give the non-symmetric diboron species $(DTBC)BB(OH)_2$. Further esterification to yield the symmetric $B_2(DTBC)_2$ has not been detected. Lewis acidic $(DTBC)BB(OH)_2$ can coordinate one molecule of redox-active ester **3** and one of DMF solvent (intermediate **A**), or alternatively the solvent alone (intermediate **B**). Upon irradiation, radical fragmentation of aggregate **A** occurs, generating the cyclopropyl radical intermediate **C** and initiating the radical chain. The DMF adduct **B** can react with radical **C** to yield the final cyclopropyl boronate **5** *via* intermediate **D**. In principle, the DMF adduct of $B_2(OH)_4$ could also be responsible for the radical capture, but we deem this possibility unlikely based on the higher stereoselectivities observed. In turn, the generation of **5** produces the reductant **E**,^{86a} that can propagate the radical chain by single electron transfer to the substrate **3**, ultimately generating boronic acid derivative **F**.

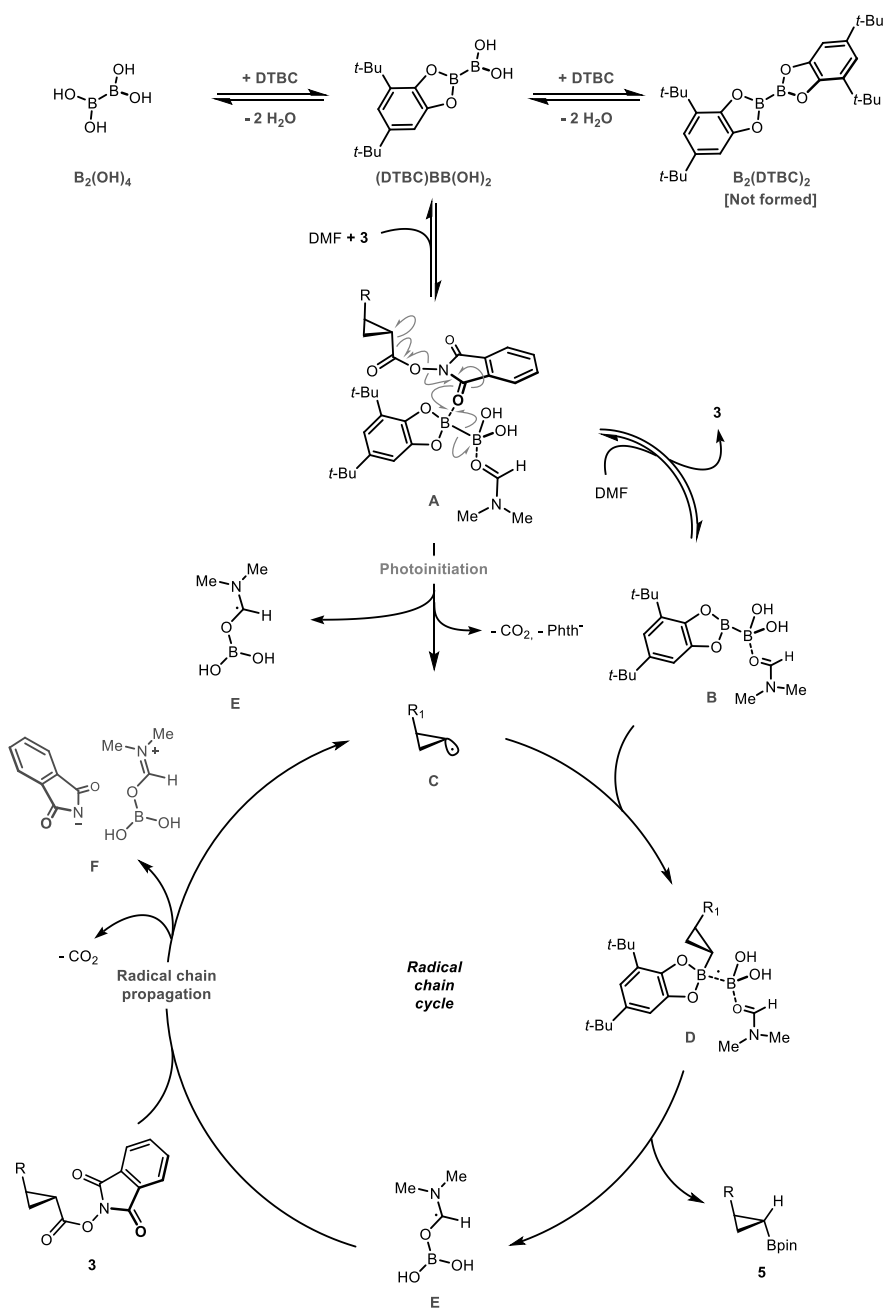


Figure 28: Mechanistic proposal for the photo-organocatalytic borylation reaction.

5.4 Conclusions and outlook

In summary, the decarboxylative borylation was investigated by means of NMR spectroscopy and kinetic analysis. The insights gathered from this study allowed to identify the origin of the irreproducibility of this transformation and recognized for the first time non-symmetrical diboronic acid monoesters as the reaction mediators. Importantly, we were able to utilize this information to develop a new catalytic and robust protocol towards boronic acid derivatives, which was implemented in a telescoped cyclopropanation/borylation reaction. In particular, this methodology provided superior diastereoselectivity compared to existing methods. Overall, this approach enables the synthesis of valuable borylated building blocks in a straightforward and highly efficient manner. More results in terms of scope and mechanistic investigation are ongoing in our laboratories and will provide a comprehensive understanding of the processes operating in this photo-organocatalytic system.

6. Concluding remarks

The thesis presented herein describes different approaches towards the enantio- and diastereoselective synthesis of functionalized cyclopropanes exploiting the chemistry of redox-active carbene precursors. In **Chapter 2**, a unified asymmetric synthesis of cyclopropanes decorated with different functionalities is reported. These important molecules previously required long synthetic sequences due to the instability of the functionalized methylenes that would be required. To overcome these difficulties, a redox-active diazocompound reagent (NHPI-DA) was developed and its use in asymmetric cyclopropanation reactions was explored. It was found that with the metallacyclic ruthenium catalyst RuPheox this transformation could be carried out on an unprecedented wide-range of olefin substrates, including challenging aliphatic and electron-deficient ones. The use of RuPheox and NHPI-DA in this transformation allowed for the synthesis of unrelated cyclopropane families (*i.e.* cyclopropylboronates, cyclopropylamines, cyclopropanols, etc.) from a single precursor, exploiting the diverse chemistry of redox-active esters. The synthesis of the same classes of compounds was previously achieved using tailored methodologies that required specific starting materials (such as allylic alcohols, cyclopropenes and Michael acceptors), customized catalysts for each substrate class (transition-metal complexes or artificial enzymes) and tailored carbene precursors. The utility of the methodology reported herein was illustrated with the synthesis of chiral cyclopropane fragments of drug and bioactive compounds (Ticagrelor, Grazoprevir and belactosin A), a building block towards (–)-spongidepsin, and the total synthesis of the natural product (–)-dictyopterene. These compounds were previously obtained by much longer synthetic routes involving expensive reagents or pre-formed starting materials, and can now be assembled with a single carbene precursor and catalyst combination through a unified synthetic strategy. In **Chapter 3**, the performance of the NHPI-DA/RuPheox system was investigated in a combined experimental and computational work, in collaboration with the Himo group (Stockholm University). This study required the use of experimental techniques (nucleophilic benchmarking, nitrogen evolution monitoring, *in situ* HRMS analysis and variable-time normalization analysis) in combination with DFT calculations to gain insight on this rapid carbene-transfer reaction. This work demonstrated how the unparalleled performance of NHPI-DA in the cyclopropanation of unactivated olefins stems from the intrinsically low nucleophilicity of the diazocompound, minimizing the dimerization side-reaction. Diazocompound nucleophilicity was previously not recognized as a focus area in the development of carbene-transfer reactions. Moreover, the possibility of a migratory insertion of the carbene in the cyclometallated ligand was deemed favorable by DFT calculations, and although a set of control experiments demonstrated that this species does not play a major role in carbene-transfer to styrene substrates, it should be considered in future studies of related reactions. In **Chapter 4**, the enantioselective synthesis of *cis*-diarylcyclopropanes from styrenes is described. These highly strained molecules previously required allylic alcohol substrates, enantiopure boronate intermediates or stoichiometric chiral benzyldiene complexes with a limited scope. In

contrast, the alternative synthesis of these compounds reported herein takes advantage of dirhodium(II)-catalyzed asymmetric cyclopropanation using the redox-active aryldiazoacetates recently developed in our group. The intermediate cyclopropyl redox-active esters were converted in situ into *cis*-diarylcyclopropanes through a new efficient and stereoselective reaction mediated by 2-substituted benzothiazolines (BTAs). These reagents were not known to act as self-sensitized photoreductants, and their features have been thoroughly investigated by means of excited-state lifetime measurements, fluorescence and NMR spectroscopy. This study revealed that benzothiazolines operate through an electron donor-acceptor complex with the redox-active ester substrate. Unlike related photo-decarboxylations mediated by dihydropyridines (such as Hantzsch esters and nicotinamides), benzothiazolines did not operate *via* a radical-chain mechanism. In **Chapter 5**, the development of a new decarboxylative borylation reaction and preliminary applications are reported. These findings are a consequence of a mechanistic study aimed at determining the origin of fluctuations in the performance of the known photochemical decarboxylative borylation employing bis(catecholato)diboron. It became apparent that the water content of the solvent plays accelerates the rate of this transformation, and the alkylboronate product was unstable in the reaction conditions. It was possible to identify a new species, the non-symmetrical diboronic acid monoester (cat)BB(OH)₂, as the dominant species during the faster reactions. This led to the development of a photo-organocatalytic decarboxylative borylation reaction employing catalytic amounts of 3,5-di-*tert*-butylcatechol, and the cheaper and more stable diboronic acid as stoichiometric boron source. This reaction was implemented in a telescoped cyclopropanation/borylation protocol towards enantioenriched cyclopropyl boronates, with excellent results. Importantly, when using conformationally flexible olefin substrates, we observed a significant increase in the diastereoselectivity of the reaction compared to the original process using bis(catecholato)diboron by Aggarwal and co-workers. These observations support the different reactivity of non-symmetrical diboronic acid monoesters in the borylation of alkyl radicals. Further mechanistic experiments and scope investigations are currently ongoing in our group.

Appendix A – Contribution list

- I. Synthesized 50% of the final products reported. Optimized the cyclopropanation reaction together with Dr. Marc Montesinos-Magraner. Synthetic applications together with Dr. Marc Montesinos-Magraner. Assisted in writing the manuscript and the supporting information.
- II. Took part in the design of the project. Performed the stoichiometric and sequential cyclopropanation experiments. Performed the branching ratio kinetic experiments. Performed the VTNA analysis of the cyclopropanation reaction of 1-hexene. Performed the *in situ* HRMS study. Took part in discussions regarding the DFT calculations performed by Dr. Ferran Planas. Wrote the experimental section of the manuscript and wrote the experimental supporting information.
- III. Took part in the design of the project. Optimized the cyclopropanation reaction and the decarboxylative reduction. Synthesized all the final products reported. Performed the mechanistic control experiments. Performed the photophysical studies. Wrote the manuscript and the supporting information.
- IV. Synthesized the final products reported in the scope study and benchmarking against the Aggarwal's decarboxylative borylation protocol.

Appendix B – Reprint permissions

Reprint permissions were granted by the publishers for each publication (listed by their roman numerals):

- I. Montesinos-Magraner, M.†; Costantini, M.†; Ramirez-Contreras, R.; Muratore, M. E.; Johansson, M. J.; Mendoza, A.
Angew. Chem. Int. Ed. **2019**, 58, 5930–5935.
Copyright © 2019 Wiley-VCH Verlag GmbH & Co. KGaA, Weinheim.
- II. Planas, F. †; Costantini, M. †; Montesinos-Magraner, M.; Himo, F.; Mendoza, A.
ACS Catal. **2021**, 11, 10950–10963.
Copyright © 2021 The American Chemical Society.
- III. Costantini, M.; Mendoza, A.
Pre-print DOI: 10.33774/chemrxiv-2021-2f4mc.

Appendix C – Experimental Data for Chapter 2-4

Full experimental data and supporting information for Chapter 2 can be found at:
<https://onlinelibrary.wiley.com/doi/10.1002/anie.201814123>

Raw NMR, HPLC and HRMS data for Chapter 2 can be downloaded at:
<https://doi.org/10.5281/zenodo.2542646>

Raw crystallographic data for Chapter 2 can be downloaded at:
<https://doi.org/10.5281/zenodo.2542759>

Full experimental data and supporting information for Chapter 3 can be found at:
<https://pubs.acs.org/doi/10.1021/acscatal.1c02540?ref=PDF>

Full experimental data and supporting information for Chapter 4 can be found at:
<https://chemrxiv.org/engage/chemrxiv/article-details/60ccaea5926ad04a6301eb05>

Acknowledgments

I would like to thank *Dr. Abraham Mendoza* for support and mentorship throughout these years of research, and for his supervision during the development of these projects.

My gratitude goes to *Prof. Belén Martin-Matute* and my co-supervisor *Prof. Joseph Samec* for proof-reading this thesis and for their valuable comments. I would also like to thank *Prof. Fahmi Himo* and *Dr. Ferran Planas* for their great contribution to our joint mechanistic study, and our collaborators at AstraZeneca, *Dr. Magnus J. Johansson* and *Dr. Michael E. Muratore* for their collaboration in my first project. Finally, I am thankful to all the *PI's* of the department for sharing their interesting research and their suggestions.

I would like to thank *Prof. Armido Studer* for accepting to be the opponent of this doctoral dissertation, *Prof. Christine Dyrager*, *Prof. Peter Dinér* and *Prof. Annette Bayer* for being members of the examination committee.

Thanks to all the *TA staff*, past and present, for their continuous support.

To *Alba (Helena) Pérez Jimeno*, *Dr. Alberto Abengózar*, *Beatriz Meana*, *Carolin Kalff*, *Catarina Santos*, *Dr. Elisa Martinez de Castro*, *Emanuele Silvi*, *Dr. Gàbor Elek*, *Jesper Schwarz*, *Dr. Kilian Colas*, *Lara Lavrenčič*, *Dr. Marc Montesinos-Magraner*, *Dr. My Linh Tong*, half-doctor *Rajdip Chowdhury*, *Dr. Rodrigo Ramirez*, *Dr. Stef(ph)anie Kohlhepp*, *Dr. Stefano Parisotto*, *Xandro Vidal*, *Dr. Xiang Yin*, *Dr. Zhunzhun Yu*, *Zainab Alsaman*, thank you. With our discussions and fun moments, you made my stay in Stockholm one of the best experiences of my life.

A big thank you to all the people of the department that I have been hanging out with, who made these years an amazing time beyond expectations! Here are some of the names (although I will forget someone for sure): *Alba Carretero Cerdán*, *Alejandro Valiente Sanchez*, *Alessandro Ruda*, *Axel Furevi*, *Bram Peters*, *Dr. Cristiana Margarita*, *Daria Lebedeva*, *Dr. Davide Di Francesco*, *Davide Rigo*, *Dr. Elena Subbotina*, *Ester Di Tommaso*, *Federico Riu*, *Flavia Ferrara*, *Dr. Gabriella Kervefors*, *Gonzalo Castiella Ona*, *Dr. Gurpreet Kaur*, *Dr. Haibo Wu*, *Igor Lebedev*, *Jianping Yang*, *Kuntawit Witthayolankowit*, *Dr. Laura Castoldi*, *Luca Massaro*, *Marie Deliaval*, *Mario Prejanò*, *Dr. Marvin Lübcke*, *Dr. Pablo Martínez Pardo*, *Pedro Tortajada Palmero*, *Phan Vu Duc Ha*, *Suthawan Muangmeesri*, *Dr. Sybrand Jonker*, *Dr. Thanya Rukkijakan*, *Víctor García Vázquez*. Also, *Brando Adranno*, *Fabio Begnini*, *Francesco Nosenzo*, *Riccardo Costalunga*, *Tran Nguyen Quynh Chau* and *Yajuan Peng*, who are not from the department but still meant a lot.

Last but not least, to my *family*. Siete sempre stati al mio fianco, nonostante la distanza che ci separava. Non sarei stato nulla senza di voi, grazie di cuore.

References

- (a) Kulinkovich, O. G., *Cyclopropanes in Organic Synthesis*. 2015; (b) Craig, A. J.; Hawkins, B. C., The Bonding and Reactivity of α -Carbonyl Cyclopropanes. *Synthesis* **2020**, 52 (01), 27-39; (c) Pirenne, V.; Muriel, B.; Waser, J., Catalytic Enantioselective Ring-Opening Reactions of Cyclopropanes. *Chem. Rev.* **2021**, 121 (1), 227-263.
- (a) Barnes-Seeman, D.; Jain, M.; Bell, L.; Ferreira, S.; Cohen, S.; Chen, X.-H.; Amin, J.; Snodgrass, B.; Hatsis, P., Metabolically Stable tert-Butyl Replacement. *ACS Medicinal Chemistry Letters* **2013**, 4 (6), 514-516; (b) Talele, T. T., The "Cyclopropyl Fragment" is a Versatile Player that Frequently Appears in Preclinical/Clinical Drug Molecules. *J. Med. Chem.* **2016**, 59 (19), 8712-8756; (c) de Meijere, A., Bonding Properties of Cyclopropane and Their Chemical Consequences. *Angewandte Chemie International Edition in English* **1979**, 18 (11), 809-826.
- Cremer, D.; Kraka, E.; Szabo, K. J., General and Theoretical Aspects of the Cyclopropyl Group. In *PATAI'S Chemistry of Functional Groups*.
- (a) Coulson, C. A.; Moffitt, W. E., Strain in Non-Tetrahedral Carbon Atoms. *J. Chem. Phys.* **1947**, 15 (3), 151-151; (b) Coulson, C. A.; Moffitt, W. E., I. The properties of certain strained hydrocarbons. *The London, Edinburgh, and Dublin Philosophical Magazine and Journal of Science* **1949**, 40 (300), 1-35.
- (a) Walsh, A. D., Structures of Ethylene Oxide and Cyclopropane. *Nature* **1947**, 159 (4047), 712-713; (b) Walsh, A. D., Structures of Ethylene Oxide and Cyclopropane. *Nature* **1947**, 159 (4031), 165-165.
- Walborsky, H. M., The cyclopropyl radical. *Tetrahedron* **1981**, 37 (9), 1625-1651.
- (a) Fessenden, R. W.; Schuler, R. H., Electron Spin Resonance Studies of Transient Alkyl Radicals. *J. Chem. Phys.* **1963**, 39 (9), 2147-2195; (b) Kawamura, T.; Tsumura, M.; Yokomichi, Y.; Yonezawa, T., Stereochemistry of cyclopropyl radicals by electron spin resonance. *J. Am. Chem. Soc.* **1977**, 99 (25), 8251-8256.
- (a) Davies, I. W.; Gerena, L.; Castonguay, L.; Senanayake, C. H.; Larsen, R. D.; Verhoeven, T. R.; Reider, P. J., The influence of ligand bite angle on the enantioselectivity of copper(II)-catalysed Diels-Alder reactions. *Chem. Commun.* **1996**, (15), 1753-1754; (b) Chen, D. Y. K.; Pouwer, R. H.; Richard, J.-A., Recent advances in the total synthesis of cyclopropane-containing natural products. *Chem. Soc. Rev.* **2012**, 41 (13), 4631-4642; (c) Ebner, C.; Carreira, E. M., Cyclopropanation Strategies in Recent Total Syntheses. *Chem. Rev.* **2017**, 117 (18), 11651-11679.
- Perkin, W. H., Ueber die Einwirkung von Aethylenbromid auf Malonsäureäther. *Berichte der deutschen chemischen Gesellschaft* **1884**, 17 (1), 54-59.
- (a) Corey, E. J.; Chaykovsky, M., Dimethylsulfoxonium Methylide. *J. Am. Chem. Soc.* **1962**, 84 (5), 867-868; (b) Corey, E. J.; Chaykovsky, M., Dimethyloxosulfonium Methylide ((CH₃)₂SOCH₂) and Dimethylsulfonium Methylide ((CH₃)₂SCH₂). Formation and Application to Organic Synthesis. *J. Am. Chem. Soc.* **1965**, 87 (6), 1353-1364.
- (a) Simmons, H. E.; Smith, R. D., A NEW SYNTHESIS OF CYCLOPROPANES FROM OLEFINS. *J. Am. Chem. Soc.* **1958**, 80 (19), 5323-5324; (b) Simmons, H. E.; Smith, R. D., A New Synthesis of Cyclopropanes. *J. Am. Chem. Soc.* **1959**, 81 (16), 4256-4264.
- (a) Poulter, C. D.; Friedrich, E. C.; Winstein, S., Stereochemistry of the methylene iodide-zinc-copper couple methylenation of cyclic allylic alcohols. *J. Am. Chem. Soc.* **1969**, 91 (24), 6892-6894; (b) Charette, A. B.; Beauchemin, A., Reinvestigation of the chemoselective cyclopropanation of allylic alcohols, allylic ethers and alkenes: a comparison between various reagents and protocols. *J. Organomet. Chem.* **2001**, 617-618, 702-708.
- von E. Doering, W.; Hoffmann, A. K., The Addition of Dichlorocarbene to Olefins. *J. Am. Chem. Soc.* **1954**, 76 (23), 6162-6165.
- Cory, R. M.; McLaren, F. R., Carbon atom insertion: an efficient synthesis of isowarane. *Journal of the Chemical Society, Chemical Communications* **1977**, (17), 587-588.
- (a) de Frémont, P.; Marion, N.; Nolan, S. P., Carbenes: Synthesis, properties, and organometallic chemistry. *Coord. Chem. Rev.* **2009**, 253 (7), 862-892; (b) Moss, R. A.; Doyle, Michael P., *Contemporary Carbene Chemistry*. John Wiley & Sons, Inc.: Hoboken, New Jersey, 2014.
- Silberrad, O.; Roy, C. S., XXIV.—Gradual decomposition of ethyl diazoacetate. *Journal of the Chemical Society, Transactions* **1906**, 89 (0), 179-182.
- Padwa, A.; Austin, D. J.; Hornbuckle, S. F.; Semones, M. A.; Doyle, M. P.; Protopopova, M. N., Control of chemoselectivity in catalytic carbenoid reactions. Dirhodium(II) ligand effects on relative reactivities. *J. Am. Chem. Soc.* **1992**, 114 (5), 1874-1876.
- (a) Silveira, C. C.; Braga, A. L.; Fiorin, G. L., Arylseleno and 1-Chloro-1-arylseleno Cyclopropanes from P.T.C. and Ultrasound Conditions. *Synth. Commun.* **1994**, 24 (14), 2075-2080; (b) Schreiner, P. R.; Reisenauer, H. P.; Ley, D.; Gerbig, D.; Wu, C.-H.; Allen, W. D., Methylhydroxycarbene: Tunneling Control of a Chemical Reaction. *Science* **2011**, 332 (6035), 1300-1303; (c) Benoit, G.; Charette,

A. B., Diastereoselective Borocyclopropanation of Allylic Ethers Using a Boromethylzinc Carbenoid. *J. Am. Chem. Soc.* **2017**, *139* (4), 1364-1367; (d) Greb, A.; Poh, J.-S.; Greed, S.; Battilocchio, C.; Pasau, P.; Blakemore, D. C.; Ley, S. V., A Versatile Route to Unstable Diazo Compounds via Oxadiazolines and their Use in Aryl-Alkyl Cross-Coupling Reactions. *Angew. Chem. Int. Ed.* **2017**, *56* (52), 16602-16605; (e) Herlé, B.; Holstein, P. M.; Echavarren, A. M., Stereoselective cis-Vinylcyclopropanation via a Gold(I)-Catalyzed Retro-Buchner Reaction under Mild Conditions. *ACS Catal.* **2017**, *7* (5), 3668-3675; (f) Eckhardt, A. K.; Schreiner, P. R., Spectroscopic Evidence for Aminomethylene (H-C-NH₂)—The Simplest Amino Carbene. *Angew. Chem. Int. Ed.* **2018**, *57* (19), 5248-5252; (g) Rullière, P.; Benoit, G.; Allouche, E. M. D.; Charette, A. B., Safe and Facile Access to Nonstabilized Diazoalkanes Using Continuous Flow Technology. *Angew. Chem. Int. Ed.* **2018**, *57* (20), 5777-5782.

19. Crabtree, R. H., *The organometallic chemistry of the transition metals*. John Wiley & Sons, Inc.

: Hoboken, New Jersey, 2014.

20. (a) Davies, H. M. L.; Bruzinski, P. R.; Lake, D. H.; Kong, N.; Fall, M. J., Asymmetric Cyclopropanations by Rhodium(II) N-(Arylsulfonyl)proline Catalyzed Decomposition of Vinyl diazomethanes in the Presence of Alkenes. Practical Enantioselective Synthesis of the Four Stereoisomers of 2-Phenylcyclopropan-1-amino Acid. *J. Am. Chem. Soc.* **1996**, *118* (29), 6897-6907; (b) Doyle, M. P., Perspective on Dirhodium Carboxamides as Catalysts. *J. Org. Chem.* **2006**, *71* (25), 9253-9260.
21. Maas, G., Ruthenium-catalysed carbenoid cyclopropanation reactions with diazo compounds. *Chem. Soc. Rev.* **2004**, *33* (3), 183-190.
22. Che, C.-M.; Huang, J.-S.; Lee, F.-W.; Li, Y.; Lai, T.-S.; Kwong, H.-L.; Teng, P.-F.; Lee, W.-S.; Lo, W.-C.; Peng, S.-M.; Zhou, Z.-Y., Asymmetric Inter- and Intramolecular Cyclopropanation of Alkenes Catalyzed by Chiral Ruthenium Porphyrins. Synthesis and Crystal Structure of a Chiral Metalloporphyrin Carbene Complex. *J. Am. Chem. Soc.* **2001**, *123* (18), 4119-4129.
23. (a) Nishiyama, H.; Itoh, Y.; Sugawara, Y.; Matsumoto, H.; Aoki, K.; Itoh, K., *Bull. Chem. Soc. Jpn.* **1995**, *68*, 1247; (b) Nishiyama, H.; Soeda, N.; Naito, T.; Motoyama, Y., Single-Chiral Bis(Oxazoliny)pyridine (pybox). Efficiency in Asymmetric Catalytic Cyclopropanation. *Tetrahedron: Asymmetry* **1998**, *9*, 2865.
24. Chanthamath, S.; Phomkeona, K.; Shibatomi, K.; Iwasa, S., Highly stereoselective Ru(II)-Pheox catalyzed asymmetric cyclopropanation of terminal olefins with succinimidy diazoacetate. *Chem. Commun.* **2012**, *48* (62), 7750-7752.
25. Abu-Elfotouh, A.-M.; Phomkeona, K.; Shibatomi, K.; Iwasa, S., Asymmetric Inter- and Intramolecular Cyclopropanation Reactions Catalyzed by a Reusable Macroporous-Polymer-Supported Chiral Ruthenium(II)/Phenyloxazoline Complex. *Angew. Chem. Int. Ed.* **2010**, *49* (45), 8439-8443.
26. (a) Noels, A. F.; Demonceau, A., From olefin cyclopropanation to olefin metathesis through catalyst engineering: recent applications of olefin metathesis to fine organic synthesis and to polymer chemistry. *J. Phys. Org. Chem.* **1998**, *11* (8-9), 602-609; (b) Simal, F.; Demonceau, A.; Noels, A. F.; Knowles, D. R. T.; O'Leary, S.; Maitlis, P. M.; Gusev, O., Cp*Ru(II) and Cp*Ru(IV)-catalyzed reactions of CHX with vinyl C-H bonds: competition between double bond homologation and olefin cyclopropanation by alkyl diazoacetate. *J. Organomet. Chem.* **1998**, *558* (1), 163-170; (c) Noels, A. F.; Demonceau, A.; Jan, D., Late transition metal-based catalysts for olefin cyclopropanation or olefin metathesis. Importance of catalyst unsaturation. *Russ. Chem. Bull.* **1999**, *48* (7), 1206-1211.
27. El-Faham, A.; Albericio, F., Peptide Coupling Reagents, More than a Letter Soup. *Chem. Rev.* **2011**, *111* (11), 6557-6602.
28. Nefkens, G. H. L.; Tesser, G. I., A NOVEL ACTIVATED ESTER IN PEPTIDE SYNTHESSES. *J. Am. Chem. Soc.* **1961**, *83* (5), 1263-1263.
29. Okada, K.; Okamoto, K.; Oda, M., A new and practical method of decarboxylation: photosensitized decarboxylation of N-acyloxypthalimides via electron-transfer mechanism. *J. Am. Chem. Soc.* **1988**, *110* (26), 8736-8738.
30. (a) Barton, D. H. R.; George, M. V.; Tomoeda, M., 369. Photochemical transformations. Part XIII. A new method for the production of acyl radicals. *Journal of the Chemical Society (Resumed)* **1962**, (0), 1967-1974; (b) Barton, D. H. R.; Crich, D.; Motherwell, W. B., New and improved methods for the radical decarboxylation of acids. *Journal of the Chemical Society, Chemical Communications* **1983**, (17), 939-941.
31. (a) Eaton, P. E.; Cole, T. W., Cubane. *J. Am. Chem. Soc.* **1964**, *86* (15), 3157-3158; (b) Meinwald, J.; Shelton, J. C.; Buchanan, G. L.; Courtin, A., Highly strained bicyclic systems. XII. Synthesis and solvolysis of 1,5,5-trimethylbicyclo[2.1.1]hex-2-yl p-toluenesulfonate. *J. Org. Chem.* **1968**, *33* (1), 99-105.

32. (a) Kuivila, H. G., Reduction of Organic Compounds by Organotin Hydrides. *Synthesis* **1970**, 1970 (10), 499-509; (b) Della, E. W.; Patney, H. K., Decarboxylation of Bridgehead Carboxylic Acids. Synthesis of Deuterium-Labelled Polycyclic Hydrocarbons. *Synthesis* **1976**, 1976 (04), 251-252.
33. (a) Okada, K.; Okamoto, K.; Morita, N.; Okubo, K.; Oda, M., Photosensitized decarboxylative Michael addition through N-(acyloxy)phthalimides via an electron-transfer mechanism. *J. Am. Chem. Soc.* **1991**, 113 (24), 9401-9402; (b) Okada, K.; Okubo, K.; Morita, N.; Oda, M., Reductive decarboxylation of N-(acyloxy)phthalimides via redox-initiated radical chain mechanism. *Tetrahedron Lett.* **1992**, 33 (48), 7377-7380.
34. (a) Huihui, K. M. M.; Caputo, J. A.; Melchor, Z.; Olivares, A. M.; Spiewak, A. M.; Johnson, K. A.; DiBenedetto, T. A.; Kim, S.; Ackerman, L. K. G.; Weix, D. J., Decarboxylative Cross-Electrophile Coupling of N-Hydroxyphthalimide Esters with Aryl Iodides. *J. Am. Chem. Soc.* **2016**, 138 (15), 5016-5019; (b) Jiang, M.; Yang, H.; Fu, H., Visible-Light Photoredox Synthesis of Chiral α -Selenoamino Acids. *Org. Lett.* **2016**, 18 (9), 1968-1971; (c) Qin, T.; Cornella, J.; Li, C.; Malins, L. R.; Edwards, J. T.; Kawamura, S.; Maxwell, B. D.; Eastgate, M. D.; Baran, P. S., A general alkyl-alkyl cross-coupling enabled by redox-active esters and alkylzinc reagents. *Science* **2016**, 352 (6287), 801-805; (d) Wang, J.; Qin, T.; Chen, T.-G.; Wimmer, L.; Edwards, J. T.; Cornella, J.; Vokits, B.; Shaw, S. A.; Baran, P. S., Nickel-Catalyzed Cross-Coupling of Redox-Active Esters with Boronic Acids. *Angew. Chem. Int. Ed.* **2016**, 55 (33), 9676-9679; (e) Candish, L.; Teders, M.; Glorius, F., Transition-Metal-Free, Visible-Light-Enabled Decarboxylative Borylation of Aryl N-Hydroxyphthalimide Esters. *J. Am. Chem. Soc.* **2017**, 139 (22), 7440-7443; (f) Edwards, J. T.; Merchant, R. R.; McClymont, K. S.; Knouse, K. W.; Qin, T.; Malins, L. R.; Vokits, B.; Shaw, S. A.; Bao, D.-H.; Wei, F.-L.; Zhou, T.; Eastgate, M. D.; Baran, P. S., Decarboxylative alkenylation. *Nature* **2017**, 545 (7653), 213-218; (g) Fawcett, A.; Pradeilles, J.; Wang, Y.; Mutsuga, T.; Myers, E. L.; Aggarwal, V. K., Photoinduced decarboxylative borylation of carboxylic acids. *Science* **2017**, 357 (6348), 283-286; (h) Hu, D.; Wang, L.; Li, P., Decarboxylative Borylation of Aliphatic Esters under Visible-Light Photoredox Conditions. *Org. Lett.* **2017**, 19 (10), 2770-2773; (i) Li, C.; Wang, J.; Barton, L. M.; Yu, S.; Tian, M.; Peters, D. S.; Kumar, M.; Yu, A. W.; Johnson, K. A.; Chatterjee, A. K.; Yan, M.; Baran, P. S., Decarboxylative borylation. *Science* **2017**, 356 (6342); (j) Qin, T.; Malins, L. R.; Edwards, J. T.; Merchant, R. R.; Novak, A. J. E.; Zhong, J. Z.; Mills, R. B.; Yan, M.; Yuan, C.; Eastgate, M. D.; Baran, P. S., Nickel-Catalyzed Barton Decarboxylation and Giese Reactions: A Practical Take on Classic Transformations. *Angew. Chem. Int. Ed.* **2017**, 56 (1), 260-265; (k) Smith, J. M.; Qin, T.; Merchant, R. R.; Edwards, J. T.; Malins, L. R.; Liu, Z.; Che, G.; Shen, Z.; Shaw, S. A.; Eastgate, M. D.; Baran, P. S., Decarboxylative Alkynylation. *Angew. Chem. Int. Ed.* **2017**, 56 (39), 11906-11910; (l) Xue, W.; Oestreich, M., Copper-Catalyzed Decarboxylative Radical Silylation of Redox-Active Aliphatic Carboxylic Acid Derivatives. *Angew. Chem. Int. Ed.* **2017**, 56 (38), 11649-11652; (m) Mao, R.; Balon, J.; Hu, X., Decarboxylative C(sp³)-O Cross-Coupling. *Angew. Chem. Int. Ed.* **2018**, 57 (41), 13624-13628; (n) Mao, R.; Frey, A.; Balon, J.; Hu, X., Decarboxylative C(sp³)-N cross-coupling via synergetic photoredox and copper catalysis. *Nat. Catal.* **2018**, 1 (2), 120-126; (o) Proctor, R. S. J.; Davis, H. J.; Phipps, R. J., Catalytic enantioselective Minisci-type addition to heteroarenes. *Science* **2018**, 360 (6387), 419-422; (p) Tlahuext-Aca, A.; Candish, L.; Garza-Sanchez, R. A.; Glorius, F., Decarboxylative Olefination of Activated Aliphatic Acids Enabled by Dual Organophotoredox/Copper Catalysis. *ACS Catal.* **2018**, 8 (3), 1715-1719; (q) Wang, J.; Shang, M.; Lundberg, H.; Feu, K. S.; Hecker, S. J.; Qin, T.; Blackmond, D. G.; Baran, P. S., Cu-Catalyzed Decarboxylative Borylation. *ACS Catal.* **2018**, 8 (10), 9537-9542; (r) Xiang, J.; Shang, M.; Kawamata, Y.; Lundberg, H.; Reisberg, S. H.; Chen, M.; Mykhailiuk, P.; Beutner, G.; Collins, M. R.; Davies, A.; Del Bel, M.; Gallego, G. M.; Spangler, J. E.; Starr, J.; Yang, S.; Blackmond, D. G.; Baran, P. S., Hindered dialkyl ether synthesis with electrogenerated carbocations. *Nature* **2019**, 573 (7774), 398-402; (s) Huang, H.-M.; Koy, M.; Serrano, E.; Pflüger, P. M.; Schwarz, J. L.; Glorius, F., Catalytic radical generation of π -allylpalladium complexes. *Nat. Catal.* **2020**, 3 (4), 393-400; (t) Kakeno, Y.; Kusakabe, M.; Nagao, K.; Ohmiya, H., Direct Synthesis of Dialkyl Ketones from Aliphatic Aldehydes through Radical N-Heterocyclic Carbene Catalysis. *ACS Catal.* **2020**, 10 (15), 8524-8529; (u) Sheng, T.; Zhang, H.-J.; Shang, M.; He, C.; Vantourout, J. C.; Baran, P. S., Electrochemical Decarboxylative N-Alkylation of Heterocycles. *Org. Lett.* **2020**, 22 (19), 7594-7598; (v) Shibutani, S.; Kodo, T.; Takeda, M.; Nagao, K.; Tokunaga, N.; Sasaki, Y.; Ohmiya, H., Organophotoredox-Catalyzed Decarboxylative C(sp³)-O Bond Formation. *J. Am. Chem. Soc.* **2020**, 142 (3), 1211-1216; (w) Barton, L. M.; Chen, L.; Blackmond, D. G.; Baran, P. S., Electrochemical borylation of carboxylic acids. *Proceedings of the National Academy of Sciences* **2021**, 118 (34), e2109408118; (x) Kobayashi, R.; Shibutani, S.; Nagao, K.; Ikeda, Z.; Wang, J.; Ibáñez, I.; Reynolds, M.; Sasaki, Y.; Ohmiya, H., Decarboxylative N-Alkylation of Azoles through Visible-Light-Mediated Organophotoredox Catalysis. *Org. Lett.* **2021**, 23 (14), 5415-5419; (y) Nakagawa, M.; Nagao, K.; Ikeda, Z.; Reynolds, M.; Ibáñez, I.; Wang, J.; Tokunaga, N.; Sasaki, Y.; Ohmiya, H., Organophotoredox-Catalyzed Decarboxylative N-Alkylation of Sulfonamides. *ChemCatChem* **2021**, 13 (18), 3930-3933.
35. Staudinger, H.; Ruzicka, L., Insektentötende Stoffe I. Über Isolierung und Konstitution des wirksamen Teiles des dalmatinischen Insektenpulvers. *Helvetica Chimica Acta* **1924**, 7 (1), 177-201.

36. (a) Doyle, M. P.; Forbes, D. C., Recent Advances in Asymmetric Catalytic Metal Carbene Transformations. *Chem. Rev.* **1998**, *98* (2), 911-936; (b) Lebel, H.; Marcoux, J.-F.; Molinaro, C.; Charette, A. B., Stereoselective Cyclopropanation Reactions. *Chem. Rev.* **2003**, *103* (4), 977-1050; (c) Pellissier, H., Recent developments in asymmetric cyclopropanation. *Tetrahedron* **2008**, *64* (30), 7041-7095.
37. (a) Charette, A. B.; Juteau, H., Design of Amphoteric Bifunctional Ligands: Application to the Enantioselective Simmons-Smith Cyclopropanation of Allylic Alcohols. *J. Am. Chem. Soc.* **1994**, *116* (6), 2651-2652; (b) Lacasse, M.-C.; Poulard, C.; Charette, A. B., Iodomethylzinc Phosphates: Powerful Reagents for the Cyclopropanation of Alkenes. *J. Am. Chem. Soc.* **2005**, *127* (36), 12440-12441.
38. Kunz, R. K.; MacMillan, D. W. C., Enantioselective Organocatalytic Cyclopropanations. The Identification of a New Class of Iminium Catalyst Based upon Directed Electrostatic Activation. *J. Am. Chem. Soc.* **2005**, *127* (10), 3240-3241.
39. den Hartog, T.; Rudolph, A.; Maciá, B.; Minnaard, A. J.; Feringa, B. L., Copper-Catalyzed Enantioselective Synthesis of trans-1-Alkyl-2-substituted Cyclopropanes via Tandem Conjugate Addition-Intramolecular Enolate Trapping. *J. Am. Chem. Soc.* **2010**, *132* (41), 14349-14351.
40. (a) Didier, D.; Delaye, P.-O.; Simaan, M.; Island, B.; Eppe, G.; Eijssberg, H.; Kleiner, A.; Knochel, P.; Marek, I., Modulable and Highly Diastereoselective Carbometalations of Cyclopropanes. *Chem. Eur. J.* **2014**, *20* (4), 1038-1048; (b) Müller, D. S.; Marek, I., Asymmetric Copper-Catalyzed Carbozincation of Cyclopropanes en Route to the Formation of Diastereo- and Enantiomerically Enriched Polysubstituted Cyclopropanes. *J. Am. Chem. Soc.* **2015**, *137* (49), 15414-15417; (c) Dian, L.; Müller, D. S.; Marek, I., Asymmetric Copper-Catalyzed Carbomagnesiation of Cyclopropanes. *Angew. Chem. Int. Ed.* **2017**, *56* (24), 6783-6787; (d) Dian, L.; Marek, I., Asymmetric Preparation of Polysubstituted Cyclopropanes Based on Direct Functionalization of Achiral Three-Membered Carbocycles. *Chem. Rev.* **2018**, *118* (18), 8415-8434; (e) Cohen, Y.; Augustin, A. U.; Levy, L.; Jones, P. G.; Werz, D. B.; Marek, I., Regio- and Diastereoselective Copper-Catalyzed Carbomagnesiation for the Synthesis of Penta- and Hexa-Substituted Cyclopropanes. *Angew. Chem. Int. Ed.* **2021**, *60* (21), 11804-11808.
41. (a) Rubina, M.; Rubin, M.; Gevorgyan, V., Transition Metal-Catalyzed Hydro-, Sila-, and Stannastannation of Cyclopropanes: Stereo- and Regioselective Approach toward Multisubstituted Cyclopropyl Synthons. *J. Am. Chem. Soc.* **2002**, *124* (39), 11566-11567; (b) Rubina, M.; Rubin, M.; Gevorgyan, V., Catalytic Enantioselective Hydroboration of Cyclopropanes. *J. Am. Chem. Soc.* **2003**, *125* (24), 7198-7199; (c) Rubina, M.; Rubin, M.; Gevorgyan, V., Catalytic Enantioselective Hydrostannation of Cyclopropanes. *J. Am. Chem. Soc.* **2004**, *126* (12), 3688-3689; (d) Trofimov, A.; Rubina, M.; Rubin, M.; Gevorgyan, V., Highly Diastereo- and Regioselective Transition Metal-Catalyzed Additions of Metal Hydrides and Bimetallic Species to Cyclopropanes: Easy Access to Multisubstituted Cyclopropanes. *J. Org. Chem.* **2007**, *72* (23), 8910-8920.
42. (a) Evans, D. A.; Woerpel, K. A.; Hinman, M. M.; Faul, M. M., Bis(oxazolines) as chiral ligands in metal-catalyzed asymmetric reactions. Catalytic, asymmetric cyclopropanation of olefins. *J. Am. Chem. Soc.* **1991**, *113* (2), 726-728; (b) Nishiyama, H.; Itoh, Y.; Matsumoto, H.; Park, S.-B.; Itoh, K., New Chiral Ruthenium Bis(oxazolonyl)pyridine Catalyst. Efficient Asymmetric Cyclopropanation of Olefins with Diazoacetates. *J. Am. Chem. Soc.* **1994**, *116* (5), 2223-2224; (c) Doyle, M. P.; Austin, R. E.; Bailey, A. S.; Dwyer, M. P.; Dyatkin, A. B.; Kalinin, A. V.; Kwan, M. M. Y.; Liras, S.; Oalman, C. J., Enantioselective Intramolecular Cyclopropanations of Allylic and Homoallylic Diazoacetates and Diazoacetamides Using Chiral Dirhodium(II) Carboxamide Catalysts. *J. Am. Chem. Soc.* **1995**, *117* (21), 5763-5775; (d) Lo, M. M. C.; Fu, G. C., A New Class of Planar-Chiral Ligands: Synthesis of a C2-Symmetric Bisazaferrocene and Its Application in the Enantioselective Cu(I)-Catalyzed Cyclopropanation of Olefins. *J. Am. Chem. Soc.* **1998**, *120* (39), 10270-10271; (e) Suematsu, H.; Kanchiku, S.; Uchida, T.; Katsuki, T., Construction of Aryliridium-Salen Complexes: Enantio- and Cis-Selective Cyclopropanation of Conjugated and Nonconjugated Olefins. *J. Am. Chem. Soc.* **2008**, *130* (31), 10327-10337; (f) Zhu, S.; Xu, X.; Perman, J. A.; Zhang, X. P., A General and Efficient Cobalt(II)-Based Catalytic System for Highly Stereoselective Cyclopropanation of Alkenes with α -Cyanodiazooacetates. *J. Am. Chem. Soc.* **2010**, *132* (37), 12796-12799; (g) Lindsay, V. N. G.; Nicolas, C.; Charette, A. B., Asymmetric Rh(II)-Catalyzed Cyclopropanation of Alkenes with Diazo Acceptor Compounds: p-Methoxyphenyl Ketone as a General Stereoselectivity Controlling Group. *J. Am. Chem. Soc.* **2011**, *133* (23), 8972-8981; (h) Coelho, P. S.; Brustad, E. M.; Kannan, A.; Arnold, F. H., Olefin Cyclopropanation via Carbene Transfer Catalyzed by Engineered Cytochrome P450 Enzymes. *Science* **2013**, *339* (6117), 307-310; (i) Key, H. M.; Dydio, P.; Clark, D. S.; Hartwig, J. F., Abiological catalysis by artificial haem proteins containing noble metals in place of iron. *Nature* **2016**, *534* (7608), 534-537; (j) Key, H. M.; Dydio, P.; Liu, Z.; Rha, J. Y. E.; Nazarenko, A.; Seyedkazemi, V.; Clark, D. S.; Hartwig, J. F., Beyond Iron: Iridium-Containing P450 Enzymes for Selective Cyclopropanations of Structurally Diverse Alkenes. *ACS Cent. Sci.* **2017**, *3* (4), 302-308; (k) Xu, X.; Wang, Y.; Cui, X.; Wojtas, L.; Zhang, X. P., Metalloradical activation of α -formyldiazoacetates for the catalytic asymmetric radical cyclopropanation of alkenes. *Chem. Sci.* **2017**, *8*

- (6), 4347-4351; (l) Knight, A. M.; Kan, S. B. J.; Lewis, R. D.; Brandenberg, O. F.; Chen, K.; Arnold, F. H., Diverse Engineered Heme Proteins Enable Stereodivergent Cyclopropanation of Unactivated Alkenes. *ACS Cent. Sci.* **2018**, *4* (3), 372-377.
43. (a) Papageorgiou, C. D.; Cubillo de Dios, M. A.; Ley, S. V.; Gaunt, M. J., Enantioselective Organocatalytic Cyclopropanation via Ammonium Ylides. *Angew. Chem. Int. Ed.* **2004**, *43* (35), 4641-4644; (b) Carreras, J.; Caballero, A.; Pérez, P. J., Enantio- and Diastereoselective Cyclopropanation of 1-Alkenylboronates: Synthesis of 1-Boryl-2,3-Disubstituted Cyclopropanes. *Angew. Chem. Int. Ed.* **2018**, *57* (9), 2334-2338.
44. Coombs, J. R.; Morken, J. P., Catalytic Enantioselective Functionalization of Unactivated Terminal Alkenes. *Angew. Chem. Int. Ed.* **2016**, *55* (8), 2636-2649.
45. (a) Mayr, H. Database of reactivity parameter; (b) Mayr, H.; Bug, T.; Gotta, M. F.; Hering, N.; Irrgang, B.; Janker, B.; Kempf, B.; Loos, R.; Ofial, A. R.; Remennikov, G.; Schimmel, H., Reference Scales for the Characterization of Cationic Electrophiles and Neutral Nucleophiles. *J. Am. Chem. Soc.* **2001**, *123* (39), 9500-9512; (c) Bug, T.; Hartnagel, M.; Schlierf, C.; Mayr, H., How Nucleophilic Are Diazo Compounds? *Chem. Eur. J.* **2003**, *9* (17), 4068-4076; (d) Mayr, H.; Kempf, B.; Ofial, A. R., π -Nucleophilicity in Carbon-Carbon Bond-Forming Reactions. *Accounts of Chemical Research* **2003**, *36* (1), 66-77.
46. (a) Schnaars, C.; Hennum, M.; Bonge-Hansen, T., Nucleophilic Halogenations of Diazo Compounds, a Complementary Principle for the Synthesis of Halodiazo Compounds: Experimental and Theoretical Studies. *J. Org. Chem.* **2013**, *78* (15), 7488-7497; (b) Wang, Z.; Herraiz, A. G.; del Hoyo, A. M.; Suero, M. G., Generating carbyne equivalents with photoredox catalysis. *Nature* **2018**, *554* (7690), 86-91; (c) Wang, Z.; Jiang, L.; Sarro, P.; Suero, M. G., Catalytic Cleavage of C(sp²)-C(sp²) Bonds with Rh-Carbynyds. *J. Am. Chem. Soc.* **2019**, *141* (39), 15509-15514; (d) Jiang, L.; Wang, Z.; Armstrong, M.; Suero, M. G., β -Diazocarbonyl Compounds: Synthesis and their Rh(II)-Catalyzed 1,3 C-H Insertions. *Angew. Chem. Int. Ed.* **2021**, *60* (11), 6177-6184.
47. (a) Sakhautdinov, I. M.; Lakeev, S. N.; Halikov, I. G.; Abdullin, M. F.; Galin, F. Z., *Bashk. Khim. Zh.* **2004**, *11*, 32-35; (b) Ma, M.; Peng, L.; Li, C.; Zhang, X.; Wang, J., Highly Stereoselective [2,3]-Sigmatropic Rearrangement of Sulfur Ylide Generated through Cu(I) Carbene and Sulfides. *J. Am. Chem. Soc.* **2005**, *127* (43), 15016-15017; (c) Hashimoto, T.; Miyamoto, H.; Naganawa, Y.; Maruoka, K., Stereoselective Synthesis of α -Alkyl- β -keto Imides via Asymmetric Redox C-C Bond Formation between α -Alkyl- α -diazocarbonyl Compounds and Aldehydes. *J. Am. Chem. Soc.* **2009**, *131* (32), 11280-11281; (d) Hashimoto, T.; Nakatsu, H.; Yamamoto, K.; Maruoka, K., Chiral Brønsted Acid-Catalyzed Asymmetric Trisubstituted Aziridine Synthesis Using α -Diazoacyl Oxazolidinones. *J. Am. Chem. Soc.* **2011**, *133* (25), 9730-9733.
48. Montesinos-Magraner, M.; Costantini, M.; Ramírez-Contreras, R.; Muratore, M. E.; Johansson, M. J.; Mendoza, A., General Cyclopropane Assembly by Enantioselective Transfer of a Redox-Active Carbene to Aliphatic Olefins. *Angew. Chem. Int. Ed.* **2019**, *58* (18), 5930-5935.
49. Haym, I.; Brimble, M. A., The Kulinkovich hydroxycyclopropanation reaction in natural product synthesis. *Org. Biomol. Chem.* **2012**, *10* (38), 7649-7665.
50. (a) Alexander, K.; Cook, S.; Gibson, C. L., cis-Selective cyclopropanations using chiral 5,5-diaryl bis(oxazoline) catalysts. *Tetrahedron Lett.* **2000**, *41* (36), 7135-7138; (b) Niimi, T.; Uchida, T.; Irie, R.; Katsuki, T., Co(II)-salen-catalyzed highly cis- and enantioselective cyclopropanation. *Tetrahedron Lett.* **2000**, *41* (19), 3647-3651; (c) Uchida, T.; Irie, R.; Katsuki, T., cis- and Enantio-selective Cyclopropanation with Chiral (ON⁺)Ru-Salen Complex as a Catalyst. *Tetrahedron* **2000**, *56* (22), 3501-3509; (d) Bachmann, S.; Furler, M.; Mezzetti, A., Cis-Selective Asymmetric Cyclopropanation of Olefins Catalyzed by Five-Coordinate [RuCl(PNNP)]⁺ Complexes. *Organometallics* **2001**, *20* (10), 2102-2108; (e) Hu, W.; Timmons, D. J.; Doyle, M. P., In Search of High Stereocontrol for the Construction of cis-Disubstituted Cyclopropane Compounds. Total Synthesis of a Cyclopropane-Configured Urea-PETT Analogue That Is a HIV-1 Reverse Transcriptase Inhibitor. *Org. Lett.* **2002**, *4* (6), 901-904; (f) Bonaccorsi, C.; Mezzetti, A., Optimization or Breakthrough? The First Highly cis- and Enantioselective Asymmetric Cyclopropanation of 1-Octene by "Electronic and Counterion" Tuning of [RuCl(PNNP)]⁺ Catalysts. *Organometallics* **2005**, *24* (21), 4953-4960; (g) Zhu, S.; Perman, J. A.; Zhang, X. P., Acceptor/Acceptor-Substituted Diazo Reagents for Carbene Transfers: Cobalt-Catalyzed Asymmetric Z-Cyclopropanation of Alkenes with α -Nitrodiazoacetates. *Angew. Chem. Int. Ed.* **2008**, *47* (44), 8460-8463; (h) Rosenberg, M. L.; Vlašaná, K.; Gupta, N. S.; Wragg, D.; Tilset, M., Highly cis-Selective Rh(I)-Catalyzed Cyclopropanation Reactions. *J. Org. Chem.* **2011**, *76* (8), 2465-2470; (i) Piou, T.; Romanov-Mikhailidis, F.; Ashley, M. A.; Romanova-Michaelides, M.; Rovis, T., Stereodivergent Rhodium(III)-Catalyzed cis-Cyclopropanation Enabled by Multivariate Optimization. *J. Am. Chem. Soc.* **2018**, *140* (30), 9587-9593.
51. Xu, F.; Zhong, Y.-L.; Li, H.; Qi, J.; Desmond, R.; Song, Z. J.; Park, J.; Wang, T.; Truppo, M.; Humphrey, G. R.; Ruck, R. T., Asymmetric Synthesis of Functionalized trans-Cyclopropoxy Building Block for Grazoprevir. *Org. Lett.* **2017**, *19* (21), 5880-5883.

52. Larionov, O. V.; de Meijere, A., Enantioselective Total Syntheses of Belactosin A, Belactosin C, and Its Homoanalogue. *Org. Lett.* **2004**, *6* (13), 2153-2156.
53. Larionov, Oleg V.; Savel'eva, Tatyana F.; Kochetkov, Konstantin A.; Ikonnikov, Nikolai S.; Kozhushkov, Sergei I.; Yufit, Dmitrii S.; Howard, Judith A. K.; Khrustalev, Viktor N.; Belokon, Yuri N.; de Meijere, A., Productive Asymmetric Synthesis of All Four Diastereomers of 3-(trans-2-Nitrocyclopropyl)alanine from Glycine with (S)- or (R)-2-[(N-Benzylpropyl)amino]benzophenone as a Reusable Chiral Auxiliary. *Eur. J. Org. Chem.* **2003**, *2003* (5), 869-877.
54. Lin, H.; Tian, L.; Krauss, I. J., Enantioselective syn and anti Homocrotylation of Aldehydes: Application to the Formal Synthesis of Spongidepsin. *J. Am. Chem. Soc.* **2015**, *137* (40), 13176-13182.
55. Moore, R. E.; Pettus, J. A.; Mistysyn, J., Odoriferous C11 hydrocarbons from Hawaiian Dictyopteris. *J. Org. Chem.* **1974**, *39* (15), 2201-2207.
56. Armstrong, R. J.; Niwetmarin, W.; Aggarwal, V. K., Synthesis of Functionalized Alkenes by a Transition-Metal-Free Zweifel Coupling. *Org. Lett.* **2017**, *19* (10), 2762-2765.
57. Hohn, E.; Paleček, J.; Pietruszka, J.; Frey, W., Enantiomerically Pure Vinylcyclopropylboronic Esters. *Eur. J. Org. Chem.* **2009**, *2009* (22), 3765-3782.
58. (a) Hoffmann, H. M. R.; Otte, A. R.; Wilde, A.; Menzer, S.; Williams, D. J., Isolation and X-Ray Crystal Structure of a Palladacyclobutane: Insight into the Mechanism of Cyclopropanation. *Angewandte Chemie International Edition in English* **1995**, *34* (1), 100-102; (b) Rasmussen, T.; Jensen, J. F.; Østergaard, N.; Tanner, D.; Ziegler, T.; Norrby, P.-O., On the Mechanism of the Copper-Catalyzed Cyclopropanation Reaction. *Chem. Eur. J.* **2002**, *8* (1), 177-184; (c) Bernardi, F.; Bottoni, A.; Miscione, G. P., DFT Study of the Olefin Metathesis Catalyzed by Ruthenium Complexes. *Organometallics* **2003**, *22* (5), 940-947.
59. (a) Fraile, J. M.; Garcia, J. I.; Martínez-Merino, V.; Mayoral, J. A.; Salvatella, L., Theoretical (DFT) Insights into the Mechanism of Copper-Catalyzed Cyclopropanation Reactions. Implications for Enantioselective Catalysis. *J. Am. Chem. Soc.* **2001**, *123* (31), 7616-7625; (b) Tagliatesta, P.; Pastorini, A., Remarkable selectivity in the cyclopropanation reactions catalysed by an halogenated iron meso-tetraphenylporphyrin. *Journal of Molecular Catalysis A: Chemical* **2003**, *198* (1), 57-61.
60. Guptill, D. M.; Davies, H. M. L., 2,2,2-Trichloroethyl Aryldiazoacetates as Robust Reagents for the Enantioselective C–H Functionalization of Methyl Ethers. *J. Am. Chem. Soc.* **2014**, *136* (51), 17718-17721.
61. (a) Hansen, J. H.; Parr, B. T.; Pelphrey, P.; Jin, Q.; Autschbach, J.; Davies, H. M. L., Rhodium(II)-Catalyzed Cross-Coupling of Diazo Compounds. *Angew. Chem. Int. Ed.* **2011**, *50* (11), 2544-2548; (b) Rivilla, I.; Sameera, W. M. C.; Alvarez, E.; Díaz-Requejo, M. M.; Maseras, F.; Pérez, P. J., Catalytic cross-coupling of diazo compounds with coinage metal-based catalysts: an experimental and theoretical study. *Dalton Transactions* **2013**, *42* (12), 4132-4138.
62. (a) Frutos, M. R.; Belderrain, T. R.; Nicasio, M. C.; Nolan, S. P.; Kaur, H.; Díaz-Requejo, M. M.; Pérez, P. J., Complete Control of the Chemoselectivity in Catalytic Carbene Transfer Reactions from Ethyl Diazoacetate: An N-Heterocyclic Carbene–Cu System That Suppresses Diazo Coupling. *J. Am. Chem. Soc.* **2004**, *126* (35), 10846-10847; (b) Wei, B.; Sharland, J. C.; Lin, P.; Wilkerson-Hill, S. M.; Fullilove, F. A.; McKinnon, S.; Blackmond, D. G.; Davies, H. M. L., In Situ Kinetic Studies of Rh(II)-Catalyzed Asymmetric Cyclopropanation with Low Catalyst Loadings. *ACS Catal.* **2020**, *10* (2), 1161-1170; (c) Chirila, A.; Brands, M. B.; de Bruin, B., Mechanistic investigations into the cyclopropanation of electron-deficient alkenes with ethyl diazoacetate using [Co(MeTAA)]. *Journal of Catalysis* **2018**, *361*, 347-360.
63. (a) Li, Y.; Qi, Z.; Wang, H.; Yang, X.; Li, X., Ruthenium(II)-Catalyzed C–H Activation of Imidamides and Divergent Couplings with Diazo Compounds: Substrate-Controlled Synthesis of Indoles and 3H-Indoles. *Angew. Chem. Int. Ed.* **2016**, *55* (39), 11877-11881; (b) Borah, G.; Ramaiah, D.; Patel, P., Synthesis of Isoquinoline from Benzimidates via Ru(II)-Catalyzed C–H Alkylation/Annulations with Diazo Compounds. *ChemistrySelect* **2018**, *3* (37), 10333-10337; (c) Su, L.; Yu, Z.; Ren, P.; Luo, Z.; Hou, W.; Xu, H., Ruthenium(ii)-catalyzed synthesis of indazoline-fused cinnolines via C–H coupling with diazo compounds. *Org. Biomol. Chem.* **2018**, *16* (39), 7236-7244; (d) Wang, C.; Maity, B.; Cavallo, L.; Rueping, M., Manganese Catalyzed Regioselective C–H Alkylation: Experiment and Computation. *Org. Lett.* **2018**, *20* (10), 3105-3108; (e) Kumar, G. S.; Khot, N. P.; Kapur, M., Oxazolinyl-Assisted Ru(II)-Catalyzed C–H Functionalization Based on Carbene Migratory Insertion: A One-Pot Three-Component Cascade Cyclization. *Adv. Synth. Catal.* **2019**, *361* (1), 73-78.
64. Planas, F.; Costantini, M.; Montesinos-Magraner, M.; Himo, F.; Mendoza, A., Combined Experimental and Computational Study of Ruthenium N-Hydroxyphthalimido Carbene in Alkene Cyclopropanation Reactions. *ACS Catal.* **2021**, 10950-10963.
65. (a) Burès, J., A Simple Graphical Method to Determine the Order in Catalyst. *Angew. Chem. Int. Ed.* **2016**, *55* (6), 2028-2031; (b) Burès, J., Variable Time Normalization Analysis: General Graphical Elucidation of Reaction Orders from Concentration Profiles. *Angew. Chem. Int. Ed.* **2016**, *55*

- (52), 16084-16087; (c) Nielsen, C. D. T.; Burés, J., Visual kinetic analysis. *Chem. Sci.* **2019**, *10* (2), 348-353.
66. Planas, F. Doctoral dissertation thesis, 2020.
67. Wipf, P.; Skoda, E. M.; Mann, A., Chapter 11 - Conformational Restriction and Steric Hindrance in Medicinal Chemistry. In *The Practice of Medicinal Chemistry (Fourth Edition)*, Wermuth, C. G.; Aldous, D.; Raboisson, P.; Rognan, D., Eds. Academic Press: San Diego, 2015; pp 279-299.
68. (a) Shimamoto, K.; Ohfuné, Y., Syntheses and Conformational Analyses of Glutamate Analogs: 2-(2-Carboxy-3-substituted-cyclopropyl)glycines as Useful Probes for Excitatory Amino Acid Receptors. *J. Med. Chem.* **1996**, *39* (2), 407-423; (b) Sekiyama, T.; Hatsuya, S.; Tanaka, Y.; Uchiyama, M.; Ono, N.; Iwayama, S.; Oikawa, M.; Suzuki, K.; Okunishi, M.; Tsuji, T., Synthesis and Antiviral Activity of Novel Acyclic Nucleosides: Discovery of a Cyclopropyl Nucleoside with Potent Inhibitory Activity against Herpesviruses. *J. Med. Chem.* **1998**, *41* (8), 1284-1298; (c) Martin, S. F.; Dwyer, M. P.; Hartmann, B.; Knight, K. S., Cyclopropane-Derived Peptidomimetics. Design, Synthesis, and Evaluation of Novel Enkephalin Analogs. *J. Org. Chem.* **2000**, *65* (5), 1305-1318; (d) Kazuta, Y.; Hirano, K.; Natsume, K.; Yamada, S.; Kimura, R.; Matsumoto, S.-i.; Furuichi, K.; Matsuda, A.; Shuto, S., Cyclopropane-Based Conformational Restriction of Histamine. (1S,2S)-2-(2-Aminoethyl)-1-(1H-imidazol-4-yl)cyclopropane, a Highly Selective Agonist for the Histamine H3 Receptor, Having a cis-Cyclopropane Structure. *J. Med. Chem.* **2003**, *46* (10), 1980-1988; (e) Yonezawa, S.; Yamamoto, T.; Yamakawa, H.; Muto, C.; Hosono, M.; Hattori, K.; Higashino, K.; Yutsudo, T.; Iwamoto, H.; Kondo, Y.; Sakagami, M.; Togame, H.; Tanaka, Y.; Nakano, T.; Takemoto, H.; Arisawa, M.; Shuto, S., Conformational Restriction Approach to β -Secretase (BACE1) Inhibitors: Effect of a Cyclopropane Ring To Induce an Alternative Binding Mode. *J. Med. Chem.* **2012**, *55* (20), 8838-8858.
69. (a) Aggarwal, V. K.; de Vicente, J.; Bonnert, R. V., Catalytic Cyclopropanation of Alkenes Using Diazo Compounds Generated in Situ. A Novel Route to 2-Arylcyclopropylamines. *Org. Lett.* **2001**, *3* (17), 2785-2788; (b) Fang, G.-H.; Yan, Z.-J.; Deng, M.-Z., Palladium-Catalyzed Cross-Coupling of Stereospecific Potassium Cyclopropyl Trifluoroborates with Aryl Bromides. *Org. Lett.* **2004**, *6* (3), 357-360; (c) Solorio-Alvarado, C. R.; Echavarren, A. M., Gold-Catalyzed Annulation/Fragmentation: Formation of Free Gold Carbenes by Retro-Cyclopropanation. *J. Am. Chem. Soc.* **2010**, *132* (34), 11881-11883; (d) Solorio-Alvarado, C. R.; Wang, Y.; Echavarren, A. M., Cyclopropanation with Gold(I) Carbenes by Retro-Buchner Reaction from Cycloheptatrienes. *J. Am. Chem. Soc.* **2011**, *133* (31), 11952-11955; (e) Verdecchia, M.; Tubaro, C.; Biffis, A., Olefin cyclopropanation with aryl diazo compounds upon catalysis by a dirhodium(II) complex. *Tetrahedron Lett.* **2011**, *52* (10), 1136-1139; (f) Ringger, D. H.; Chen, P., Rational Design of a Gold Carbene Precursor Complex for a Catalytic Cyclopropanation Reaction. *Angew. Chem. Int. Ed.* **2013**, *52* (17), 4686-4689; (g) Lévesque, É.; Goudreau, S. R.; Charette, A. B., Improved Zinc-Catalyzed Simmons-Smith Reaction: Access to Various 1,2,3-Trisubstituted Cyclopropanes. *Org. Lett.* **2014**, *16* (5), 1490-1493; (h) Spencer, J. A.; Jamieson, C.; Talbot, E. P. A., One-Pot, Three-Step Synthesis of Cyclopropylboronic Acid Pinacol Esters from Synthetically Tractable Propargylic Silyl Ethers. *Org. Lett.* **2017**, *19* (14), 3891-3894; (i) Carden, R. G.; Widenhoefer, R. A., Gold Sulfonium Benzylidene Complexes Undergo Efficient Benzylidene Transfer to Alkenes. *Chem. Eur. J.* **2019**, *25* (47), 11026-11030; (j) Sugawara, M.; Yoshida, J.-i., Remarkable γ -Effect of Tin: Acid-Promoted Cyclopropanation Reactions of α -((Alkoxy carbonyl)oxy)stannanes with Alkenes. *J. Am. Chem. Soc.* **1997**, *119* (49), 11986-11987.
70. (a) Yamaguchi, K.; Kazuta, Y.; Abe, H.; Matsuda, A.; Shuto, S., Construction of a cis-Cyclopropane via Reductive Radical Decarboxylation. Enantioselective Synthesis of cis- and trans-1-Arylpiperazyl-2-phenylcyclopropanes Designed as Antidopaminergic Agents. *J. Org. Chem.* **2003**, *68* (24), 9255-9262; (b) Ty, N.; Pontikis, R.; Chabot, G. G.; Devillers, E.; Quentin, L.; Bourg, S.; Florent, J.-C., Synthesis and biological evaluation of enantiomerically pure cyclopropyl analogues of combretastatin A4. *Bioorg. Med. Chem.* **2013**, *21* (5), 1357-1366; (c) Brookhart, M.; C.Buck, R., Enantioselective benzylidene transfer reactions using the chiral-at-iron benzylidene complexes (SFeSc)- and (RFeSc)-Cp(CO)(Ph)2R★P₂Fe=CH6H5+ (R★ = (S-2-methylbutyl) and SFe- and (RFe)-Cp(CO)P(tBu)3Fe=CHC6H5+. *J. Organomet. Chem.* **1989**, *370* (1), 111-127; (d) Brookhart, M.; Liu, Y.; Goldman, E. W.; Timmers, D. A.; Williams, G. D., Enantioselective cyclopropane syntheses using the chiral carbene complexes (SFe)- and (RFe)-C5H5(CO)(PR3)Fe:CHCH3+. A mechanistic analysis of the carbene transfer reaction. *J. Am. Chem. Soc.* **1991**, *113* (3), 927-939; (e) Seitz, W. J.; Hossain, M. M., Iron Lewis acid catalyzed reactions of phenyldiazomethane and olefins: Formation of cyclopropanes with very high cis selectivity. *Tetrahedron Lett.* **1994**, *35* (41), 7561-7564; (f) Theys, R. D.; Hossain, M. M., Asymmetric cyclopropanation reactions via iron carbene complexes having chirality at the carbene ligand. *Tetrahedron Lett.* **1995**, *36* (29), 5113-5116; (g) Wang, Q.; Mayer, M. F.; Brennan, C.; Yang, F.; Hossain, M. M.; Grubisha, D. S.; Bennett, D., A New Approach to Diastereoselective and Enantioselective Cyclopropane Syntheses Using the Chiral Iron Carbene Complexes S- and R-[(η 5-C5H5)(CO)2FeCH[(η 6-o-CH3OC6H4)Cr(CO)3]]+. *Tetrahedron* **2000**, *56* (28), 4881-4891; (h) Wang, Q.; Försterling, F. H.; Hossain, M. M., Enantiospecific Cis-Cyclopropane Synthesis Using the Chiral Iron Carbene Complexes S-

and R-(η^5 -C₅H₅)(CO)₂FeCH[(η^6 -o-CH₃C₆H₄)Cr(CO)₃]⁺. *Organometallics* **2002**, *21* (13), 2596-2598;

(i) Wang, Q.; Försterling, F. H.; Hossain, M. M., Study of the origin of enantioselectivity in cyclopropanation reactions using the chiral iron carbene complex [(η^5 -C₅H₅)(CO)₂FeCH[(η^6 -o-MeOC₆H₄)Cr(CO)₃]]⁺. *J. Organomet. Chem.* **2005**, *690* (24), 6238-6246; (j) Goudreau, S. R.; Charette, A. B., In Situ Generation of Zinc Carbenoids from Diazo Compounds and Zinc Salts: Asymmetric Synthesis of 1,2,3-Substituted Cyclopropanes. *J. Am. Chem. Soc.* **2009**, *131* (43), 15633-15635; (k) E. A. Luthle, J.; Pietruszka, J.; Witt, A., Enantiomerically pure 1,3,2-dioxaborolanes: new reagents for the hydroboration of alkynes. *Chem. Commun.* **1998**, (23), 2651-2652.

71. Yu, Z.; Mendoza, A., Enantioselective Assembly of Congested Cyclopropanes using Redox-Active Aryldiazoacetates. *ACS Catal.* **2019**, *9* (9), 7870-7875.

72. Boche, G.; Schneider, D. R., Configurational stability of cyclopropyl radicals in electron-transfer reactions with naphthalene radical anion. *Tetrahedron Lett.* **1978**, *19* (26), 2327-2330.

73. (a) Patra, T.; Mukherjee, S.; Ma, J.; Strieth-Kalthoff, F.; Glorius, F., Visible-Light-Photosensitized Aryl and Alkyl Decarboxylative Functionalization Reactions. *Angew. Chem. Int. Ed.* **2019**, *58* (31), 10514-10520; (b) Ko, E. J.; Savage, G. P.; Williams, C. M.; Tsanakisidis, J., Reducing the Cost, Smell, and Toxicity of the Barton Reductive Decarboxylation: Chloroform as the Hydrogen Atom Source. *Org. Lett.* **2011**, *13* (8), 1944-1947.

74. (a) Zheng, C.; Wang, G.-Z.; Shang, R., Catalyst-free Decarboxylation and Decarboxylative Giese Additions of Alkyl Carboxylates through Photoactivation of Electron Donor-Acceptor Complex. *Adv. Synth. Catal.* **2019**, *361* (19), 4500-4505; (b) Wang, P.-Z.; Chen, J.-R.; Xiao, W.-J., Hantzsch esters: an emerging versatile class of reagents in photoredox catalyzed organic synthesis. *Org. Biomol. Chem.* **2019**, *17* (29), 6936-6951; (c) van Leeuwen, T.; Buzzetti, L.; Perego, L. A.; Melchiorre, P., A Redox-Active Nickel Complex that Acts as an Electron Mediator in Photochemical Giese Reactions. *Angew. Chem. Int. Ed.* **2019**, *58* (15), 4953-4957; (d) Milligan, J. A.; Phelan, J. P.; Badir, S. O.; Molander, G. A., Alkyl Carbon–Carbon Bond Formation by Nickel/Photoredox Cross-Coupling. *Angew. Chem. Int. Ed.* **2019**, *58* (19), 6152-6163; (e) Huang, W.; Cheng, X., Hantzsch Esters as Multifunctional Reagents in Visible-Light Photoredox Catalysis. *Synlett* **2017**, *28* (02), 148-158; (f) Buzzetti, L.; Prieto, A.; Roy, S. R.; Melchiorre, P., Radical-Based C–C Bond-Forming Processes Enabled by the Photoexcitation of 4-Alkyl-1,4-dihydropyridines. *Angew. Chem. Int. Ed.* **2017**, *56* (47), 15039-15043.

75. Chowdhury, R.; Yu, Z.; Tong, M. L.; Kohlhepp, S. V.; Yin, X.; Mendoza, A., Decarboxylative Alkyl Coupling Promoted by NADH and Blue Light. *J. Am. Chem. Soc.* **2020**, *142* (47), 20143-20151.

76. (a) Chikashita, H.; Miyazaki, M.; Itoh, K., 2-Phenylbenzothiazoline as a Reducing Agent in the Conjugate Reduction of α,β -Unsaturated Carbonyl Compounds. *Synthesis* **1984**, *1984* (04), 308-310; (b) Chikashita, H.; Miyazaki, M.; Itoh, K., Lewis acid-promoted conjugate reduction of α,β -unsaturated carbonyl compounds by 2-phenylbenzothiazoline (2-phenyl-2,3-dihydrobenzothiazole). *J. Chem. Soc., Perkin Trans. 1* **1987**, (0), 699-706; (c) Zhu, C.; Akiyama, T., Benzothiazoline: Highly Efficient Reducing Agent for the Enantioselective Organocatalytic Transfer Hydrogenation of Ketimines. *Org. Lett.* **2009**, *11* (18), 4180-4183; (d) Enders, D.; Liebich, J. X.; Raabe, G., Organocatalytic Asymmetric Synthesis of trans-1,3-Disubstituted Tetrahydroisoquinolines via a Reductive Amination/Aza-Michael Sequence. *Chem. Eur. J.* **2010**, *16* (32), 9763-9766; (e) Henseler, A.; Kato, M.; Mori, K.; Akiyama, T., Chiral Phosphoric Acid Catalyzed Transfer Hydrogenation: Facile Synthetic Access to Highly Optically Active Trifluoromethylated Amines. *Angew. Chem. Int. Ed.* **2011**, *50* (35), 8180-8183; (f) Saito, K.; Akiyama, T., Enantioselective organocatalytic reductive amination of aliphatic ketones by benzothiazoline as hydrogen donor. *Chem. Commun.* **2012**, *48* (38), 4573-4575; (g) Zhu, C.; Saito, K.; Yamanaka, M.; Akiyama, T., Benzothiazoline: Versatile Hydrogen Donor for Organocatalytic Transfer Hydrogenation. *Accounts of Chemical Research* **2015**, *48* (2), 388-398.

77. (a) Tarantino, K. T.; Liu, P.; Knowles, R. R., Catalytic Ketyl-Olefin Cyclizations Enabled by Proton-Coupled Electron Transfer. *J. Am. Chem. Soc.* **2013**, *135* (27), 10022-10025; (b) Slutskyy, Y.; Jamison, C. R.; Lackner, G. L.; Müller, D. S.; Dieskau, A. P.; Untiedt, N. L.; Overman, L. E., Short Enantioselective Total Syntheses of trans-Clerodane Diterpenoids: Convergent Fragment Coupling Using a trans-Decalin Tertiary Radical Generated from a Tertiary Alcohol Precursor. *J. Org. Chem.* **2016**, *81* (16), 7029-7035; (c) Chen, J.; Huang, W.; Li, Y.; Cheng, X., Visible-Light-Induced Difluoropropargylation Reaction with Benzothiazoline as a Reductant. *Adv. Synth. Catal.* **2018**, *360* (7), 1466-1472; (d) Li, L.; Guo, S.; Wang, Q.; Zhu, J., Acyl Radicals from Benzothiazolines: Synthons for Alkylation, Alkenylation, and Alkynylation Reactions. *Org. Lett.* **2019**, *21* (14), 5462-5466; (e) Bhunia, A.; Studer, A., Recent advances in radical chemistry proceeding through pro-aromatic radicals. *Chem* **2021**.

78. (a) Mori, T.; Inoue, Y., Charge-transfer excitation: unconventional yet practical means for controlling stereoselectivity in asymmetric photoreactions. *Chem. Soc. Rev.* **2013**, *42* (20), 8122-8133; (b) Lima, C. G. S.; de M. Lima, T.; Duarte, M.; Jurberg, I. D.; Paixão, M. W., Organic Synthesis Enabled by Light-Irradiation of EDA Complexes: Theoretical Background and Synthetic Applications. *ACS Catal.* **2016**, *6* (3), 1389-1407.

79. (a) Renny, J. S.; Tomasevich, L. L.; Tallmadge, E. H.; Collum, D. B., Method of Continuous Variations: Applications of Job Plots to the Study of Molecular Associations in Organometallic Chemistry. *Angew. Chem. Int. Ed.* **2013**, *52* (46), 11998-12013; (b) Zheng, L.; Cai, L.; Tao, K.; Xie, Z.; Lai, Y.-L.; Guo, W., Progress in Photoinduced Radical Reactions using Electron Donor-Acceptor Complexes. *Asian Journal of Organic Chemistry* **2021**, *10* (4), 711-748.
80. (a) Buzzetti, L.; Crisenza, G. E. M.; Melchiorre, P., Mechanistic Studies in Photocatalysis. *Angew. Chem. Int. Ed.* **2019**, *58* (12), 3730-3747; (b) Gehlen, M. H., The centenary of the Stern-Volmer equation of fluorescence quenching: From the single line plot to the SV quenching map. *Journal of Photochemistry and Photobiology C: Photochemistry Reviews* **2020**, *42*, 100338.
81. Aganda, K. C. C.; Kim, J.; Lee, A., Visible-light-mediated direct C3-arylation of 2H-indazoles enabled by an electron-donor-acceptor complex. *Org. Biomol. Chem.* **2019**, *17* (45), 9698-9702.
82. Cismesia, M. A.; Yoon, T. P., Characterizing chain processes in visible light photoredox catalysis. *Chem. Sci.* **2015**, *6* (10), 5426-5434.
83. Su, Y.; Li, Q.-F.; Zhao, Y.-M.; Gu, P., Preparation of Optically Active cis-Cyclopropane Carboxylates: Cyclopropanation of α -Silyl Stryenes with Aryldiazoacetates and Desilylation of the Resulting Silyl Cyclopropanes. *Org. Lett.* **2016**, *18* (17), 4356-4359.
84. (a) Goetz, F. J., Heterocyclic tautomerisms. I. An investigation of the 2-arylbenzothiazoline-2-(benzylideneamino)thiophenol tautomerism. Part 1. *Journal of Heterocyclic Chemistry* **1967**, *4* (1), 80-84; (b) Goetz, F. J., Heterocyclic tautomerisms. III. An investigation of the 2-arylbenzothiazoline-2-(benzylideneamino)thiophenol tautomerism. Part 3. *Journal of Heterocyclic Chemistry* **1968**, *5* (4), 509-512; (c) Mashraqui, S. H.; Kellogg, R. M., A ring expansion method for the preparation of 2,3-dihydro-1,4-benzothiazines from 2-aryl-2,3-dihydrobenzothiazoles. *Tetrahedron Lett.* **1985**, *26* (11), 1457-1460.
85. Friese, F. W.; Studer, A., New avenues for C-B bond formation via radical intermediates. *Chem. Sci.* **2019**, *10* (37), 8503-8518.
86. (a) Cheng, Y.; Mück-Lichtenfeld, C.; Studer, A., Metal-Free Radical Borylation of Alkyl and Aryl Iodides. *Angew. Chem. Int. Ed.* **2018**, *57* (51), 16832-16836; (b) Cheng, Y.; Mück-Lichtenfeld, C.; Studer, A., Transition Metal-Free 1,2-Carboboration of Unactivated Alkenes. *J. Am. Chem. Soc.* **2018**, *140* (20), 6221-6225; (c) Mazzarella, D.; Magagnano, G.; Schweitzer-Chaput, B.; Melchiorre, P., Photochemical Organocatalytic Borylation of Alkyl Chlorides, Bromides, and Sulfonates. *ACS Catal.* **2019**, *9* (7), 5876-5880.
87. Friese, F. W.; Studer, A., Deoxygenative Borylation of Secondary and Tertiary Alcohols. *Angew. Chem. Int. Ed.* **2019**, *58* (28), 9561-9564.
88. (a) Hu, J.; Wang, G.; Li, S.; Shi, Z., Selective C-N Borylation of Alkyl Amines Promoted by Lewis Base. *Angew. Chem. Int. Ed.* **2018**, *57* (46), 15227-15231; (b) Sandfort, F.; Strieth-Kalthoff, F.; Klauck, F. J. R.; James, M. J.; Glorius, F., Deaminative Borylation of Aliphatic Amines Enabled by Visible Light Excitation of an Electron Donor-Acceptor Complex. *Chem. Eur. J.* **2018**, *24* (65), 17210-17214; (c) Wu, J.; He, L.; Noble, A.; Aggarwal, V. K., Photoinduced Deaminative Borylation of Alkylamines. *J. Am. Chem. Soc.* **2018**, *140* (34), 10700-10704.
89. (a) Blackmond, D. G., Reaction Progress Kinetic Analysis: A Powerful Methodology for Mechanistic Studies of Complex Catalytic Reactions. *Angew. Chem. Int. Ed.* **2005**, *44* (28), 4302-4320; (b) Mathew, J. S.; Klussmann, M.; Iwamura, H.; Valera, F.; Futran, A.; Emanuelsson, E. A. C.; Blackmond, D. G., Investigations of Pd-Catalyzed ArX Coupling Reactions Informed by Reaction Progress Kinetic Analysis. *J. Org. Chem.* **2006**, *71* (13), 4711-4722.
90. (a) Scheffler, J. E.; Cottrell, C. E.; Berliner, L. J., An inexpensive, versatile sample illuminator for photo-CIDNP on any NMR spectrometer. *Journal of Magnetic Resonance (1969)* **1985**, *63* (1), 199-201; (b) Feldmeier, C.; Bartling, H.; Riedle, E.; Gschwind, R. M., LED based NMR illumination device for mechanistic studies on photochemical reactions – Versatile and simple, yet surprisingly powerful. *Journal of Magnetic Resonance* **2013**, *232*, 39-44; (c) Ji, Y.; DiRocco, D. A.; Kind, J.; Thiele, C. M.; Gschwind, R. M.; Reibarkh, M., LED-Illuminated NMR Spectroscopy: A Practical Tool for Mechanistic Studies of Photochemical Reactions. *ChemPhotoChem* **2019**, *3* (10), 984-992.
91. (a) Øpstad, C. L.; Melø, T.-B.; Sliwka, H.-R.; Partali, V., Formation of DMSO and DMF radicals with minute amounts of base. *Tetrahedron* **2009**, *65* (36), 7616-7619; (b) Sugihara, Y.; O'Connor, P.; Zetterlund, P. B.; Aldabbagh, F., Chain transfer to solvent in the radical polymerization of N-isopropylacrylamide. *Journal of Polymer Science Part A: Polymer Chemistry* **2011**, *49* (8), 1856-1864; (c) Chen, Y.-y.; Zhang, X.-j.; Yuan, H.-m.; Wei, W.-t.; Yan, M., Efficient cyclization of tertiary amines and alkenes promoted by KOT-Bu-DMF. *Chem. Commun.* **2013**, *49* (93), 10974-10976; (d) Wei, W.-t.; Dong, X.-j.; Nie, S.-z.; Chen, Y.-y.; Zhang, X.-j.; Yan, M., Intramolecular Dehydrative Coupling of Tertiary Amines and Ketones Promoted by KO-t-Bu/DMF: A New Synthesis of Indole Derivatives. *Org. Lett.* **2013**, *15* (23), 6018-6021; (e) Wang, W.-j.; Zhao, X.; Tong, L.; Chen, J.-h.; Zhang, X.-j.; Yan, M., Direct Inter- and Intramolecular Addition of Amides to Arylalkenes Promoted by KOT-Bu/DMF. *J. Org. Chem.* **2014**, *79* (18), 8557-8565; (f) Ragno, D.; Zaghi, A.; Di Carmine, G.; Giovannini, P. P.; Bortolini, O.; Fogagnolo,

M.; Molinari, A.; Venturini, A.; Massi, A., Cross-benzoin and Stetter-type reactions mediated by KOtBu-DMF via an electron-transfer process. *Org. Biomol. Chem.* **2016**, *14* (41), 9823-9835; (g) Yang, Q.; Sheng, M.; Huang, Y., Potential Safety Hazards Associated with Using N,N-Dimethylformamide in Chemical Reactions. *Organic Process Research & Development* **2020**, *24* (9), 1586-1601.